Old Dominion University
ODU Digital Commons

Theses and Dissertations in Biomedical Sciences

College of Sciences

Winter 1995

Cellular Mechanisms Underlying Myogenic Reactivity in Isolated Arterioles

Hui Zou
Old Dominion University

Follow this and additional works at: https://digitalcommons.odu.edu/biomedicalsciences_etds

Part of the Animal Structures Commons, Cell Biology Commons, and the Physiology Commons

Recommended Citation
Zou, Hui. "Cellular Mechanisms Underlying Myogenic Reactivity in Isolated Arterioles" (1995). Doctor of Philosophy (PhD), dissertation, , Old Dominion University, DOI: 10.25777/5azf-9z78
https://digitalcommons.odu.edu/biomedicalsciences_etds/90

This Dissertation is brought to you for free and open access by the College of Sciences at ODU Digital Commons. It has been accepted for inclusion in Theses and Dissertations in Biomedical Sciences by an authorized administrator of ODU Digital Commons. For more information, please contact digitalcommons@odu.edu.

CELLULAR MECHANISMS UNDERLYING MYOGENIC REACTIVITY IN ISOLATED ARTERIOLES

by

Hui Zou
Baccalaureate of Engineering, July 1986, Tianjin University, China
Master of Engineering, May 1989, Tianjin University, China

A Dissertation submitted to the Faculty of Eastern Virginia Medical School
and Old Dominion University in Partial Fulfillment of the Requirement
for the Degree of

DOCTOR OF PHILOSOPHY

PHYSIOLOGY
BIOMEDICAL SCIENCES

Eastern Virginia Medical School and Old Dominion University
December, 1995

Approved by:

Michael A. Hill (Director)

Stephen J. Beebe (Member)

Peter F. Blackmore (Member)

Barbara Hargrave (Member)

Paul H. Ratz (Member)

ABSTRACT

CELLULAR MECHANISMS UNDERLYING MYOGENIC REACTIVITY IN ISOLATED ARTERIOLES

Hui Zou
Eastern Virginia Medical School and Old Dominion University, 1995
Advisor: Dr. Michael A. Hill

The myogenic reactivity provides one of the principal mechanisms for blood flow autoregulation. The aims of the performed studies described in this dissertation were to test the role of $[Ca^{2+}]_i$ and MLC phosphorylation in arteriolar myogenic reactivity and further examine the source(s) of activator Ca^{2+} required to initiate and maintain myogenic vasoconstriction. In addition, the possible underlying mechanism of contractile protein expression was also addressed.

These studies used male Sprague Dawley rats of 200~350 grams body weight. Experiments were carried out using rat cremaster first order arterioles and mesenteric vessels. Gel electrophoresis and immunoblotting techniques were employed to analyze and identify the contractile protein isoforms and myosin light chain phosphorylation while the functional aspects of the studies were performed on isolated, cannulated vessel preparations. Intracellular calcium was measured using a video based image system with fura-2 as a fluorescent Ca^{2+} indicator. A fluorescence image intensity ratio of 340nm over 380nm excitation wavelengths was accepted as a measurement of $[Ca^{2+}]_i$. Samples for measuring MLC phosphorylation were collected by quickly freezing the vessels at the desired time points after different treatments according to the

protocols. Gel scanning and result quantification were performed with the aid of a computerized image analysis system.

The following conclusions were drawn from the studies presented in this dissertation: 1) Myogenic reactivity may, in part, relate to differences in structural composition of contractile proteins; 2) $[Ca^{2+}]_i$ and MLC phosphorylation play obligatory roles in the setting of arteriolar spontaneous tone and myogenic reactivity; 3) Wall tension appears to be the detected variable and a regulatory factor during the arteriolar myogenic reactivity; 4) α-adrenergic agonist induced-arteriolar contraction also depends on increases in $[Ca^{2+}]_i$ and MLC phosphorylation, however, signaling pathways appear to differ from that described for myogenic contraction. Further, mechanisms involving the contractile element Ca^{2+} sensitization also contribute to the agonist-induced response; 5) The extracellular Ca^{2+} source is most important in the maintenance of arteriolar basal tone and the myogenic contraction. While Ca^{2+} entry from the extracellular environment, largely via VOCs, is a mandatory process, Ca^{2+} release from intracellular stores may also be involved in the myogenic constriction. An additional Ca^{2+} entry mechanism, possibly receptor-operated Ca^{2+} channels, is involved in the agonist-induced contractions.

ACKNOWLEDGMENT

I would like to express my sincere gratitude to the members of my guidance committee: Dr. Stephen J. Beebe, Dr. Peter F. Blackmore, Dr. Barbara Hargrave, Dr. Paul H. Ratz for their kind help and advice all these four and a half years. My special thanks go to Dr. Michael A. Hill, my major advisor. He led me into the world of microcirculation and started my career in life sciences which is so much fun. He has not only been an exemplary mentor, but also a valued friend. Thank you, Mike.

I would also like to thank my family: my wife Xiaojun, who gave me so much support throughout these years; my son Alex, who always cheers me up; my mom Junxiu Sun and my mother-in-law Shuqing Chen, who have been great help. I could not have made it without you. I owe you a lot.

TABLE OF CONTENTS

Page

LIST OF TABLES vii

LIST OF FIGURES viii

LIST OF ABBREVIATIONS xii

CHAPTER

I. Background and Introduction 1

Blood Flow Regulation and Myogenic Phenomenon . . 1
Smooth Muscle Contraction 5
Myosin Light Chain (MLC) Phosphorylation and Smooth Muscle Contraction. . . . 5
Latch-Bridge Hypothesis 6
Protein Kinase C Activation and Smooth Muscle Contraction 8
Thin-filament Regulation of Smooth Muscle Contraction 11
Signal Transductions Involved in Agonist Induced Smooth Muscle Contractions . . . 13
Regulation of Ca^{2+}-Sensitivity 15
Intracellular Calcium 17
Voltage Operated Ca^{2+} Channels . . . 17
Receptor Operated Ca^{2+} Channels . . . 18
Stretch Activated Ca^{2+} Channels . . . 19
Intracellular Ca^{2+} Release via Inositol 1,4,5-triphosphate (IP3) Sensitive Channels . . 19
Intracellular Ca^{2+} Release via Ryanodine Sensitive Channels and Calcium Induced Calcium Release (CICR) . 20
Ca^{2+}-ATPase Pumps 21
Na^{+}-Ca^{2+} Exchangers 23
Capacitative Calcium Entry and Superficial Buffer Barrier 24
Contractile Protein Isoforms and Their effects on Smooth Muscle Functions 26
Previous Knowledge on Myogenic Reactivity . . . 30
Wall Tension as the Sensing Parameter? . . 30

CHAPTER Page

Endothelial Modulation of Myogenic Reactivity . 31
Proposed Mechanisms for Myogenic Reactivity . 32
Aims of the Study 35

II. Materials and Methods 39

Animal Preparation 39
Preparation of Tissues and Cannulating Glass Micropipette . 39
Isolation and Cannulation of Single Arterioles 42
Method for studying Myogenic and Agonist Responses in Isolated Arterioles 43
Intracellular Ca^{2+} Measurement with Fura-2 in Isolated Arterioles 45
Calibration of the Ca^{2+} Measurement System 49
Preparation of Samples for Electrophoretic Protein Separation . 50
Electrophoretic and Western Blotting Techniques . . 55
Statistical Methods and Data Analysis 57

III. Contractile Protein Isoform Expression Along Rat Mesenteric Vascular Tree 59

Materials and Methods 60
Results 61
Discussion 69

IV. Role of Ca^{2+}_i and Myosin Phosphorylation in Arteriolar Basal Tone Setting 74

Methods and Experimental Protocols 75
Results 77
Discussion 85

V. Role of Ca^{2+}_i and Myosin Phosphorylation in Myogenic- and Agonist-induced Arteriolar Contraction 92

Methods and Experimental Protocols 93
Results 95
Discussion 108

VI. Role of Intracellular Ca^{2+} Store Release and Ca^{2+} Entry in Arteriolar Contractions 117

CHAPTER Page

Methods and Experimental Protocols 118
Results 123
Discussion 142

VII. Concluding Statements and Future Directions . . . 149

REFERENCES 156

VITA 182

LIST OF TABLES

Table Page

3-1. Myosin SM1 Heavy Chain Content (% total SM MHC) . . 68

5-1. Comparison of arteriolar responses to 30mm Hg pressure increase starting at 30 and 120mm Hg 99

LIST OF FIGURES

Figure Page

1-1. Schematic illustration of arteriolar diameter response to intraluminal pressure changes 3

1-2. Myosin phosphorylation-dephosphorylation as the primary mechanism in the regulation of smooth muscle contraction 7

1-3. Latch-bridge model. 8

1-4. Smooth muscle cellular events following the binding of NE to its receptor . . 14

2-1. Illustration of rat mesenteric (top) and cremaster (bottom) vascular bed . . 41

2-2. Illustration of glass micropipette (top) and a cannulated vessel (bottom) . . 42

2-3. Illustrations of vessel cannulation and cannulating chamber . . . 44

2-4. Excitation spectra of fura-2 46

2-5. Schematic diagram of the Ca^{2+} measurement system 48

2-6. Measurement of vessel diameter using pixel count as an index . . . 49

2-7. Absorption spectra of the optical filters 51

2-8. Illustration of the cannulating chamber for vessel sample collection . . 53

2-9. Representative gel showing the separation of myosin light chain isoforms . 56

3-1. Relationship between α actin content and small mesenteric artery diameter . 63

Figure Page

3-2. Comparison of actin isoform content of small mesenteric arteries compared to that of the corresponding small veins 64

3-3. Relative abundance of tropomyosin subunits in small mesenteric arteries . 65

3-4. Digital image showing electrophoretic separation of myosin heavy chains . 67

4-1. Relationship between arteriolar diameter, pressure and wall tension . . 79

4-2. Relationship between arteriolar $[Ca^{2+}]_i$, pressure and wall tension . . 80

4-3. Level of myosin light chain phosphorylation expressed as a percentage of total myosin light chain 82

4-4. Relationship between myosin light chain phosphorylation and diameter (A) or calculated wall tension (B) 83

4-5. Effect of the myosin light chain kinase inhibitor, ML-7, on pressure-induced changes in $[Ca^{2+}]_i$ (A) and diameter (B) . . . 84

4-6. Measured and calculated vessel diameter based on the idea that wall tension is regulated in myogenic reactivity 88

5-1. Arteriolar diameter and Ca^{2+} responses to an increase in intraluminal pressure from 70 to 100 mmHg 96

5-2. Arteriolar diameter (A) and Ca^{2+} (B) responses to pressure step increases from 30mmHg to 60mmHg and 120mmHg to 150mmHg . . 98

5-3. Arteriolar diameter (A) and Ca^{2+} (B) responses to pressure step increase from 50mmHg to 120mmHg and followed by return to 50mmHg . 101

Figure Page

5-4. Arteriolar diameter (A) and Ca^{2+} (B) responses to an acute 30-150mmHg pressure step 102

5-5. Relationship between pressure step-induced stretch and $[Ca^{2+}]_i$ increases (A), and increase in wall tension and $[Ca^{2+}]_i$ increase (B) . . 103

5-6. Arteriolar diameter (A) and Ca^{2+} (B) responses to 0.1μM, 1μM, and 5μM NE stimulations 105

5-7. MLC phosphorylation following NE stimulation 106

5-8. Comparison of arteriolar diameter (A) and Ca^{2+} (B) responses to an acute pressure increase and a comparable NE stimulation . . 107

6-1. Effect of Ca^{2+} entry blockade on arteriolar steady state basal tone (A) and $[Ca^{2+}]_i$ (B) 124

6-2. Effect of Ca^{2+} entry blockade on arteriolar diameter (A) and Ca^{2+} (B) response to an acute 50-120mmHg pressure increase . . 126

6-3. Effect of Ca^{2+} entry blockade on arteriolar basal, maximal and steady state $[Ca^{2+}]_i$ in response to an acute 50-120mmHg pressure increase . 127

6-4. Effect of Ca^{2+} entry blockade on arteriolar diameter (A) and Ca^{2+} (B) response to 0.1μM norepinephrine stimulation . . . 128

6-5. Effect of Ca^{2+} entry blockade on arteriolar diameter (A) and Ca^{2+} (B) response to 1μM norepinephrine stimulation . . . 129

6-6. Effect of Ca^{2+} entry blockade on arteriolar diameter (A) and Ca^{2+} (B) response to 5μM norepinephrine stimulation . . . 130

Figure Page

6-7. Effect of Ca^{2+} entry blockade on arteriolar maximal and steady-state Ca^{2+} response to 0.1μM (A), 1μM (B) and 5μM (C) norepinephrine stimulation . 132

6-8. Effect of Ca^{2+} entry blockade on steady-state arteriolar constriction to 0.1, 1 and 5μM norepinephrine 133

6-9. Representative tracings of Ca^{2+} response revealing the relationship between caffeine and agonist-released Ca^{2+} pools 134

6-10. Representative tracings showing the time course for the depletion of intracellular Ca^{2+} stores accessed by agonist and caffeine in the absence of extracellular Ca^{2+} 135

6-11. Representative tracings showing the effect of ryanodine on arteriolar Ca^{2+} and diameter responses to an acute 50-120mmHg pressure increase . 137

6-12. Effect of intracellular pressure on arteriolar diameter and Ca^{2+} responses to caffeine (20mM) under conditions of control and verapamil pre-treatment 138

6-13. Representative tracings detecting arteriolar intracellular Ca^{2+} release during pressure step-increase and a following caffeine stimulation . . 140

6-14. Representative tracings of fluorescence intensities of 340nm and 360nm excitation detecting intracellular Ca^{2+} release during pressure increase and NE stimulation 141

7-1. Possible signaling pathways involved in the arteriolar myogenic responses . 155

CHAPTER I

BACKGROUND AND INTRODUCTION

Arterioles (approximately 10~100μm in diameter) are the terminal branches of the arterial system. They are also termed resistance vessels because the greatest functional resistance (50-80%) to blood flow resides in this segment of the circulation, and as such, arterioles play a very important role in regulating local blood flow. The wall of resistance vessels consists primarily of smooth muscle cells wrapped circumferentially around the vessel lumen, which is lined by a monolayer of endothelial cells in contact with the blood (Rhodin, 1967). In order to provide a framework for understanding arteriolar vasomotor function, a general background introduction to the myogenic phenomenon and the related mechanisms for smooth muscle contraction are provided in the remainder of the chapter.

Blood Flow Regulation and Myogenic Phenomenon

Arterioles characteristically show **basal tone** (also called **spontaneous tone** or **myogenic tone**) - a partially constricted state of smooth muscle cells of the vessel wall from which they can relax or further constrict in response to different stimuli. It is this unique characteristic that enables the arterioles to function as the major site for local blood flow regulation.

Although variation exists between organs, the blood flow to each tissue of the body tends to be tightly controlled in relation to the tissue need. Local blood flow regulation, or autoregulation, involves several mechanisms including myogenic and metabolic responsiveness (Granger, et al., 1988; Johnson, 1986). Stabilizing tissue oxygen is the proposed ultimate goal for the metabolic mechanism. When tissue oxygenation falls below normal, a signal (possibly through releasing of vasodilator metabolites, e.g. adenosine) is transmitted to the arteriolar smooth muscle cell to elicit relaxation. Consequently, blood flow through microcirculation increases and more oxygen is transported from capillaries thereby returning tissue oxygenation to normal and providing convective washout of accumulated metabolites. According to the **myogenic mechanism**, vascular smooth muscle cells constrict in response to an increase in transmural pressure and relax following a pressure reduction. The increased (decreased) blood flow resulting from the elevation (reduction) of blood pressure is then normalized by the decrease (increase) in vessel cross-section area due to the constriction (relaxation). A relationship between blood flow and vessel cross section area (radius) is shown below:

$$\text{Flow (F)} = k\,\Delta\,Pr^4 \qquad (1\text{-}1)$$

here, k is a constant related to blood viscosity and vessel length; ΔP is blood pressure change along the vessel; and r is radius of the vessel.

In many tissues of the body, both metabolic and myogenic mechanisms are required for a complete local microcirculatory regulation. It has been considered that the metabolic mechanism dominates when tissue oxygenation is below normal, while myogenic mechanism supersedes when the prevailing tissue oxygen tension is higher than normal (Granger, et al., 1988). It was recently suggested that these mechanisms reside in different arteriolar segments:

metabolic control exerts a dominant effect on the smallest arterioles (<20µm) and myogenic control dominates in vessels 20-30µm (Kuo, et al., 1992).

In addition to blood flow and capillary pressure regulation, the myogenic response may also be critically important for the establishment of basal vascular resistance and may interact additively or negatively with other mechanisms (Kuo, et al., 1991). The control of resistance is very effective because resistance is inversely proportional to the 4th order of vessel radius. Figure 1-1 illustrates arteriolar diameter responses to changes in transmural pressure.

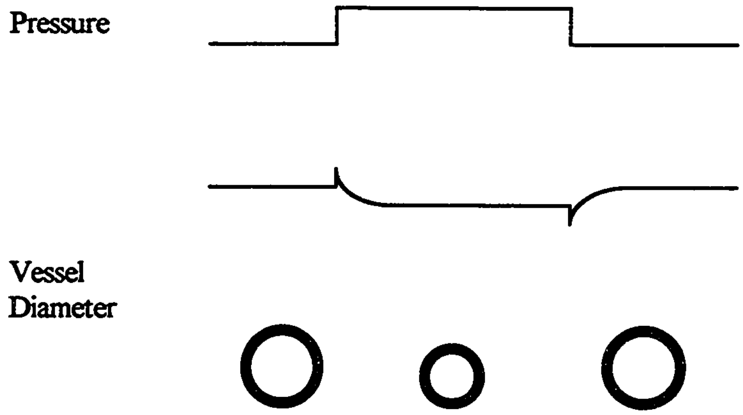

Figure 1-1. Schematic illustration of arteriolar diameter response to intraluminal pressure changes.

Myogenic activity of blood vessels was first theorized by Sir William Maddock Bayliss at the turn of the century (Bayliss, 1902). Two of the phenomena Bayliss observed in his experiments contributed most in leading to this proposition. He found that a brief reduction of perfusion pressure to the hindquarters of the dog caused expansion of the limb beyond its control volume when the pressure was restored. More directly, he also observed that when the internal pressure of an isolated carotid artery segment was elevated, it began to "writhe like a worm". However, the support for the myogenic phenomena remained weak and some other researchers suggested alternative explanations such as local accumulation of chemical factors. Until 1950's, most physiologists still regarded the blood vessels as being principally under the central control of vasodilator and vasoconstrictor nerves, with local mechanisms playing a minor role (Johnson, 1980). The studies from Folkow (1949 and 1952) provided another milestone in the study of myogenic reactivity. Using perfused cat hindquarters, he showed that despite a transient increase, flow returned towards its control level after an elevation of the arterial perfusion pressure. A transient flow decrease followed by a gradual increase towards control level was seen with a reduced perfusion pressure. Further, he demonstrated that complete denervation of muscular, cutaneous, and splanchnic vessels did not abolish vascular tone. His study provided sufficient evidence that there could be a myogenic origin for vascular tone and that it again became a matter of serious consideration.

Following Folkow's studies there was a resurgence of interest in the role of the myogenic response in local blood flow regulation. In particular, numerous studies provided descriptive data dealing with the presence or absence of myogenic behavior within specific vascular beds and at specific sites within a vascular network (for review see Johnson, 1980 and 1986). More recently, with the development of methods for studying signal transduction, the focus has shifted to understanding the cellular events which underlie myogenic vasoconstriction. Before describing such studies, a brief overview of smooth muscle contraction, signal transduction mechanisms related to contraction and the role of specific proteins in contractile function is provided. Following this the current understanding of the cellular mechanisms involved in myogenic reactivity will be presented.

Smooth Muscle Contraction

The myogenic reactivity has been proved to be smooth muscle originated and is independent of endothelium (see the section of "previous knowledge on myogenic reactivity" in this chapter). Therefore, myogenic reactivity, per se, is smooth muscle contraction. Although the sliding filament contractile mechanism for striated muscles was detailed decades ago, smooth muscle contraction had remained a mystery until the 1980's. In the late 70's, studies started to show that myosin light chain (MLC) phosphorylation mediated by myosin light chain kinase (MLCK) is a key event leading to smooth muscle contraction (Cassidy, et al., 1979; Sobieszek, 1977). Evidence supporting this thick-filament regulation hypothesis has, since, been accumulating and the activation of MLCK pathway has been demonstrated to be both necessary and sufficient to trigger contraction of smooth muscle (Driska, et al., 1981; Hai and Murphy, 1988; Itoh, et al., 1989; Murphy, 1982)

Myosin Light Chain Phosphorylation and Smooth Muscle Contraction

Intracellular calcium concentration ($[Ca^{2+}]_i$) is agreed to be the primary determinant of smooth muscle contraction, and it is now generally accepted that intracellular free Ca^{2+} binding to the protein calmodulin (CaM) forms the initial event in smooth muscle contraction. The regulatory Ca^{2+}/CaM complex ($4Ca^{2+}$-CaM) then binds to the catalytic subunit of MLCK and activates this enzyme. MLCK phosphorylates serine 19 (high concentration MLCK also phosphorylates threonine 18 *in vitro*) (Ikebe and Hartshorne, 1985) on the 20kD regulatory light chain of myosin which leads to an increase in the actin-activated myosin ATPase. Physiologically, MLC phosphorylation would be associated with attachment and cycling of cross bridges to actin and the subsequent development of force or increase in maximal shortening velocity. A decrease in $[Ca^{2+}]_i$ inactivates MLCK and dephosphorylation of MLC by a protein phosphatase (Myosin Light Chain Phosphatase, MLCP) would lead to relaxation (Kamm and Stull, 1985; Stull, et al., 1991; Walsh, 1991). A diagram of the molecular events involved in smooth muscle contraction and relaxation is shown in figure 1-2.

Latch-bridge Hypothesis

Although the proposed general scheme of MLC phosphorylation causing smooth muscle contraction is widely applicable and generally accepted, many investigations have shown that the events illustrated in figure 1-2 are not sufficient to describe all the cellular processes involved in smooth muscle contraction. Murphy and his colleagues originally observed a dissociation of force and myosin phosphorylation (Dillon, et al., 1981). Following a high K^+ stimulation of swine carotid artery, they found a correlation between MLC phosphorylation and maximum shortening velocity during force development, however, isometric force was maintained during prolonged stimulation while MLC phosphorylation decreased to about 25% from a peak value of 65%. Similar observations were also reported by other investigators using different (vascular and tracheal smooth muscles) tissues (Aksoy, et al., 1983; Kamm and Stull, 1985). To explain this, Murphy and colleagues (Dillon et al., 1981;

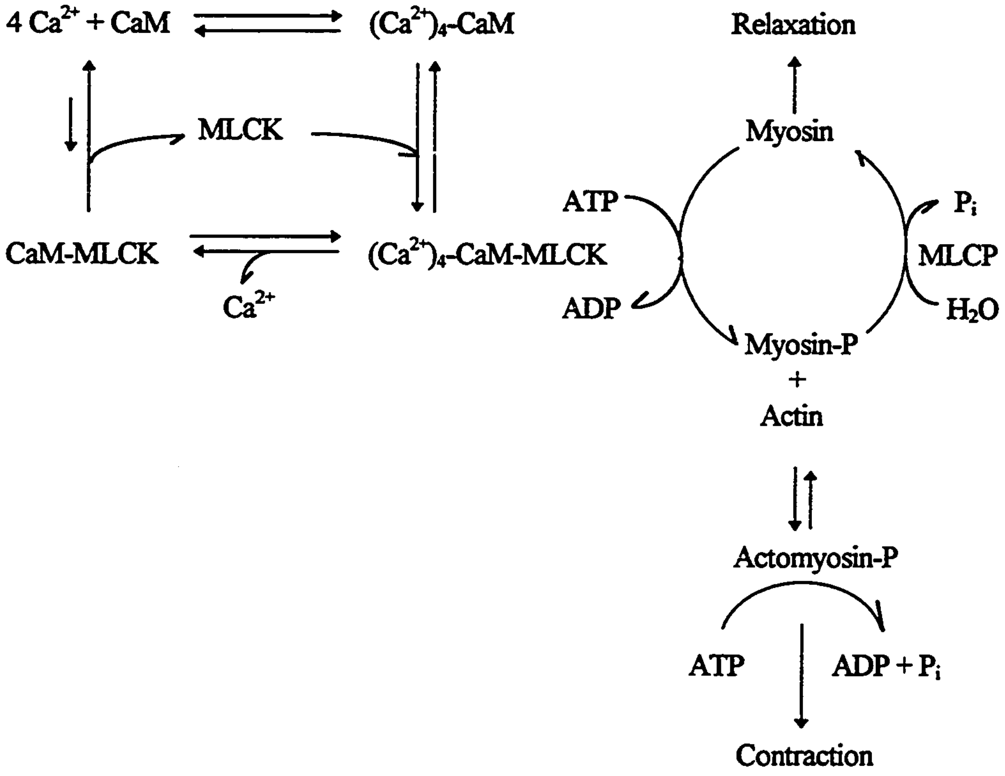
4 Ca2+ + CaM
(Ca2+)4-CaM
MLCK
CaM-MLCK
(Ca2+)4-CaM-MLCK
Ca2+
Relaxation
Myosin
ATP
ADP
Pi
MLCP
H2O
Myosin-P
+
Actin
Actomyosin-P
ATP
ADP + Pi
Contraction

Figure 1-2. Myosin phosphorylation-dephosphorylation as the primary mechanism in the regulation of smooth muscle contraction. CaM, calmodulin; MLCK, myosin light chain kinase; MLCP, myosin light chain phosphatase.

Hai and Murphy, 1988) put forward a 'Latch-bridge Hypothesis" which suggests a state of dephosphorylated myosin attaching to actin during the prolonged smooth muscle activation, forming a noncycling cross-bridge (the latch-bridge). This latch-bridge mechanism appears to function only after the initial activation and Ca^{2+} transient that lead to myosin phosphorylation and stress development (Chatterjee and Murphy, 1983). Figure 1-3 shows a schematic diagram of this proposed mechanism.

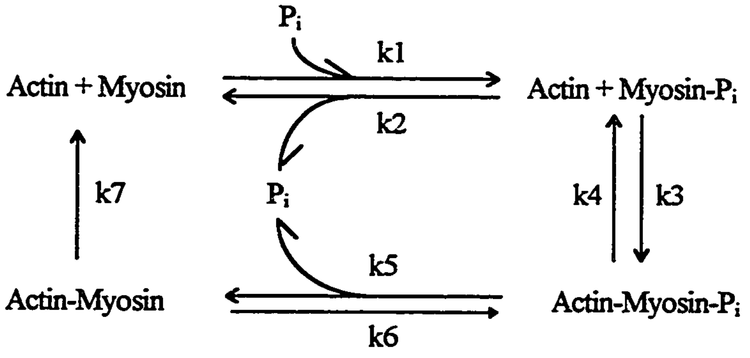

Figure 1-3. Latch-bridge model

While the physiologically based 'latch-bridge" model explains many observations relating MLC phosphorylation and force development or maximal shortening velocity, to date, there have been no biochemical studies that directly demonstrate this unique form of myosin cross bridge.

Protein Kinase C Activation and Smooth Muscle Contraction

An alternative explanation to this dissociation of force from MLC phosphorylation has been proposed by Rasmussen, et al. (1987). These investigators defined a two domain model for smooth muscle cells: caldesmon - tropomyosin - actin - myosin (CD-TM-A-M) domains and filamin - Actin - desmin (F-A-D) domains. According to this model, the latch mechanism is not caused by the formation of a specific latch bridge between actin and myosin, but to a reorganization and stabilization of the supramolecular organization of the components of the F-A-D domain. Briefly, in the early phase of contraction, the activation of MLCK by Ca^{2+}/CaM causes MLC phosphorylation which leads to the formation of cycling cross-bridges of actin and myosin and thus development of tension. During tension development, the F-A-D fibrillar domain undergoes a re-organization. In addition, the activation of protein kinase C (PKC) leads to the phosphorylation of desmin, synemin, caldesmon and several cytosolic proteins. While the MLC phosphorylation is transient and soon falls towards near basal value, tension is maintained as a consequence of the stabilization of the F-A-D domain by the late-phase phosphorylation.

Since then, involvement of PKC in smooth muscle contraction has attracted much attention. Both Ca^{2+}-dependent (α, β) and Ca^{2+}-independent PKC isoforms (ε, ζ) have been found in smooth muscle cells and both classes have been implicated in the modulation of smooth muscle contraction (Andrea and Walsh, 1992; Lee and Severson, 1994). Although biochemical studies have demonstrated that PKC directly phosphorylates MLC at serine 1, serine 2 and threonine 9 (Bengur, et al., 1987; Ikebe, et al., 1987), such phosphorylation alone has no effect on the enzymatic properties of myosin. On the other hand, PKC-catalyzed phosphorylation reduces by approximately 50% the actin-activated ATPase activity of myosin previously phosphorylated at serine 19 by MLCK (Nishikawa, et al., 1983). However, it is interesting to notice that phorbol 12,13-dibutyrate (PDB, an exogenous PKC activator) or α-agonists such as phenylephrine, which generates an endogenous PKC activator 1,2-diacylglycerol (DAG), does not cause phosphorylation at any of the PKC sites in myosin, but only at serine 19 with some phosphorylation at threonine 18 (Singer, et al., 1989). MLCK is, therefore, the primary enzyme that catalyzes the MLC phosphorylation. PKC can also phosphorylate MLCK, but, there is evidence to suggest that the phosphorylation of MLCK by PKC does not affect contractility (Stull, et al., 1990). It seems that contractions elicited by agonists that trigger phosphoinostide turnover and generation of DAG do not involve PKC-catalyzed phosphorylation of either MLC or MLCK. For example, Kitazawa et al. found (1991) found that in α-toxin skinned vessel, GTPγS, which mimics the agonist-induced G-protein activation, did not further increase MLC phosphorylation hence had no effect on MLCK activity. And this idea is also supported by the study from Rembold and Murphy (1988). They examined the $[Ca^{2+}]_i$ and MLC phosphorylation following a PDB stimulation in hog carotid artery and found that PDB can cause an increase in $[Ca^{2+}]_i$, and the subsequent increase in MLC phosphorylation, due to the elevated $[Ca^{2+}]_i$, quantitatively explains the contraction. Although other proteins such as putative thin-filament regulatory proteins, caldesmon and calponin, can also be phosphorylated by PKC *in vitro*, substrates of PKC under physiological conditions are yet to be identified to specify the role of PKC in smooth muscle contraction.

Thin-filament Regulation of Smooth Muscle Contraction

Inspired by the idea of PKC involvement, recent research from several other groups proposed another mechanism regulating contractile protein activation - thin filament regulation (Abe, et al., 1990; Marston and Redwood, 1992; Sobue and Sellers, 1991; Winder and Walsh, 1990). Caldesmon and calponin may play important roles in smooth muscle contraction according to this hypothesis. Caldesmon is a major calmodulin- and actin-binding protein found in smooth muscle and other cells (Haeberle et al., 1992; Mabuchi, et al., 1992; Lehman, et al., 1990). *In vitro* studies have demonstrated that caldesmon inhibits superprecipitation and actin-activated myosin Mg^{2+}-ATPase activity (Nagi and Walsh, 1984; Sobue, et al., 1982; Marston and Lehman, 1985) suggesting that caldesmon inhibits actomyosin interaction. There is also evidence to show that caldesmon regulates smooth muscle contraction by providing a basal resting inhibition of vascular tone and that exogenously added caldesmon relaxes permeablized smooth muscle fiber preparations (Katsuyama, et al., 1992; Taggart and Marston, 1988). Studies from Chalovich and colleagues (1993) suggested that caldesmon increases the level of MLC phosphorylation required for smooth muscle activation in skinned gizzard muscle fibers. But, these authors further pointed out that caldesmon does not act to maintain force in smooth muscle by cross-liking myosin with actin since competition of binding of caldesmon with myosin does not cause a reduction in tension. Phosphorylation of caldesmon *in vitro* by PKC reversed its inhibition on actomyosin ATPase. However, comparison of the phosphopeptide maps of caldesmon phosphorylation, from *in vitro* phosphorylation by PKC with that by phorbol ester stimulation in intact smooth muscle, suggested that the putative cellular caldesmon kinase is not PKC (Lee and Severson, 1994). It has been suggested that caldesmon from intact vascular smooth muscle was phosphorylated by mitogen-activated protein (MAP) kinase (Adam and Hathaway, 1993). Further, a recent study from Katoch and Moreland (1995) suggested that in swine carotid artery, MAP kinase is activated in response to all forms of contractile stimulation, and the activated MAP kinase phosphorylates caldesmon and releases the inhibition of caldesmon on actomyosin interaction. This disinhibition allows an inherent level of myosin ATPase activity to be expressed. However, there is also evidence against this disinhibition by the phosphorylation of caldesmon. Pinter and Marston (1992) found that *in vitro* phosphorylation of vascular smooth muscle caldesmon by endogenous kinase did not change its inhibitory effects on actin-tropomyosin activated myosin Mg^{2+}-ATPase. Incorporation of caldesmon into native or synthetic thin filament did not alter its phosphorylation by the crude mixture containing endogenous "caldesmon kinase" hence indicating a more "*in vivo*" situation in their study. A recent report from Nixon et al. (1995) demonstrated that phosphorylation of caldesmon by MAP kinase has no effect on Ca^{2+} sensitivity in rabbit smooth muscle. Due to the controversial evidence for the functions of caldesmon, further studies are needed to clarify the role of caldesmon in regulating smooth muscle contraction.

Calponin is a smooth muscle specific, 34 kD calmodulin-binding troponin T-like protein. Structural studies demonstrated that intracellular calponin is colocalized on thin filament and share an identical distribution to that of actin and tropomyosin (Takahashi, et al, 1986; Walsh, et al., 1993). It has been shown *in vitro* that calponin binds to actin and tropomyosin in a Ca^{2+}-independent manner and bind to calmodulin Ca^{2+}-dependently. Calponin inhibits the actomyosin ATPase and can be phosphorylated by PKC and Ca^{2+}/CaM-dependent protein kinase II (CaM kinase II) and dephosphorylated by a type 2A phosphatase (Winder, et al., 1992). Upon phosphorylation, the inhibitory effect of calponin is completely reversed while the dephosphorylation of calponin completely restores the ability of calponin to inhibit the actomyosin ATPase. Calponin phosphorylation also occurs in intact toad stomach smooth muscle strips which supports the hypothesis that calponin may be regulated *in vivo* by phosphorylation-dephosphorylation (Winder, et al., 1993).

Signal Transductions Involved in Agonist Induced Smooth Muscle Contractions

An agonist-induced smooth muscle contraction is initiated by the binding of agonists to their receptors on the plasma membrane. A simplified illustration diagram is shown in figure 1-4 where norepinephrine (NE), a neurotransmitter released from periarteriolar neurons, is used as an example in the diagram. Upon binding to the α_1 receptor (on smooth muscle cell membrane), NE activates a membrane bound (more exactly, membrane receptor bound) trimeric GTP-binding and hydrolyzing protein (G-protein). An activated G-protein binds to GTP and the hydrolysis of GTP to GDP causes inactivation of the protein. The activated G-protein (G_q), in turn, leads to the activation of phospholipase C_β (PLC) on cell membrane which catalyzes the hydrolysis of phosphatidylinositol 4,5-*bis*phosphate (PIP_2), a plasma membrane lipid. Although it has been considered that the α-subunit of G_q is responsible for PLC activation, the $\beta\gamma$-dimer is also suggested play a role in the signaling (Clapham and Neer, 1993). Two important cellular messengers are generated as the products of this hydrolysis:

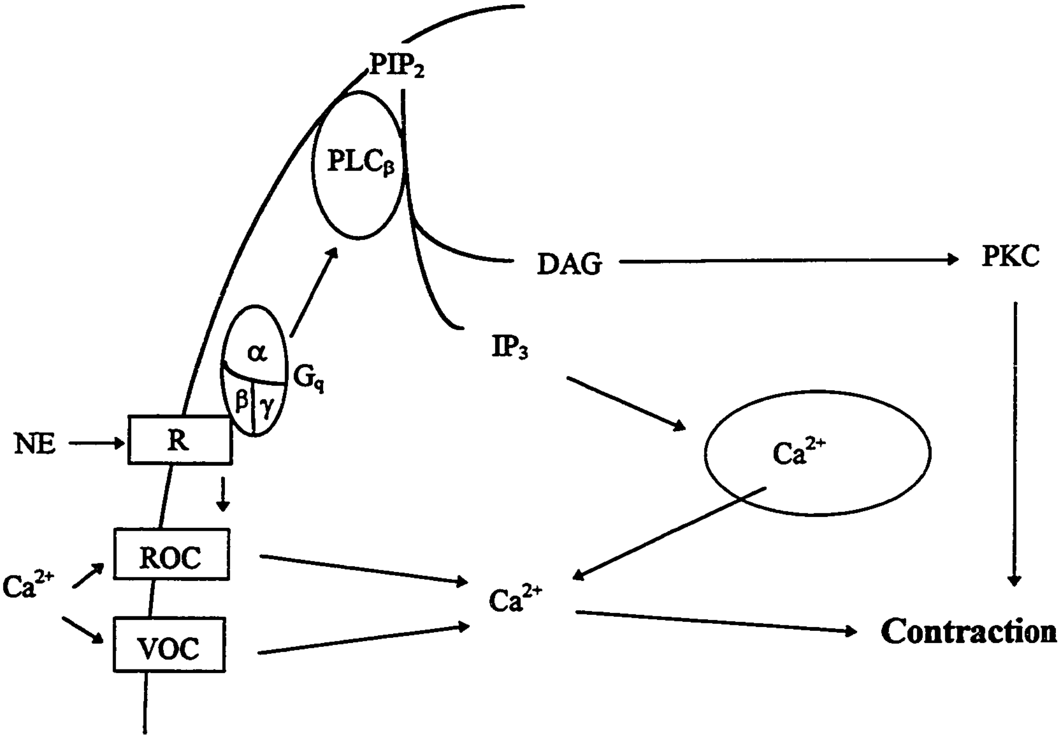
PIP2
PLCβ
DAG
PKC
IP3
α
Gq
β
γ
NE
R
Ca2+
ROC
Ca2+
VOC
Ca2+
Contraction

Figure 1-4 Smooth muscle cellular events following the binding of NE to its receptor. DAG, 1,2-diacylglycerol; NE, norepinephrine; IP_3, inositol 1,4,5-*tris*phosphate; PIP_2, phosphatidylinositol 4,5-*bis*phosphate; PKC, protein kinase C; PLC_β, phospholipase C_β; R, receptor; ROC, receptor operated channel; VOC, voltage operated channel.

1,4,5-*tri*phosphate (IP_3) and DAG. While DAG is an endogenous PKC activator, IP_3 can bind to its receptors on the membrane of sarcoplasmic reticulum (SR) and release Ca^{2+} from intracellular stores (Birnbaumer and Brown, 1990). NE, in addition to its reported capability of increasing Ca^{2+} entry through putative receptor operated Ca^{2+} channels (ROC) without significant changes in membrane potential, can also depolarize arterial smooth muscles and, therefore, increase the opening of voltage-operated-channels (VOC) (for review, see Nelson, et al., 1990). The increase in $[Ca^{2+}]_i$ will activate MLCK and lead to the contraction of smooth muscle. An increase in PKC activity following an agonist stimulation (due to the generation of DAG) is considered to have a regulatory effect on smooth muscle contraction (e.g. sensitizing the contractile apparatus).

Regulation of Ca^{2+}-Sensitivity

Studies revealed that the force/Ca^{2+} ratio is generally higher during smooth muscle activation by agonists than by a depolarization induced increase in $[Ca^{2+}]_i$ (Nishimura, et al., 1990), indicating a Ca^{2+} sensitizing effect of agonists. Furthermore, it has also been demonstrated that agonist-induced force generation can occur in the absence of increase in $[Ca^{2+}]_i$ in vascular smooth muscle preparations (Eiichi, et al., 1991; Moreland, et al., 1992). A decrease in Ca^{2+}-sensitivity was also reported in studies showing force can decline while $[Ca^{2+}]_i$ is maintained (Himpens, et al., 1989; Somlyo, 1989).

Traditionally, it has been considered that MLCK is the only enzyme that is regulated during the MLC phosphorylation while MLCP activity, in particular, remains constant. However, recent findings suggest that the protein phosphatase that dephosphorylates Serine 19 of MLC can also be regulated (inhibited) . It appears that the inhibition of this phosphatase, possibly by PKC, is the main mechanism of G-protein coupled Ca^{2+}-sensitization (Collins, et al., 1992; Itoh, et al., 1993; Katsuyama and Morgan, 1993; Kitazawa, et al., 1991). Inhibition of the phosphatase increases MLC phosphorylation and hence the force at given $[Ca^{2+}]_i$. Recently, arachidonic acid (AA) has also been implicated as a potential cellular messenger that mediates signaling from membrane receptors to the myosin bound phosphatase (Gong, et al, 1992; Somlyo and Somlyo, 1994).

Although the conventional heterotrimeric G-protein is considered to play a primary role in Ca^{2+}-sensitization, the possibility for the contribution of monomeric G-protein family has not been ruled out. Satoh et al. (1993) recently reported that H-ras p21 proteins increase Ca^{2+}-responsiveness of smooth muscle contraction in β-escin skinned guinea pig small mesenteric arteries, suggesting involvement of tyrosine kinase pathway in vascular smooth muscle contraction.

Phosphorylation of MLCK at a specific serine residue in the CaM-binding domain (site A) by several kinases reduces its affinity for CaM and consequently its kinase activity (Stull, 1991). Phosphorylation of MLCK by one of these kinases, CaM kinase II, occurs in vivo and is suggested as a physiological mechanism for Ca^{2+}-desensitization. But, it requires a higher $[Ca^{2+}]_i$ than activation of MLCK does due to the lower affinity of CaM kinase for Ca^{2+}/CaM than that of MLCK.

Intracellular Calcium

The $[Ca^{2+}]_i$ is precisely regulated and is maintained at a level of about 100nM under resting conditions, despite extracellular $[Ca^{2+}]$ and the SR $[Ca^{2+}]$ in the mM range. Upon activation, $[Ca^{2+}]_i$ can increase dramatically to 500-700 nM (Williams and Fay, 1986). This increased Ca^{2+} comes from either the extracellular pool via various Ca^{2+} channels in the plasma membrane or the intracellular pools (presumably SR) via different release mechanisms. The removal of Ca^{2+} from cytosol is accomplished by extrusion via Na^+-Ca^{2+} exchangers and Ca^{2+}-ATPase pumps in sarcolemma or uptake into intracellular stores by Ca^{2+}-ATPase on SR membrane. To help understanding the Ca^{2+} homeostasis, especially those studies discussed in chapter 6, the $[Ca^{2+}]_i$ adjustment mechanisms that may be involved in smooth muscle contraction are briefly described below.

Voltage Operated Ca^{2+} Channels

The VOCs are channels that are gated by the membrane potential: opening at more positive potentials (depolarized states) and closing at more negative potentials (hyperpolarized states). The thresholds for VOC opening are different among different channel types. The arterial smooth muscle cells, *in vivo,* have stable resting membrane potentials between -60 and -75mV (Nelson, et al., 1990). More positive potentials (depolarization) can open the VOC and cause an influx of Ca^{2+} to increase $[Ca^{2+}]_i$. Several types of Ca^{2+} VOCs have been found: Long-lasting, large capacitance (L-) type, transient (T-) type, P-type, Q-type, and neuron specific (N-) type. Studies on P-, Q- and N-type VOCs have been mostly limited to neuronal cells. Although T-type channels are also reported to be present in some, but not all, smooth muscle cells (Benham, et al., 1987; Nelson and Worley, 1989), L-type channels are the ones that have been extensively studied because the maintained arterial tone depends strongly on this channel and transient Ca^{2+} influxes are likely to play a minimal role in the steady state (Nelson, et al., 1990). The activity of the L-type VOCs can be modulated by different agonists (e.g. Bay K8644) and antagonists (e.g. nifedipine). Cell depolarization using high K^+ solution is the most commonly used pharmacological method for VOC study. Although Ca^{2+} release from intracellular stores is considered to contribute most of the $[Ca^{2+}]_i$ rise following an agonist stimulation, opening of VOCs by depolarizing cell membrane has also been observed (for review, see Nelson, et al., 1990). Three classes of L-type Ca^{2+} VOC blockers have been developed: the phenylalkylamines (e.g., verapamil), the dihydropyridines (e.g., nifedipine) and the benzothiazepines (e.g., diltiazem).

Receptor Operated Ca^{2+} Channels

ROCs have been suggested to exist in many cell types (Felder, et al., 1992; Llopis, et al., 1992; Osage, et al., 1989). By definition, binding of agonist to the receptor directly operates the opening and closing of the channel. These channels are proposed to be distinct form VOCs and their activities are independent of membrane potential. However, the presence of smooth muscle ROCs remains more putative and controversial. It seems that for each of the reasons indicating the presence of ROC in smooth muscle cells there is an alternative explanation (Nelson, et al., 1990). Also, the studies have been limited to the contractility studies and $^{45}Ca^{2+}$-influx experiments using intact tissues or the studies of Ca^{2+} current across membrane patches (Kwan, 1991). There are studies showed that a group of ginsenosides block

ROCs, and these drugs may represent a class of novel ROC antagonists (Guan, et al., 1988; and Kwan, et al., 1990).

Stretch Activated Ca^{2+} Channels

Since its discovery in cultured skeletal muscle cells in 1984 (Guharay and Sachs), mechanosensitive ion channels or stretch activated Ca^{2+} channels (SACs) have been identified in a variety of cell types. The opening of these channels depends on the stretching of the cell membrane. Such channels have also been demonstrated in both visceral (Kirber, et al., 1988) and vascular (Davis, et al., 1992) smooth muscle cells. The vascular smooth muscle SACs are not cation selective and their relative selectivities for cations are suggested as follows: $K^+ > Na^+ > Ba^{2+} > Ca^{2+}$ (Davis, et al., 1992). Their conductance for Ca^{2+} is apparently low at physiological Ca^{2+} concentration so that the Ca^{2+} entry through SACs may not be adequate to elicit a substantial contraction. However, due to the very high membrane impedance at rest ($>1\sim2G\Omega$), inward currents carried by Na^+ and Ca^{2+} through SACs ($\sim2.0pA$) could depolarize the cell sufficiently to open Ca^{2+} VOCs and lead to a contraction (Davis, et al., 1992; Benham, et al., 1987; and Matsuda, et al., 1991). An ion-selective SAC was reported to be found in rabbit mesenteric arterial smooth muscle cells which appears to be large conductance Ca^{2+} activated K^+ channels (Kirber, et al., 1992). Gadolinium (Gd^{3+}), a non-specific Ca^{2+} channel blocking trivalent cation, has been reported to block the SACs (Yang and Sachs, 1989).

Intracellular Ca^{2+} Release via Inositol 1,4,5-trisphosphate Sensitive Channels

IP_3, a cellular messenger generated upon receptor activation, causes release of Ca^{2+} from intracellular stores in many cells, including smooth muscle. It is generally accepted that both IP_3 and DAG are formed by the hydrolysis of an inositol lipid precursor stored in the plasma membrane - PIP_2. Although PLC is the identified enzyme catalyzing the reaction, two major distinct signaling pathways have been suggested: one initiated by a family of G-protein linked receptors and the other by receptors associated with tyrosine kinases (Berridge, 1993). Different PLC isoforms, respectively PLC_β and PLC_γ, are involved in these separate receptor mechanisms, and $PLC_{\beta 1}$ is the isoform most likely to be responsible for PIP_2 hydrolysis in vascular smooth muscle in response to α1-agonists (Lee and Severson, 1994). Meyer et al. (1990) proposed that IP_3 induced Ca^{2+} release depends on IP_3 binding sequentially to the its receptors on intracellular store. The kinetics of this release was examined *in vitro* using synaptosomes (Finch et al., 1990), according to his study the response is extremely fast, reaching a maximum within 140ms of adding IP_3. This finding is in agreement with that the transient increase in $[Ca^{2+}]_i$ following agonist stimulation is due to the Ca^{2+} release from intracellular stores. Heparin, which has been reported to be an antagonist to the IP_3 receptor in smooth muscle cells (Chadwick, et al., 1990), can be used as a tool to examine the role of Ca^{2+} release in agonist-induced responses.

Intracellular Ca^{2+} Release via Ryanodine Sensitive Channels and Calcium Induced Calcium Release

Ryanodine sensitive channels represent another principal intracellular Ca^{2+} channel responsible for mobilizing stored Ca^{2+} and as such may contribute to vascular smooth muscle contraction. Although the functions of ryanodine were not apparent until a few years ago, this plant alkaloid has been extensively studied due to its capability in releasing Ca^{2+} from intracellular stores. Three different ryanodine receptor genes have been identified in mammals and are designated as the skeletal, cardiac and brain ryanodine receptor genes or *ryr*-1, *ryr*-2 and *ryr*-3, respectively (McPherson and Campbel, 1993). While caffeine is another commonly used ryanodine receptor agonist, it also inhibits cyclic nucleotide phosphodiesterase which causes increases in cytosolic cAMP and cGMP and consequently leads to smooth muscle relaxation by lowering $[Ca^{2+}]_i$.

It is well known that calcium-induced calcium release (CICR), an influx of Ca^{2+} through the sarcolemma triggering the release of additional Ca^{2+} from SR, plays a very important role in cardiac muscle contraction. Recent studies from cultured smooth muscle cell line as well as skinned taenia caeci preparations indicated that this mechanism may also exist in smooth muscle (Blatter and Wier, 1992; Iino, 1989; Iino, 1990). Further, the CICR channels from smooth muscle cells show properties similar to those observed for skeletal and cardiac CICR channels: it can be activated by Ca^{2+}, ATP and caffeine and inhibited by Mg^{2+} (Himpens, et al., 1995). The channel can be locked in an open state by the plant alkaloid ryanodine.

Ca^{2+}-ATPase Pumps

Ca^{2+}-ATPase pumps belong to a class of transmembrane proteins that transduce the energy liberated by ATP hydrolysis into the transport of ions against a steep electrochemical gradient. While catalyzing this transport the enzyme cycles through two major conformations: one with high Ca^{2+} affinity and the other with low Ca^{2+} affinity. Ca^{2+}-ATPase Pumps are present in plasma membrane as well as in the membrane of intracellular stores, presumably the

SR or a subcompartment of it. They work in concert to maintain a low $[Ca^{2+}]_i$ and to bring $[Ca^{2+}]_i$ back to resting levels when stimuli are removed.

Two distinct families of Ca^{2+}-ATPase pumps have been found to exist in smooth muscle cells. These two types of pumps are encoded by multiple genes and their regulation for activation are also different (Raeymaekers and Wuytack, 1993). The plasma membrane Ca^{2+}-ATPase pump has a molecular weight of 130kD and is stimulated by CaM, while the SR Ca^{2+}-ATPase pump does not require CaM for activation and has a molecular weight of 105kD.

Phospholamban is a SR Ca^{2+}-ATPase regulatory protein. Although the phosphorylation of this protein has been associated with an increased SR Ca^{2+}-ATPase activity in cardiac muscle, its role in smooth muscle is not clear, because many other SR proteins are also phosphorylated (Raeymaekers and Jones, 1986). Recent insight into the role of cAMP- and cGMP-dependent protein kinases in smooth muscle relaxation has indicated that phospholamban could mediate some of their effects on smooth muscle relaxation. For example, Lincoln and Cornwell (1991, 1993) suggested that elevation of cAMP in smooth muscle lead to activation of both cAMP kinase and cGMP kinase, and activation of the latter leads to a reduction in $[Ca^{2+}]_i$. This $[Ca^{2+}]_i$ reduction may result from phospholamban phosphorylation, enhancing SR Ca^{2+}-ATPase activity, and from IP_3 receptor phosphorylation, inhibiting Ca^{2+} release.

Thapsigargin, a tumor promoter first found to transiently increase $[Ca^{2+}]_i$ without generating IP_3 in neuronal cells (Thastrup, et al., 1990), is identified to be a microsomal Ca^{2+}-ATPase inhibitor. It blocks the Ca^{2+} uptake by Ca^{2+}-ATPase and subsequently empties intracellular Ca^{2+} stores. Cyclopiazonic acid (CPA), an indole tetramic acid metabolite of *Aspergillus* and *Penicillium*, has also been shown to be a highly selective inhibitor of the Ca^{2+}-ATPase (Low, et al., 1992; Omote and Mizusawa, 1994). With the aid of these useful pharmacological agents, various studies on Ca^{2+} signaling can be performed by functionally removing intracellular Ca^{2+} stores.

Na^+-Ca^{2+} Exchangers

Sodium-Calcium (Na^+-Ca^{2+}) exchanger is a countertransport system that translocates Na^+ and Ca^{2+} across the plasma membrane. Under physiological conditions, with the driving force being electrochemical gradient of Na^+ across the membrane ($[Na^+]_i$ = 10mM, $[Na^+]_o$ = 140mM), it allows three Na^+ to enter the cell in exchange for one Ca^{2+}. This exchange system can also transport ions in opposite directions by manipulating the extracellular Na^+ concentrations during experiments. The activity of the Na^+-Ca^{2+} exchanger has been reported to be regulated by ions (for review, see Matlib 1991; O'Donnell and Owen, 1994). For example, inhibition of Na^+-K^+ pump, which increases the intracellular Na^+ concentration, will promote Na^+-Ca^{2+} exchange. However, there is no evidence to suggest a second messenger-dependent direct modification of the system. It has been hypothesized that a physiological role of Na^+-Ca^{2+} exchanger in vascular smooth muscle is reducing the amplitude and duration of Ca^{2+} signals induced by Ca^{2+} mobilizing hormones. For example, at a $[Ca^{2+}]_i$ of 400nM, the Na^+-Ca^{2+} exchanger is responsible for nearly half of the rate of Ca^{2+} removal from the cell, while the Ca^{2+}-ATPase is presumably responsible for the removal of the remaining Ca^{2+} at that concentration (Fay, et al., 1992).

Further, it was suggested that the Na^+-Ca^{2+} exchanger function is more important for long-term homeostasis of intracellular Ca^{2+} (O'Donnell and Owen, 1994).

Capacitative Calcium Entry and Superficial Buffer Barrier Hypothesis

A model for receptor-regulated Ca^{2+} entry, capacitative calcium entry, is proposed by Putney in 1986 and revised in 1990 (Putney, 1990). According to his model, Ca^{2+} content of an agonist- and IP_3-regulated intracellular pool regulates the permeability of the plasma membrane to Ca^{2+}. The essence of the hypothesis is that the depletion of an intracellular Ca^{2+} store by IP_3 somehow triggers the opening of a pathway for its replenishment from extracellular space. As long as IP_3 was present, the store would remain empty and Ca^{2+} entry across the plasma membrane, into the store and subsequently into the cytoplasm would continue. A postulation follows this model would be that the depletion of the intracellular store by any means will activate the same Ca^{2+} entry mechanism. Putney's model explains the observed phenomenon that, in non-excitable cells as well as in smooth muscle cells, agonist-induced Ca^{2+} mobilization was a response of transient release from intracellular stores followed by sustained activation of Ca^{2+} entry across plasma membrane (Bohr, 1973; Putney, 1978; Stolze and Schulz, 1980). This proposition was also supported by the study from Takemura, et al. (1989) using thapsigargin. They found, in parotid acinar cells, that this intracellular store Ca^{2+}-ATPase inhibitor caused a sustained increase in $[Ca^{2+}]_i$ in presence of extracellular Ca^{2+} and the addition of methacholine, an agonist that has been proved to release intracellular Ca^{2+} and increase Ca^{2+} influx (Takemura and Putney, 1989), failed to further increase the Ca^{2+} entry.

Although this model proposed a possible mechanism for the initiation of Ca^{2+} entry, it does not provide a strong enough argument regarding the pathway(s) for Ca^{2+} to enter the intracellular store from the extracellular space. Together with other findings the observations that Ca^{2+} entry is usually associated with an increase in $[Ca^{2+}]_i$ (Takemura and Putney, 1989) and existence of an efficient refilling system from cytosol (Kwan, et al., 1990) led to a skepticism regarding the concept of continuous direct filling of the store as initially proposed in the model. Recently, a soluble mediator (Ca^{2+} influx factor, CIF), which is released from intracellular organelles upon Ca^{2+} depletion, is found in a lymphocyte cell line (Randriamampita and Tsien, 1993). This messenger can cause Ca^{2+} influx when applied to several other cells and is presumably responsible for mediating the signal from intracellular Ca^{2+} stores to plasma membrane. The discovery of this novel cell messenger gave further support to Ca^{2+} capacitative entry hypothesis.

Based on studies of smooth muscle cells, van Breemen and Saida (1989) proposed another model for regulating Ca^{2+} entry - the superficial buffer barrier hypothesis. According to this model, peripheral or superficial SR, in addition to Ca^{2+} uptake and discharge during smooth muscle relaxation and contraction respectively, also functions as a superficial buffer barrier to Ca^{2+} entry from extracellular space into the cytoplasm: a) the superficial SR removes Ca^{2+} entering through sarcolemma before it can activate myofilaments; b) the state of the SR with respect to its permeability to Ca^{2+} and its rate of

Ca^{2+}-ATPase activity partly determines the steady state cellular Ca^{2+} concentration; and c) a variable Ca^{2+} gradient exists near the inner plasmalemmal surface, with Ca^{2+} activity increasing nearer that surface. The model was supported by and partially based on ultrastructural studies showing that a portion of the SR is located close to the inner surface of the sarcolemma to which it occasionally joins with via special junctions and the lumen of all SR network is probably contiguous (Somlyo and Franzini-Armstrong, 1985). Although the SR membrane comes close to sarcolemma, there is no evidence for any continuity between the extracellular space and the SR lumen.

According to this model, the superficial buffer barrier is likely to be an important mechanism for increasing the informational content of the Ca^{2+} signal in smooth muscle. In addition, it may be a safety factor in protecting small cells having a high surface:volume ratio against the relatively large unregulated Ca^{2+} leak (van Breemen et al., 1995).

Contractile Protein Isoforms and Their effects on Smooth Muscle Function

Actin, myosin and tropomyosin are usually considered the major contractile proteins and play the primary role in muscle contraction. While the same contractile proteins are found in striated and smooth muscles in general, different isoforms have been identified in different muscle types or within the same muscle type from different tissues. A number of studies have suggested that differences in muscle function reside, to a great extent, in the contractile protein isoform compositions (Aikawa, et al., 1993; Borrione, et al., 1989; Murphy, 1992; Murphy, et al., 1974; Owens, et al., 1986; Somlyo, 1993). Basic knowledge regarding actin, myosin and tropomyosin isoforms is given below to provide background information for the studies described in Chapter 3.

Actin is a cytoskeletal protein that constitutes the major part of the thin filament. Under low ionic conditions, purified actin exists as a single polypeptide chain of 42kD. This monomer is designated as G-actin because of its globular shape. In intact muscle, or under physiological conditions, G-actin polymerizes and form filamentous actin (F-actin). High-resolution electron microscopic studies reveal F-actin as two braid α-helical strands of globular actin monomers. Actin is such an extraordinarily highly conserved molecule that over 90% homology exists amongst the different isoforms and the difference between the four muscle-specific forms are only a few amino acids concentrated in the N-terminal end of the protein (Vandekerckhove and Weber, 1978). At least six actin isoforms have been found: α-skeletal, α-cardiac, α-smooth muscle (SM), γ-SM, β-nonmuscle (NM), and γ-NM, and the latter four isoforms are all found in smooth muscle cells. These actin isoforms are encoded by different genes (Chang, et al., 1984).

Studies on cellular contractile protein content have been performed among different porcine smooth muscle cells (Cohen and Murphy, 1978). While cellular myosin contents were found to be similar in each tissue (both arterial and nonarterial) tested, the contents of actin, tropomyosin and the calculated weight ratio of average actin:myosin in arterial tissues are significantly higher. In terms of actin and tropomyosin content, smooth muscles have been grouped into arterial smooth muscle and nonarterial smooth muscle (Murphy, 1992). Arterial smooth muscle appears to have about 30% more actin than the other type and this extra is the α-SM isoform (Cohen and Murphy, 1978; Fatigati and Murphy, 1984). However, no functional significance has been established regarding this finding. Fatigati and Murphy (1984) also showed that muscles that are normally relaxed (visceral tissues) primarily express γ-actin (presumably γ-SM) while muscles that are normally contracted contain greater amounts of α-SM actin. They also found that in cultured smooth muscle cells, α-SM actin content decreases with time while β-NM actin and γ-SM and NM isoforms increase. An increase in NM-actin isoform expression characterized the cell with a proliferative, synthetic and secretory phenotype while SM-isoforms are primarily expressed in non-dividing, contractile cells *in vivo*.

Myosin is the primary protein of the thick filament in smooth muscle and is a hexamer of two heavy chains and two sets of two light chains. Two smooth muscle myosin heavy chain (MHC) isoforms were identified by Rovner, Thompson and Murphy (1986) according to their migration rate in sodium dodecyl sulfate (SDS) polyacrylamide gel electrophoresis (PAGE). SM1 and SM2 were assigned to the heavier isoform (~204kD) and the faster migrating isoform (~200kD), respectively. Studies from Babij and Periasamy (1989) demonstrated that the isoform diversity is produced by alternative splicing of the same smooth muscle MHC gene which results in a 43 amino acid difference at the carboxyl terminal. This result gave support to the earlier finding by Eddinger and Murphy (1988) that the two smooth muscle MHCs differ in their light meromyosin. The SM1/SM2 ratios vary in different smooth muscles and appears to be a characteristic for smooth muscle tissues, i.e. it is reasonably constant for a particular tissue (Boels, et al., 1991; Mohammad and Sparrow, 1988; Rovner, Murphy and Owens, 1986). Smooth muscle MHCs can form either homodimers or heterodimers (Kelley, et al., 1992; Tsao and Eddinger, 1993). Non-muscle (NM) type MHCs are also found in smooth muscle cells (Eddinger and Wolf, 1993; Gaylinn, et al., 1989; Rovner, Murphy and Owens, 1986). These isoforms are encoded by different genes (Katsuragawa, et al., 1989) and are mapped to different chromosomes from the smooth muscle MHCs (Matsuoka, 1993). However, the localization and the function of the NM MHCs in smooth muscle cell is unknown.

The two 17 kD myosin light chains (MLC_{17a} and MLC_{17b}) found in smooth muscle have been identified to be the products of a single gene by alternative splicing (Nabeshima, et al., 1987). MLC_{17a} is the more acidic isoform and MLC_{17b} is the more basic one. The ATPase of myosin is lower in proportion to the relative expression of MLC_{17b} (Helper, et al., 1988) and the maximum shortening velocity estimated from zero load is inversely proportional to the relative amount of MLC_{17b} (Malmqvst and Arner, 1991). The regulatory smooth muscle light chain (MLC_{20}, 20kD) and nonmuscle light chain expressed in smooth muscle are highly conserved among species and there are no reports suggesting that isoform variants affect function (Somlyo, 1993).

Tropomyosin is another important protein of the thin filament. Tropomyosin molecules lie in the groove of actin helix and consist 284 amino acids (Clayton, et al., 1988). Tropomyosin is a dimer of two coiled-coil polypeptide chains with close to 100% α-helical content, binds end-to-end along actin and thereby imparts coopereativity to the regulation of contraction. Two subunit isoforms have been found in smooth muscle, the acidic isoform and the basic one. In addition to isoelectric points, their molecular weights are slightly different as well (Fatigati and Murphy, 1984). The subunit composition of tropomyosin remained in question although it has been known for sometime that smooth muscle tropomyosin contains about 50% of each isoform (Cummins and Perry, 1974). Reports from *in vitro* studies showed evidence both for homodimers (Graceffa, 1989) and for the heterodimer (Sanders, et al., 1986). More recently, Jancsó and Graceffa (1991), using anion-exchange chromatography and native gel electrophoresis techniques, demonstrated that the native protein is composed of more than 90% heterodimer. Although tropomyosin heterodimer composition predominates in several smooth muscle types, its functional significance is not clear.

Previous Knowledge on Myogenic Reactivity

A general introduction to myogenic phenomenon and its physiological importance, smooth muscle contraction and contractile proteins in smooth muscles has been provided in the previous parts of the chapter. Although smooth muscle studies have made many breakthroughs during the past decades, many gaps still remain in our understanding of myogenic reactivity. For example, little is known about the cellular basis for this phenomenon regarding what is sensed, what is controlled, what are the involved signal transduction pathways and how they contribute to this vasoregulatory event. The following section will summarize previous studies related to arteriolar myogenic response.

Wall Tension as the Sensing Parameter?

A tension sensor has been suggested as the mechanosensor involved in arteriolar myogenic reactivity (Johnson, 1980). According to this hypothesis, it is the increase in wall tension, not pressure, that induces vessel constriction. This constriction leads to a reduction in wall tension (according to Laplace relationship) and thereby inhibits any further constriction.

The apparent effect of this negative feedback system is that vessel diameter is regulated against changes in transmural pressure. The pressure- or stretch-increased smooth muscle sensitivity to agonist stimulation (Meininger and Faber, 1991; Lombard, et al., 1990) can also be explained by the increase of tension. A recent study from VanBavel and Mulvany (1994), using rat mesenteric artery, gave more support to this proposal. With an automatic feedback adjustment system, they were able to test the arterial responsiveness to agonists under isometric as well as isobaric conditions. They found that isometric vessels were significantly more sensitive to norepinephrine and vasopresin than isobaric vessels. Similar results were reported by Bevan and colleagues (Dunn, et al., 1994) in isolated rabbit mesenteric vessels. However, how the vessel wall tension is sensed and how the signal is converted to smooth muscle contraction is unknown.

Endothelial Modulation of Myogenic Reactivity

It is now generally agreed that myogenic reactivity is a characteristic of the smooth muscle cells (Meininger and Davis, 1992). Although some studies suggest endothelial cells play a crucial role in arteriolar myogenic response (Harder, 1987; Katusic, et al., 1987; Rubanyi, 1988), the particular experimental conditions and protocols involved in these studies might not be physiological. For example, removal of endothelium with enzymes such as elastase and collagenase appears to damage the underlying vascular smooth muscle cells. Further, Liu et al. (1994) showed that even a nonchemical method for endothelium removal, air perfusion, can still damage dog kidney arteries and hence impair myogenic responsiveness, providing more evidence for the idea that inhibition of myogenic reactivity is due to the damage of smooth muscle cells rather than loss of endothelium. Convincing evidence has been accumulated showing that an intact endothelium is not required for normal myogenic reactivity of the vessel and that the removal of the endothelial layer does not change basal tone and myogenic responsiveness (Bulow and Nilsson, 1991; Falcone, et al., 1991; MacPherson, et al., 1991; McCarron, et al., 1989). However, the endothelium may indeed play a possible role in modulating myogenic reactivity (for review see Kuo, et al., 1992). For example, in response to shear stress caused by blood flow, endothelial cells may release vasoactive compounds such as substance P, EDRF (Endothelium Derived Relaxation Factor, now identified to be nitric oxide) or prostaglandins, which modulate guanylate or adenylate cyclase activity in vascular smooth muscle. Also noticed was that most of the studies suggesting that endothelium play a crucial role came from those performed on cerebral arteries. It is possible that the control of blood flow or capillary pressure is more efficient and essential in brain and that it requires the involvement of both endothelial and smooth muscle cells. Another possible explanation to the discrepancy regarding the role of endothelium would be species or tissue specific differences.

Proposed Mechanisms for Myogenic Reactivity

It is well known that in isolated arterial/arteriolar preparations removal of extracellular Ca^{2+} will eliminate myogenic responsiveness (Harder, et al., 1987; Jackson and Duling, 1989). Davis, Meininger and Zawieja (1992) demonstrated that stretching of the isolated pig coronary arterial smooth muscle cells results in an increase in Ca^{2+} influx which occurs in part via a nifedipine-resistant pathway. This pathway has been identified to be a SAC (Davis, Donovitz and Hood, 1992), hence suggesting that stretch activated Ca^{2+} influx may, in part, account for pressure-induced activation of intact blood vessels.

Membrane depolarization has been observed in isolated dog renal artery and cat cerebral artery preparations (Harder, 1984; Harder, et al., 1987) as well as in ferret trachealis smooth muscle (Coburn, 1987). Also, VOCs are considered to be implicated in calcium entry during arteriolar myogenic reactions (Harder, et al., 1987, Hill and Meininger, 1994). Using rabbit facial vein, which demonstrates stretch-induced as well as temperature-sensitive tone, Laher and Bevan (1989) found that the stretch-induced smooth muscle tone is associated with increases in Ca^{2+} influx, $[Ca^{2+}]_i$, and MLC phosphorylation. However, none of these parameters were further increased while this stretch activated tone was potentiated by PKC, hence, indicating an increasing sensitivity in contractile apparatus to Ca^{2+} following PKC activation (Laporte, et al., 1993). The idea of PKC involvement in arteriolar myogenic reactivity has been reported by several investigators. For example, Hill et al. (1990), using both *in vivo* and *in vitro* preparations of rat cremaster arterioles, demonstrated that inhibitors of PKC attenuated the myogenic response to pressure increase while a PKC activator, indolactam, enhanced it.

Ca^{2+} release from intracellular stores has been reported following a mechanical stretching on porcine coronary arterial smooth muscle (Tanaka, et al., 1993 and 1994). This stretch induced Ca^{2+} release is believed to be mediated by IP_3. Evidence supporting this idea also comes from studies demonstrating that stretch can activate PLC activity in vascular smooth muscles (Matsumoto, et al., 1995; Osol, et al., 1993). It is reported that PLC activity is significantly increased in rabbit aortic muscle within 200-300 ms post-stretch and Ca^{2+} influx via gadolinium-sensitive ion channels is involved in this PLC activation (Matsumoto, et al., 1995). Increased PLC activity has also been noticed during pressurization in isolated renal arteries (Narayanan, et al., 1994). However, the studies of Matsumoto were performed on conduit vessels which do not typically contract to increases in intraluminal pressure while the results from Narayanan et al. were acquired 15 minutes after the pressure increase, a time point that would be expected to reflect only steady state conditions.

Increases in MLC phosphorylation have been reported after a mechanical stretch of arterial and non-vascular smooth muscles (Barany, et al., 1990; Csabina, et al., 1986), indicating an activation of MLCK following stretch. However, the experimental approaches in their studies, e.g. stretching of the smooth muscle strips to about 1.7 times their resting lengths, were not physiological stimulations and therefore, the results may not reflect an *in vivo* situation.

Based on the known knowledge, possible cellular mechanisms involved in the vascular myogenic response were proposed by Meininger and Davis (1992). According to their suggested scheme of events, stretch of vascular smooth muscle acts principally at the cell membrane to alter ion conductance and perhaps initiate hydrolysis of membrane phospholipids. While the stretch induced breakdown of membrane phospholipids may produce sufficient IP_3 to release Ca^{2+} from intracellular stores, the change in membrane ion conductance increases influx of Na^+ and Ca^{2+} through SACs. This influx of cations results in membrane depolarization which in turn activate Ca^{2+} VOCs augmenting Ca^{2+} influx. Ca^{2+} entered through SACs could directly initiate contraction or act to trigger Ca^{2+} release from internal stores. The increased $[Ca^{2+}]_i$ then is assumed to activate MLCK which leads to contraction. Concomitant activation of PKC, through DAG generated by phospholipid hydrolysis, is hypothesized to initiate a Ca^{2+} sensitizing mechanism.

Aims of the study

The background material provided in the previous section gives a brief overview of arteriolar myogenic responsiveness, including its role in local microvascular blood flow autoregulation, and mechanisms underlying vascular smooth muscle contraction. However, it is apparent that comparatively little is certain as to the actual intracellular biochemical pathways which lead to the generation of basal microvascular tone and the ability to adjust arteriolar diameter appropriately in response to changes in intraluminal pressure. Thus a major goal of the studies described in this thesis is to extend our mechanistic knowledge of vascular smooth muscle contraction to the level of the microvasculature. Such studies are of direct physiologic significance as the microvasculature represents a major site for the control of peripheral vascular resistance and the control of local blood flow and pressure. Further, the data are required for our full understanding of pathophysiologic states affecting the microcirculation, such as hypertension and diabetic microangiopathy, and may provide potential avenues for development of rationale pharmacological intervention.

As can be appreciated from the background section above contraction of vascular smooth muscle is a complex process with some uncertainty as to the exact cellular and molecular mechanisms which give rise to contraction. Variation in functional properties of smooth muscle cells in different tissues may result from a number of factors including differences in either 1) the structural composition of proteins participating in the contractile process; or 2) the underlying signaling pathways. These two alternatives represent both a long-term (through structural composition) and a rapid (short-term generation of signaling molecules) mechanism for regulating arteriolar smooth muscle contractile function. To date, few studies have been performed on arteriolar smooth muscle cells regarding the contractile protein composition aspect. Our knowledge of contractile protein isoform expression and mechanisms for smooth muscle contraction is largely derived from studies of conduit vessels and non-vascular smooth muscles. Further, whether the generally accepted or "textbook" mechanism for smooth muscle contraction - Ca^{2+}/CaM activated MLC phosphorylation - is an obligatory requirement for the generation of arteriolar tone and myogenic reactivity is not known. Therefore, the specific aims of this study were to test the hypotheses that:

1. *Contractile protein isoforms vary between vessels of different sizes with the contractile isoforms exist more abundant in more active vessels.* These studies are described in Chapter 3 and, in addition to describing contractile protein isoforms in small arterial vessels, they provided the basis for establishing electrophoretic techniques for measurement of arteriolar myosin light chain phosphorylation which was used in subsequent sections.

2. *Pressure-dependent steady-state arteriolar myogenic tone is dependent on* $[Ca^{2+}]_i$ *and MLC phosphorylation:* These studies detailed in Chapter 4 were conducted to establish whether arteriolar tone is dependent on the generally accepted mechanism for smooth muscle contraction, i.e. Ca^{2+}/CaM/MLCK mediated phosphorylation of the myosin regulatory light chain. This data was required before considering the possibility of an

obligatory involvement of non-classical contractile mechanisms (e.g. involvement of protein kinase C) or examining temporal aspects of the Ca^{2+}/phosphorylation signaling pathway.

3. *The myogenic contraction to an acute pressure increase is* $[Ca^{2+}]_i$ *and MLC phosphorylation dependent and that the temporal changes in these parameters will exhibit a distinct pattern compared to that occurring during an agonist-induced contraction.* These studies described in Chapter 5 were designed to extend the steady-state data and, in particular, examine whether there was apparent dissociation between the diameter response and Ca^{2+}/MLC phosphorylation levels during the time course of the contraction. Comparisons with the response to the α_1-adrenergic agonist, norepinephrine, were included as a larger database exists in the literature for agonist-induced smooth muscle activation than for activation in response to mechanical stimuli.

4. *The* Ca^{2+} *requirements for basal arteriolar tone and acute myogenic reactivity are met through a combination of* Ca^{2+} *entry from the extracellular environment, release from intracellular stores and* Ca^{2+} *sensitization processes.* These studies described in Chapter 6 were performed to address the question of the source of activator Ca^{2+} (e.g. extracellular compared with sarcoplasmic reticulum) that is required for basal tone and acute myogenic responses. As in the previous chapter comparisons were made between the pressure-induced response and that occurring after exposure to norepinephrine to facilitate interpretation of the data in context of the available literature. Further, the use of pharmacological agents such as L-type Ca^{2+} channel blocker (verapamil) and compounds

acting on the sarcoplasmic reticulum (caffeine, ryanodine) was exploited to manipulate the Ca^{2+} supply.

While the studies relating to these aims are described in individual chapters an overall discussion is provided in Chapter 7 to address the general question of regulation of arteriolar tone and myogenic reactivity via mechanisms involving intracellular Ca^{2+} and contractile protein modification.

CHAPTER II

MATERIALS AND METHODS

The general methods used in the studies are described below. Specific methods and protocols are included in the individual chapters.

Animal Preparation

Studies used male Sprague-Dawley rats between 6-9 weeks of age, weighing 200~350 grams. Rats were housed in a temperature and humidity controlled facility with a 12 hour light/dark cycle. Before use in experiments rats were allowed free access to a standard rat chow diet and drinking water. Use of animals was approved by the Animal Care Use Committee at Eastern Virginia Medical School.

Prior to vessel isolation, rats were anesthetized with sodium thiopental (Pentothal, 20mg/100g body weight) administrated by a single intramuscular injection on the outer hind leg. If a surgical plane of anesthesia was not reached, a second supplementary dose of anesthetic [subcutaneous injection of ~0.1ml of the drug (100mg/ml in saline)] was administered.

Preparation of tissues and cannulating glass micropipette

Small mesenteric arteries and cremaster muscle first order arterioles were used in the described studies. While cremaster arterioles have been used in earlier studies by the mentor (Hill, et al., 1990; Hill and Meininger, 1994) and showed strong myogenic reactivity, mesenteric arteries were chosen due to their size, ease of accessibility and that electrophoretic separations can be performed on single vessel segments. It is important to note that cannulated small mesenteric arteries are also capable of exhibiting spontaneous tone and myogenic reactivity. Figure 2-1 shows illustrations of rat mesenteric and cremaster vascular beds with arteries and arterioles labeled.

Cremaster arterioles Anesthetized rats were placed on a plastic dissecting board and held in position with tapes. Cremaster muscles were removed in the anesthetized state (as compared to post mortem for mesenteric vessels) to ensure that the vessels contained a blood column which facilitates visualization of the vessels for dissection. Cremaster muscle(s) was opened and separated from skin by gently pulling off the connective tissues with tweezers. Then the muscle(s) was removed by disrupting the connective tissue fascia, which joins the cremaster muscle to the epididymis and testis, and transferred to a dissection chamber containing a cold (<4°C) buffer solution [3mM 3-(N-morpholino)-propane-sulfonic acid (MOPS), 145mM NaCl, 5mM KCl, 2mM $CaCl_2.2H_2O$, 1.2mM $MgSO_4.7H_2O$, 1.4mM NaH_2PO_4, 0.02mM EDTA, 2mM pyruvate, 5mM glucose and 1% albumin]. The cremaster muscle was allowed to equilibrate in the chamber for 15-20 minutes before starting arteriole dissection.

Small mesenteric arteries Immediately before opening the abdomen, rats were killed by cervical dislocation. This is to prevent over-bleeding when dissecting out mesentery. Through an abdominal cut, rat mesentery was spread over saline (0.9% NaCl solution) wet gauze pads and kept moist with cold saline. Part of the mesentery was removed by carefully cutting along the small intestine (the 4th order arteries run parallel along the intestinal wall while the 5th

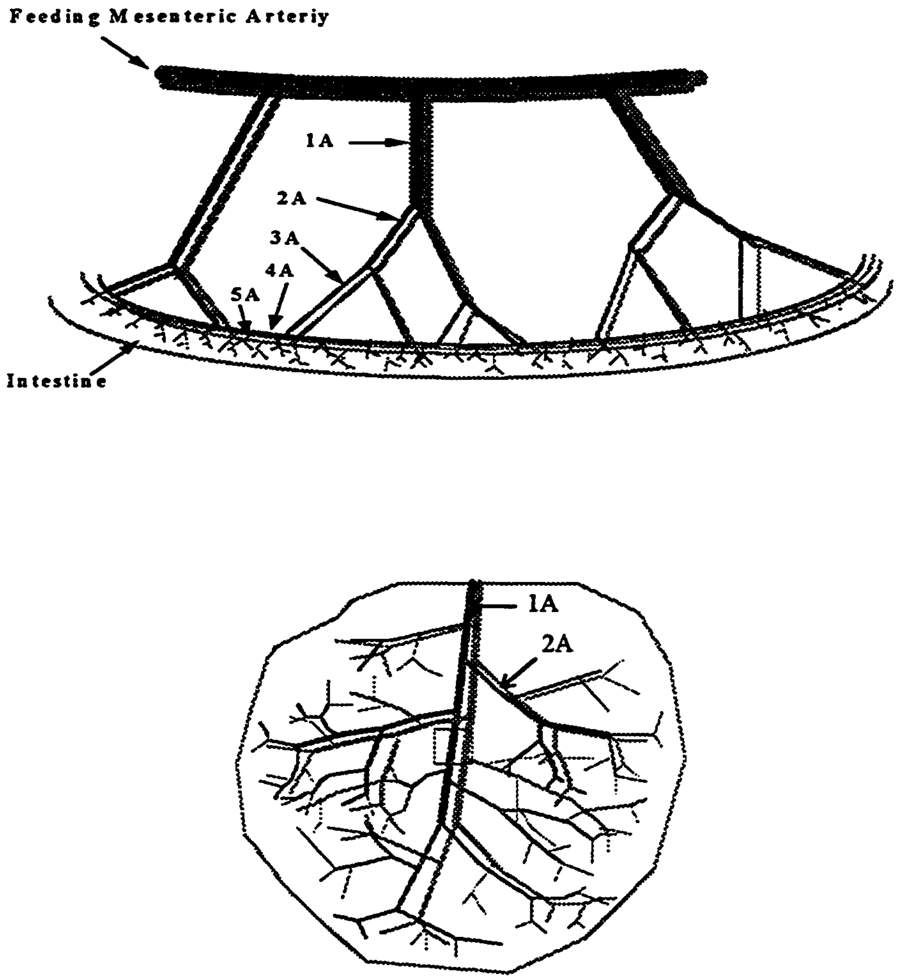
Feeding Mesenteric Arteriy
1A
2A
3A
4A
5A
Intestine
1A
2A

Figure 2-1. Illustration of rat mesenteric (top) and cremaster (bottom) vascular bed. The rectangular frame on the cremaster muscle indicates where the vessel segment is usually taken from.

order vessels typically penetrate the gut wall). Then the mesentery was transferred to the dissecting chamber and equilibrated for 15-20 minutes as was done for cremaster muscle.

Cannulating pipette preparation Glass tubes (o.d. 0.047", i.d. 0.040", Drummond Scientific Company, PA.) were first pulled with a Sachs Flaming Micropipette Puller (Model PC-84, Sutter Instrument, CA) to form a tapering tip. Then the tip was shaped and polished with the use of a microforge manipulator (Stoelting Co.) to the final form.

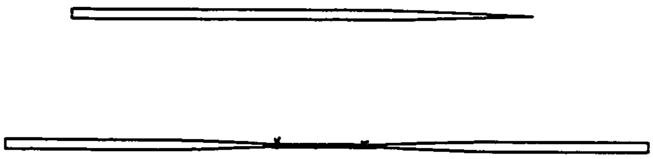

Figure 2-2. Illustration of glass micropipette (top) and a cannulated vessel (bottom).

Isolation and Cannulation of Single Arterioles

Dissection was performed with the aid of a dissecting microscope (Olympus, Japan). The chamber was illuminated with a Fiber-LiteR high intensity illuminator (model 180, Dolan Jenner Industries Co.). To prevent tissue from moving during the dissection, cremaster muscle or mesentery was pinned onto the silicon layer covering the bottom of the chamber with #27 needles. The silicon layer was made from a 184 Silicone Elastomer Kit (Dow Corning Corp., MI). Vessels were cleared from surrounding tissues using ultrafine microsurgical instruments (Fine Science Tools, Inc., CA). Arteriole segments were then cannulated, secured with 10-0 nylon suture (Alcon Surgical Inc. TX), onto glass micropipettes and mounted in a custom designed microperfusion system as shown in figures 2-2 and 2-3. The perfusion system was then transferred to the stage of a Nikon Diaphot microscope coupled to a high resolution video system comprising of a CCD camera, a video recorder, a time/date generator, and a display monitor. Vessels were gradually warmed to 34-35°C for cremaster arteriole, and 36-37°C for mesenteric arteries, and allowed to develop spontaneous tone while slowly pressurized to a level expected in vivo (70mmHg for cremaster first order arteriole and 90mmHg for small mesenteric arteries). During experiments vessels were superfused with Krebs Ringer bicarbonate buffer solution [111mM NaCl, 25.7mM $NaHCO_3$, 4.9mM KCl, 2.5mM $CaCl_2$, 1.2mM $MgSO_4$, 1.2mM KH_2PO_4, 11.5mM Glucose, and 10mM N-2-hydroxyethylpiperazine-N'-2-ethane-sulfonic acid (HEPES)] maintained at physiologic conditions with respect to temperature, pH, pO_2 and pCO_2. To be considered viable and suitable for study, arterioles needed to exhibit spontaneous tone, myogenic responsiveness and be free of pressure leaks.

Method for studying Myogenic and Agonist Responses in Isolated Arterioles

Intraluminal pressure in the isolated arteriolar segment was controlled by adjusting the height of a fluid reservoir which was connected via polyethylene tubling to one of the cannulating pipettes. All experiments were performed in the absence of intraluminal flow to enable responses to transmural pressure to be studied without shearing forces. To quantitate the response of an arteriole to a given change in transmural pressure or to agonist

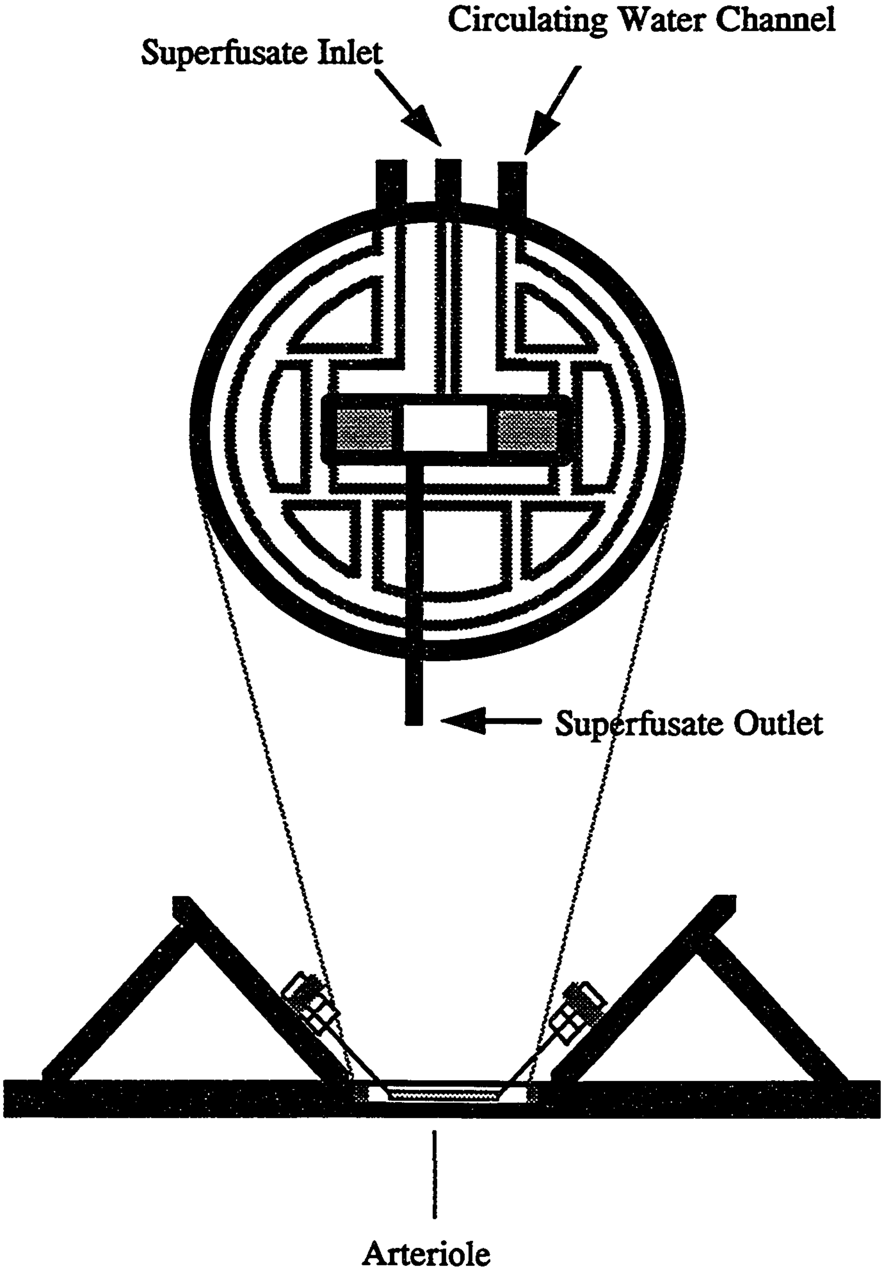
Circulating Water Channel
Superfusate Inlet
Superfusate Outlet
Arteriole

Figure 2-3. Illustrations of vessel cannulation and cannulating chamber.

stimulations, vessel lumen diameter was measured directly on the video monitor using a calibrated electronic caliper (Made by the Microcirculation Research Institute, Texas A&M University, TX). Experiments were videotaped for subsequent analysis when necessary.

Intracellular Ca^{2+} Measurement with Fura-2 in Isolated Arterioles

Due to the privotal importance of Ca^{2+} in cellular signal transduction, many techniques have been developed to measure the $[Ca^{2+}]_i$, among them is the fluorescent indicators. Fura-2 is currently the most popular Ca^{2+} indicator for microscopic studies. Upon Ca^{2+} binding,, its excitation spectrum shifts approximately 30nm towards shorter wavelengths while the green emission from fura-2 maintains its peak at 505-520nm. A diagram showing the excitation spectrum of fura-2 is given in figure 2-4. Therefore, the ratio of fluorescence emission intensities obtained from 340/380nm excitation pair provides a measure of $[Ca^{2+}]_i$ which is generally unaffected by variable dye content or cell thickness (Tsien, 1989). Fluorescent emission does not change with Ca^{2+} binding when excited at 360nm.

The acetomethoxy ester form of fura-2 (fura-2 AM, 50µg/vial, Molecular Probes, OR) was dissolved in DMSO (50µl, final concentration 0.5%) and then diluted in Krebs bicarbonate buffer (10 ml) containing 0.01% Pluronic F-127 (1 mg, Molecular Probes, OR) to facilitate dispersion and loading of the dye. The cell-permeant AM ester passively crosses the plasma membrane, and once inside the cell, is cleaved to a cell-impermeant product by intracellular esterases. Pluronic also helps to prevent the compartmentalization of fura-2 (information sheet on AM esters, Molecular Probes, Inc.). Arterioles were loaded with 5µM fura-2, applied to the exterior of the vessel, for 60 minutes at room temperature. Lowering the loading temperature

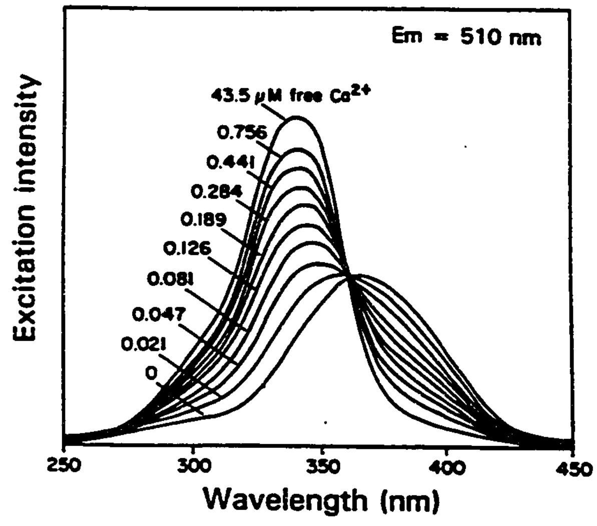

Figure 2-4. Excitation spectra of fura-2.

was to reduce the possibility for compartmentalization of fura-2 . Under these conditions, abluminal application of fura-2 has been shown previously (Meininger, et al., 1991) to restrict loading to the smooth muscle layer without substantial access to the endothelium. Loading was followed by an extensive washout, 30 minutes, using Krebs bicarbonate solution. Excitation was provided by a 75W Xenon light source directed through a quartz collector lens then passing through either a 340nm or a 380nm (or 360nm when doing Mn^{2+} quench experiments) filter; excitation wavelength was controlled by a computer driven wheel (Metaltek Instruments, NC) positioned between the light source and the microscope. A dichroic mirror reflected the excitation wavelengths through an appropriate fluorescence objective (Fluor 20X, Nikon) to the vessel segment. Fluorescence emission from the sample was passed through a bandpass filter to an intensifier (Videoscope International, Ltd.) and a CCD camera (Hamamatsu, Japan). Fluorescence intensities of the 340nm and 380nm excitation images in addition to the 340/380nm ratio were quantitated using a fluorescence image analysis system (Image 1 /FL, Universal Imaging Corp. PA). Figure 2-5 shows a schematic diagram of the computerized Ca^{2+} measurement system used in the study. A background image was taken after the system was set up in each experiment and experimental data was obtained by subtracting the background from acquired images. For each collection time point, 8 frames of images were averaged for each excitation wavelength. The microscope was focused on the outer sections of the vessel wall to maximize the contribution of the vascular smooth muscle while further minimizing any contribution from the endothelium. Previous studies from Meininger, et al. (1991) indicated that de-endothelialization of fura-2 loaded arterioles did not result in a significant alteration in Ca^{2+} related fluorescence.

Vessel diameter can also be measured from the fluorescence images using the pixel count of a region, that covers the entire vessel diameter, as an index. This measurement is illustrated in figure 2-6: as the vessel diameter changes the pixel count of the region changes accordingly. The effect of region height is canceled out when the results are expressed as relative change. Therefore, the pixel count changes, when presented as percent of basal, reflect the relative changes in vessel diameter. This function of the image system provides a practical way for simultaneous diameter measurement especially during experiments when rapid responses, such as those to NE stimulation, are expected. This method has been reported in studies by other investigators (Meininger, et al., 1991).

Figure 2-5. Schematic diagram of the Ca^{2+} measurement system.

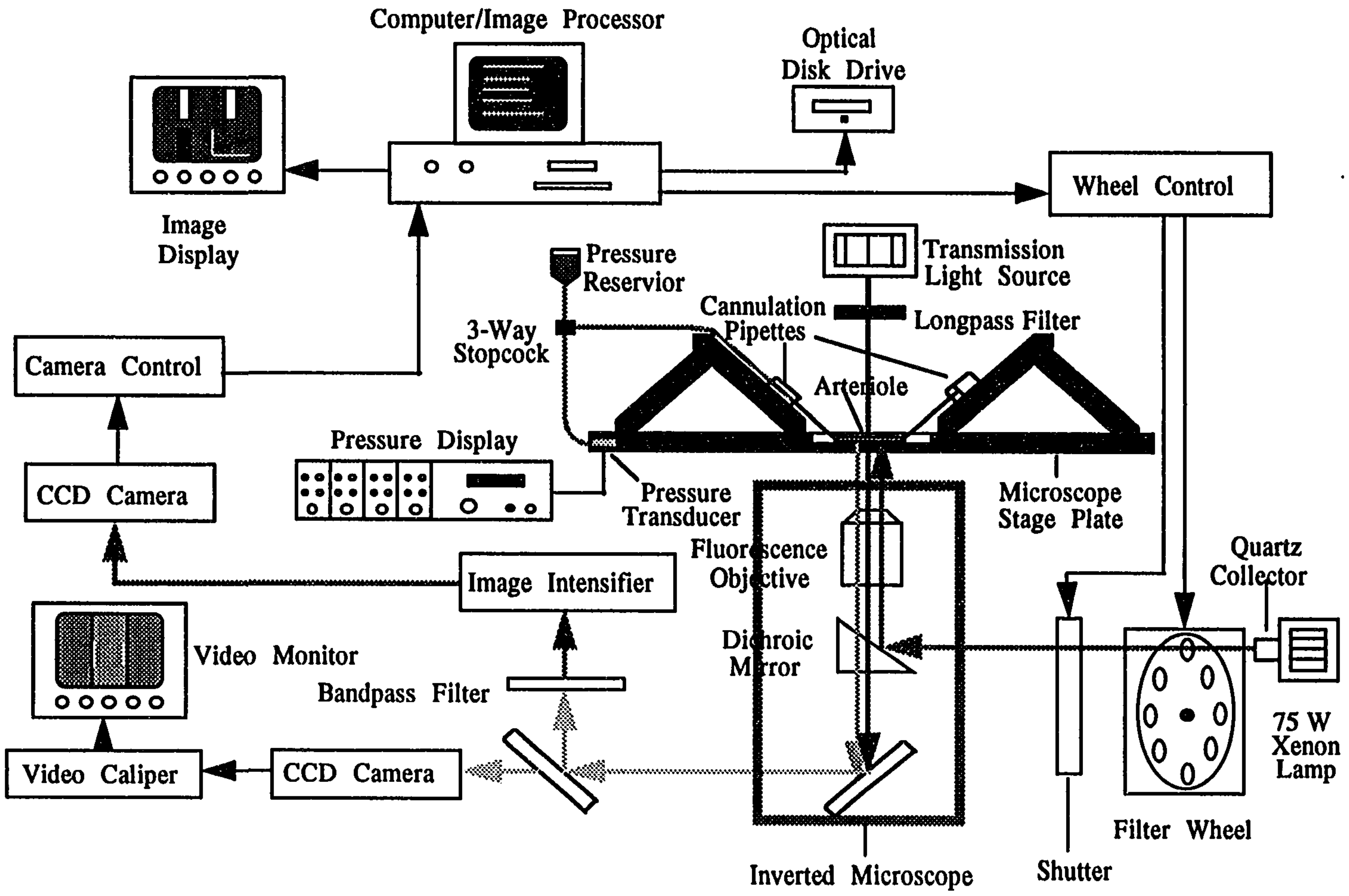
Computer/Image Processor
Optical Disk Drive
Wheel Control
Image Display
Pressure Reservior
Transmission Light Source
Cannulation Pipettes
Longpass Filter
3-Way Stopcock
Camera Control
Arteriole
Pressure Display
Pressure Transducer
Microscope Stage Plate
CCD Camera
Fluorescence Objective
Quartz Collector
Image Intensifier
Dichroic Mirror
Video Monitor
Bandpass Filter
75 W Xenon Lamp
Video Caliper
CCD Camera
Filter Wheel
Inverted Microscope
Shutter

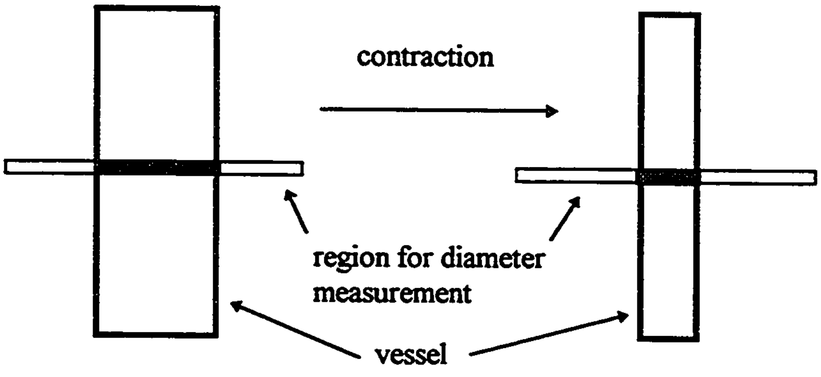

Figure 2-6. Measurement of vessel diameter using pixel count as an index. As shown in the figure, only the shaded area in the region is counted and therefore it provide an indication of changes in vessel outer diameter.

To enable continual viewing of the vessel segment, while periodically taking Ca^{2+} measurements, a transillumination (>600nm) light source coupled to a separate CCD camera and video monitor was used. This procedure did not interfere with the fluorescence measurements.

Calibration of the Ca^{2+} measurement system

While Ca^{2+} data was generally considered in terms of change in the fluorescence ratio ($R_{340/380nm}$), in situ calibrations were also performed.

R_{min} was determined by exposing the vessel segments to 2mM EGTA in Krebs buffer containing 0mM Ca^{2+}. The fluorescence emission was monitored every two minutes following the buffer change until $R_{340/380nm}$ stabilized, and that value was taken as R_{min}.

R_{max} was determined by exposing preparations to 4-bromo-calcium ionophore-A23187 (15µM, Sigma, MO) or ionomycin (14µM, Calbiochem. CA) in normal Krebs buffer containing 2.5mM Ca^{2+}. The peak value observed during the following measurement was taken as R_{max}. It was noticed that the Ca^{2+} rise was rapid and transient.

These values were used in the equation formulated by Grynkiewicz et al. (1985):

$$[Ca^{2+}]_i = K_d * (R-R_{min})/(R_{max}-R) * b \qquad (2\text{-}1)$$

where R is the measured ratio of 340/380nm; b is the ratio of the fluorescence intensity at 380nm in 0mM Ca^{2+} to that in 2.5mM Ca^{2+}; K_d, the dissociation constant, was assumed to be 224.0nM in our situation. The measured values, with calibration using 15µM bromo-A23187, used in the calibration equation were $R_{min} = 0.27$, $R_{max} = 2.02$ and $b = 0.92$.

To assure the precision measurement of $[Ca^{2+}]_i$, the absorption spectra of the optical filters used in the experiments (340nm, 360nm, and 380nm) were checked (Figure 2-7). The shift of 360nm filter spectrum towards shorter wavelength may account for the fluorescence intensity increase detected with the filter during the Mn^{2+} quench experiments.

Preparation of Samples for Electrophoretic Protein Separation

For samples that were used to measure protein isoform expression, the vessel segments were transferred to appropriate sample buffers immediately after dissection. Mesenteric tissues and samples of conduit vessels were usually ground using glass microhomogenizer (Wheaton, NJ). 2-D samples were kept cold, in ice/water mixture, while grinding because excessive heat will cause urea to covalently modify proteins producing erroneous charge modifications. For

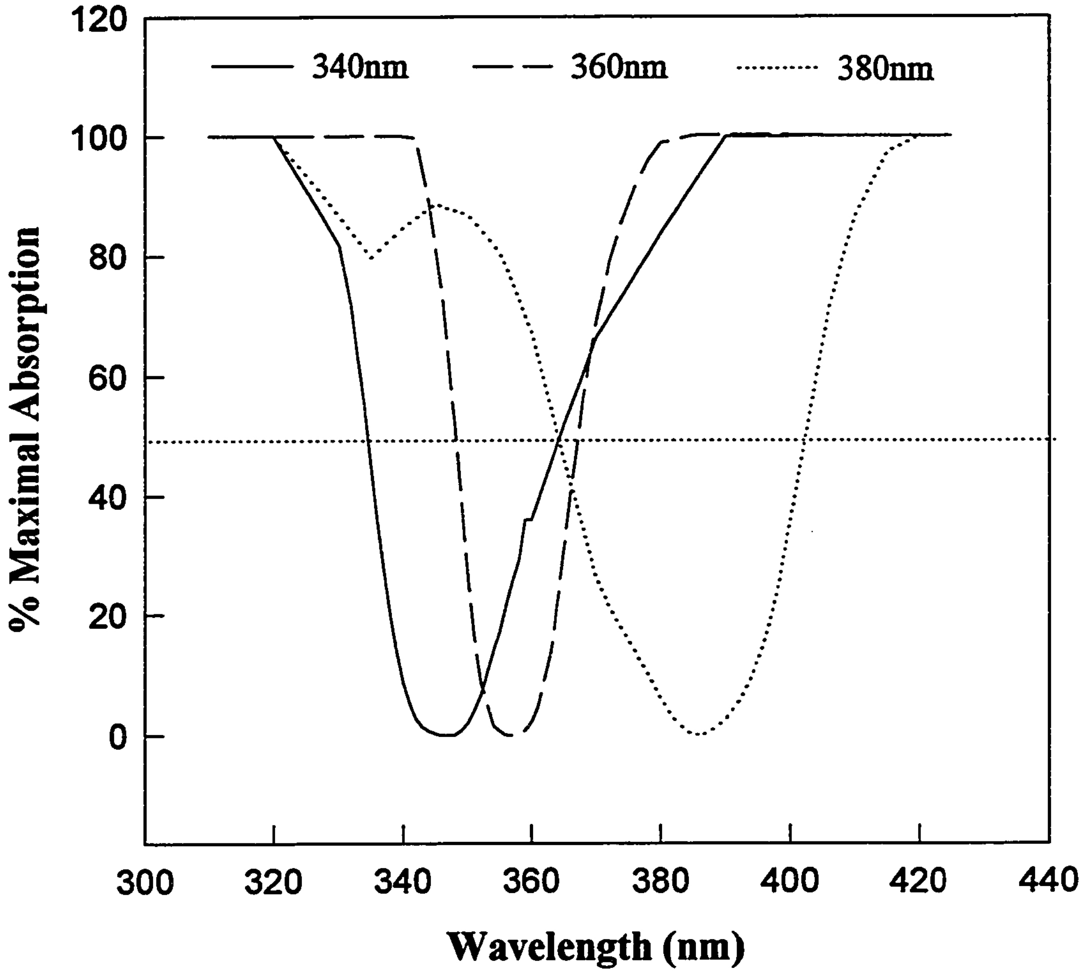

Figure 2-7. Absorption spectra of the optical filters.

the same reason, homogenization time had been limited to less than one minute when possible. 1-D samples (for separation of myosin heavy chain isoforms) were then heated in boiling water for 10 minutes to facilitate protein denaturation. Control experiments were also done without heating the sample, and it appeared that this step may be omitted.

In several studies, samples of possible contaminating tissues (adipocytes, red cells, plasma) were collected and similarly prepared for electrophoresis. Platelet homogenates were prepared from whole rat blood to provide a tissue sample expected to contain only non-muscle forms of myosin heavy chain and as such was used as a control. To assess the possible contribution of endothelial cells, actin and myosin heavy chain isoforms were also examined in vessels from which the endothelium had been removed. Endothelial removal was accomplished by introducing a glass micropipette into the vessel and physically abrading the luminal surface (Kuo, et al., 1990), after which the lumen was flushed with fresh buffer. Vessels prepared in such a manner 1) do not exhibit functional endothelium-dependent vasomotor responses and 2) have been shown histologically to be lacking an intact endothelial cell layer.

Collection of samples for myosin light chain phosphorylation measurements required more extensive preparation. After the initial set up, as described in previous sections, the arteriolar segments were treated according to the experimental protocols. At the appropriate time point, they were lifted above the superfusate by quickly turning the knob on the custom made chamber (refer to figure 2-8 for chamber structure), frozen with a pair of acetone/dry ice cooled tongs and transferred immediately to the acetone/dry ice slurry. This procedure promptly stops enzymatic reactions in the vessel and the subsequent measurement reflects the

Figure 2-8. Illustration of the cannulating chamber for vessel sample collection.

Top View of the Cannulation Chamber

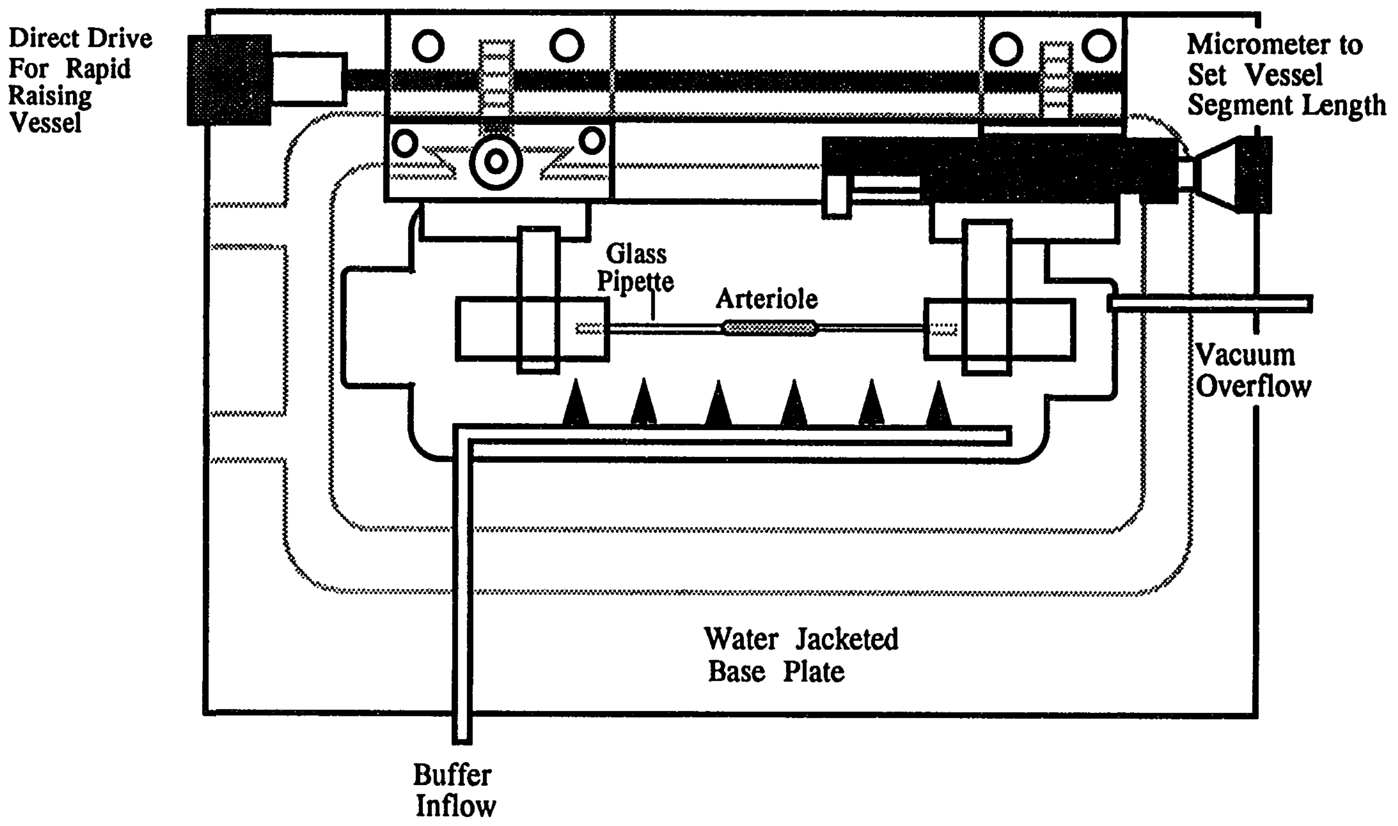
Direct Drive
For Rapid
Raising
Vessel
Micrometer to
Set Vessel
Segment Length
Glass
Pipette
Arteriole
Vacuum
Overflow
Water Jacketed
Base Plate
Buffer
Inflow

situation when the vessel was frozen (Aksoy, et al., 1983). As the vessel was slowly warmed up to room temperature, acetone replaced the water in the vessel and the dehydration maintains enzymes in an inactive state. The end portions of the vessel, distal to the ties, were eliminated from the sample as they were considered damaged during cannulation and would potentially interfere with the measurements. Then the vessel was transferred to an homogenizing buffer and subjected to sonication (Branson ultrasonic cleaner, Branson Cleaning Equipment Co., CT) for 10 minutes to extract proteins. Usually, 2-3 vessel segments (approximately 1cm in total length) were needed to provide sufficient tissue for one measurement.

Vessel samples were homogenized in buffer appropriate to the electrophoretic techniques being used: samples to be used for two dimensional (2-D) gel electrophoresis were homogenized in a solution containing 8M urea, 20mM dithiothrietol (DTT), and 2% Triton X-100 (Pierce, IL); samples for separation of myosin heavy chains using 1-D gel were homogenized in 1% SDS, 15% glycerol, 62.5% Tris-base, 15mM dithiothrietol and 0.01% bromophenol blue (P. H. Ratz, personal communication).

Protease inhibitors were not routinely included in the homogenization buffers as it has been shown that rapid homogenization in such buffers is sufficient to prevent proteolysis (Rovner, Thompson and Murphy, 1986). Further, our own preliminary studies indicated that once homogenized in these buffers proteolytic degradation could not be detected, even upon exposure of the samples to conditions which might be expected to enhance proteolytic breakdown (e.g. room temperature storage for several hours prior to freezing). All of the sample homogenates were kept at -80°C before subjected to gel electrophoresis.

Electrophoretic and Western Blotting Techniques

Isoelectric focusing (IEF) and sodium dodecyl sulfate polyacrylamide gel electrophoresis (SDS-PAGE) were used for protein separation. The mini-protein II gel system from BioRad (CA) was employed. The two dimensional (2-D) gel electrophoresis methods were mainly adopted from the studies of Driska et al. (1981) with some modification by Ratz and Murphy (1987) which has been considered a classical method for detecting MLC phosphorylation.

Actin and tropomyosin isoforms as well as phosphorylated myosin light chains were separated by 2-D gel electrophoresis. Isoelectric focusing was performed using a 4% acrylamide tube gel containing an Ampholyte range of 4.5-5.4 pH units. Gels were run at 750V for 3.5 hours after a 10-minute focusing at 500 V. The proteins were then subjected to the second dimension separation by molecular weight on a Laemmli style (Laemmli, 1970) slab gel (3.5% stacking gel and 12 or 15% separating gel). The electrophoretic condition was constant voltage at 200 V for 45 minutes. Myosin heavy chain isoforms were separated using one dimensional gels (3.5%, Laemmli style) or Giulian glycerol gels (Giulian, et al., 1983) containing 12% acrylamide and 10% glycerol. These gels were run at a constant current of 30mA for 2 hours or 40 mA for 18 hours, respectively; resolution was found to be similar in both systems. Sample loadings were optimized for the particular protein isoforms under study. Figure 2-9 shows a representative 2-D gel for MLC separation.

Figure 2-9. Representative gel showing the separation of myosin light chain isoforms.

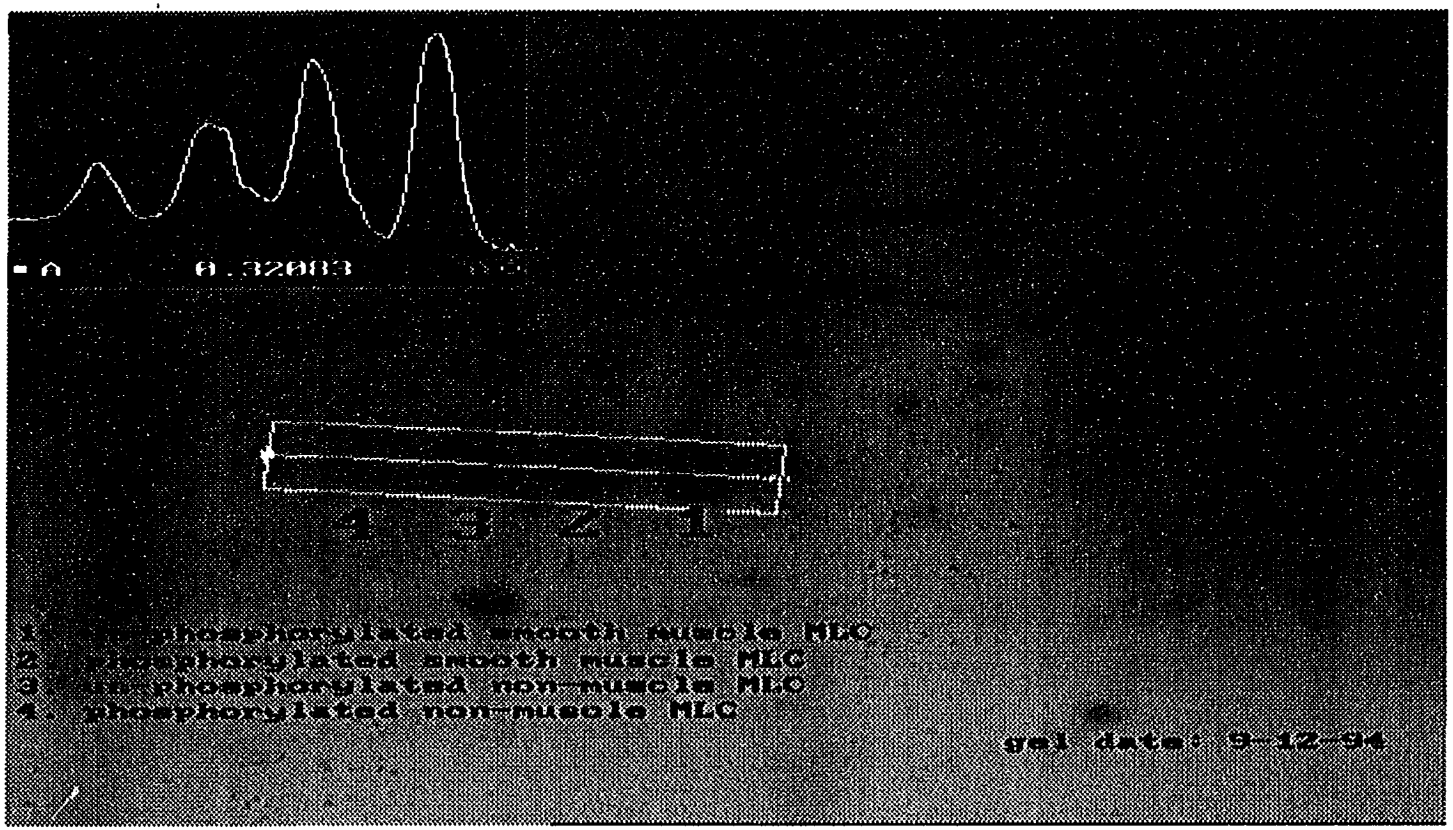
A
0.32083
4
3
2
1
1. non-phosphorylated smooth muscle MLC
2. phosphorylated smooth muscle MLC
3. non-phosphorylated non-muscle MLC
4. phosphorylated non-muscle MLC
gel date: 9-12-94

After electrophoresis, the proteins were treated differently according to the expected protein loading. For the study of myosin light chain phosphorylation, the proteins were stained with silver using BioRad Silver Stain Plus Kit. Heavily loaded samples (i.e. those for actin, tropomyosin and myosin heavy chain isoforms) were stained with Coomassie Brilliant Blue R-250. Quantitation was performed using line scan densitometry subroutine of a video based image analysis system (Image 1, Universal Imaging, PA). Results were expressed as percent of the isomer in a given protein.

Western blot techniques were performed for immunochemical identification of different actin, myosin and tropomyosin isoforms. After gel electrophoresis, proteins were transferred from gels to nitrocellulose transfer membranes (NitroPlus, 0.22μm, Micron Separations, Inc., MA) using a BioRad Mini Trans-Blot Electrophoretic Transfer Cell. Blottings were carried out in a cold transfer solution (Towbin, et al., 1979) at 100 V for 1 hour with continuous mixing. Horse radish peroxidase conjugated secondary antibodies were always used and the staining was produced using 4-chloro-1-naphthol (Pierce, IL).

Statistical Methods and Data Analysis

Based on previous experience using isolated vessel preparations it was necessary to achieve approximately 6 successful experiments for each of the manipulations described under experimental components. Where appropriate, i.e. when considering normally distributed data, simple comparisons of the mean and standard errors were performed using a two-tailed Student t-test. When considering data which is not normally distributed, levels of significance were determined by non-parametric statistics, e.g. Mann-Whitney U test. When multiple comparisons were to be made significance was determined using analysis of variance (Student-Newman-Keuls). Paired comparisons were applied when analyzing results from the same vessel with different treatments. For all comparisons significance was assumed at the $p < 0.05$ level. Data handling was performed using an IBM compatible computer (Gateway 2000, 486DX33) with appropriate spreadsheet (Microsoft Excel), graphical (SigmaPlot for Windows 5.0) and statistical (Instat) programs.

CHAPTER III

CONTRACTILE PROTEIN ISOFORM EXPRESSION ALONG RAT MESENTERIC VASCULAR TREE

It is well established that variation in contractile agonist sensitivity exists between different blood vessels. In particular, there is a tendency toward increased agonist sensitivity as arterial/arteriolar diameter decreases along the vascular network (Duling, et al., 1968 and Gore, 1972). Further, the existence of spontaneous vascular tone and the ability to control vascular resistance through local autoregulatory mechanisms (e.g. myogenic reactivity) largely resides in the small arterial vessels rather than the larger conduit arteries (Davis, 1993, Sun, et al., 1992).

While it is conceivable that such differences in function relate to variation in receptor populations or signal transduction mechanisms it is also possible that there are fundamental differences at the level of the contractile apparatus. This possibility is supported by the existence of a number of isoforms of the various contractile proteins (for review see Murphy, 1992 and Somlyo, 1993). Although the functional significance of many of these protein variants is uncertain, studies have shown that contractile protein isoform expression can be modified according to physiological and experimental situation (Babij, et al., 1992; Morano, et al., 1992), suggesting that smooth muscle can express isoforms appropriate for a given set of conditions. Further, there is evidence for developmental changes in the distribution of contractile proteins (Eddinger and Murphy, 1991; Zanellato, et al., 1990). It is also apparent that differing smooth muscle can exhibit a different complement of specific isoforms. For example, Fatigati and Murphy (1984) demonstrated that muscle specific α-actin form was more abundant in arteries compared to veins.

The present study examined 1) whether it was feasible to use electrophoretic techniques to separate and quantitate the major contractile protein isoforms that exist in small arterial vessels taken along the mesenteric vascular arcade and 2) whether evidence exists to support the suggestion that contractile function may relate to particular isoform expression. Knowledge of whether or not there is variation in contractile protein isoform expression along the vascular tree is required before the relationship between specific protein isoforms and reactivity can be systematically addressed.

Materials and Methods

Tissues were prepared as described in chapter 2. For the studies involving separation of myosin heavy chain isoforms, samples of rat aorta and femoral artery were also prepared to examine regional variations in isoform expression. In addition, samples of hog carotid artery (21 days of age, n = 9) were also examined; the rationale for studying this vessel was that it's myosin isoforms are well characterized in the literature (Eddinger and Murphy, 1991; Rovner, Thompson, and Murphy, 1986) and as such provided a suitable control.

Polyacrylamide gel electrophoresis was used to separate protein isoforms and the resolution of myosin heavy chains was found to be comparable to that previously described (e.g. Kawamoto and Adelstein, 1987).

To assist in the identification of particular isoforms of myosin heavy chain present in small mesenteric arteries Western blotting procedures were used. Rabbit anti-myosin (SM and NM) antibodies (Biomedical Technologies Inc., MA) and a Goat anti-rabbit IgG-peroxidase (Sigma Chemical Co. MO) were used as the primary and the secondary antibody, respectively.

For two dimensional separation of actin and tropomyosin, samples were loaded at approximately 1 μg actin. This was calculated assuming a tissue density of 1.055 g/cm^3 and a vascular smooth muscle actin content of approximately 20mg/g tissue in conjunction with the measurements of vessel segment diameter and length (Herlihy and Murphy, 1973).

Results

Consistent with earlier reports from large vessels, homogenates of the small mesenteric arteries consistently showed that actin stained as three distinct spots (Figure 3-1). Confirmation of the three spots being actin isoforms was obtained using an anti-actin antibody (Sigma Chemical Co.) and Western blotting procedures (data not shown). These isoforms have previously been designated as α-smooth muscle actin, β-non-muscle actin and γ-actin (mixed smooth muscle and non-muscle). The actin isoform (α-actin) migrating toward the acidic end of the gel was the most abundant and showed a significant inverse correlation ($r = 0.86$, $p < 0.001$) with vessel diameter (Figure 3-1). Comparison of 4 arteries subject to endothelial cell removal to 4 size-matched intact arteries suggested that the presence or absence of the endothelial layer did not significantly influence the results. For example, α-actin content was 56.3 ± 2.8 % of total actin in the intact arteries and 54.7 ± 2.9 % in the denuded vessels.

Compared to the corresponding small veins the arteries showed significantly more α-actin with a corresponding reduction in β-actin (Figure 3-2). The relative proportion of the two tropomyosin subunits (acidic, basic) did not appear to vary with small artery diameter and as such the data is presented in the form of group data. It can be seen that the tropomyosin subunits were present in approximately equal proportions (Figure 3-3). As described for actin above, confirmation of the two spots being tropomyosin subunits was obtained using an anti-tropomyosin antibody (Sigma Chemical Co.) and Western blotting procedures (data not shown).

One dimensional electrophoretic separations of homogenates of small arteries showed two bands in the region expected for myosin heavy chains (approximately 200kD; Figure 3-4). Consistent with the bands being muscle forms of myosin heavy chain (SM1 and SM2) their electrophoretic mobility was slightly slower than that of the platelet homogenates (Figure 3-4). Co-electrophoresis of artery and platelet homogenates show three distinct bands supporting the proposition that the predominant forms of myosin heavy chain in small mesenteric artery samples were of the muscle type as opposed to the non-muscle type (NM) reported to be present in platelets. Comparison with previously reported studies suggests that the approximate molecular weight of the bands would be

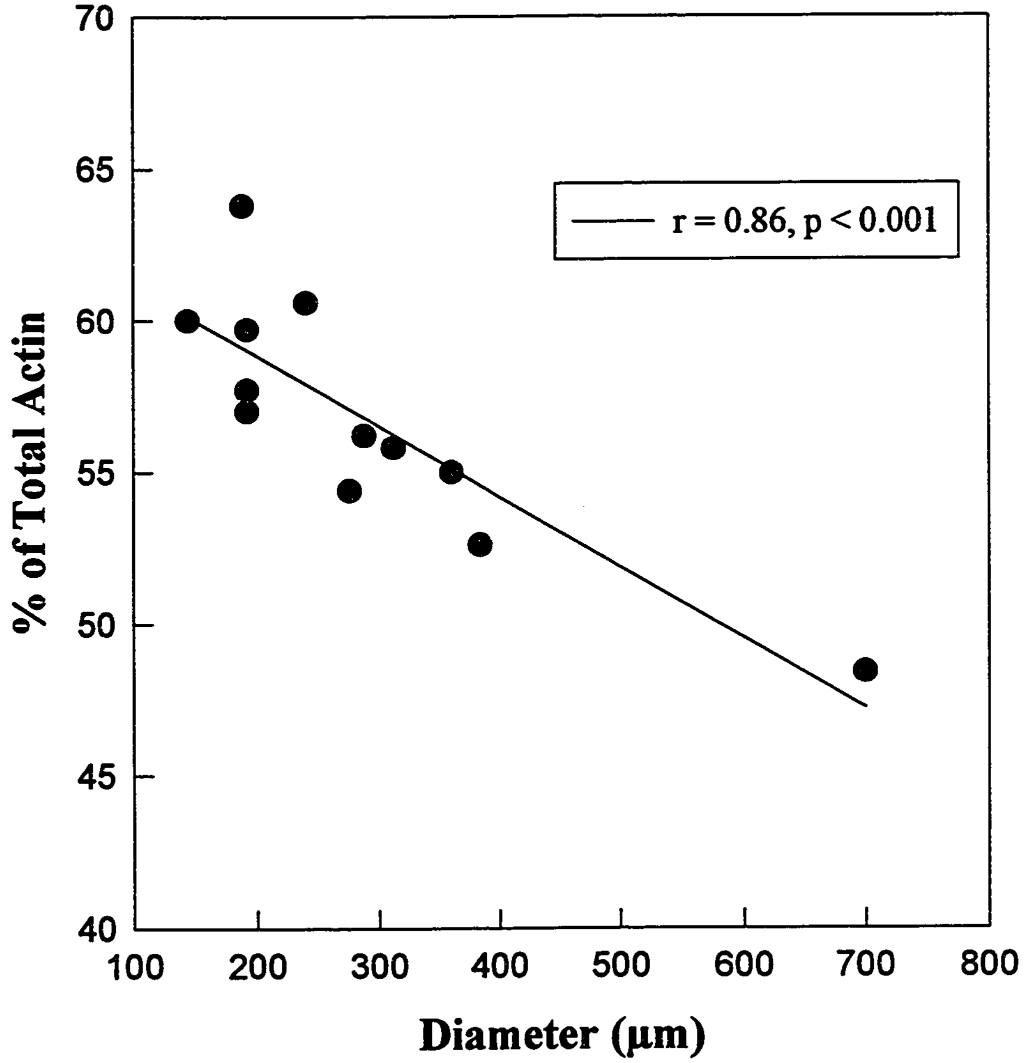

Figure 3-1. Relationship between α actin content and small mesenteric artery diameter.

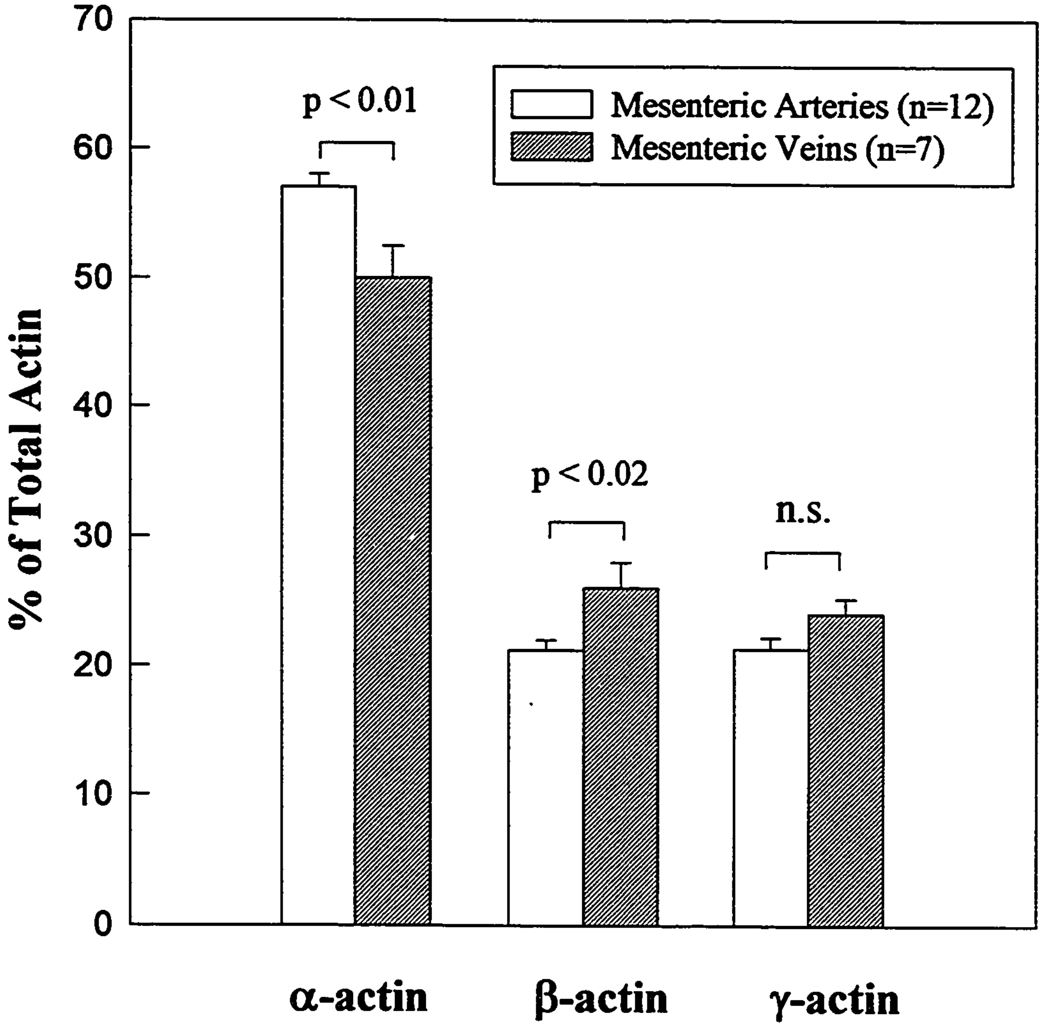

Figure 3-2. Comparison of actin isoform content of small mesenteric arteries compared to that of the corresponding small veins. Results are expressed as mean ± SEM.

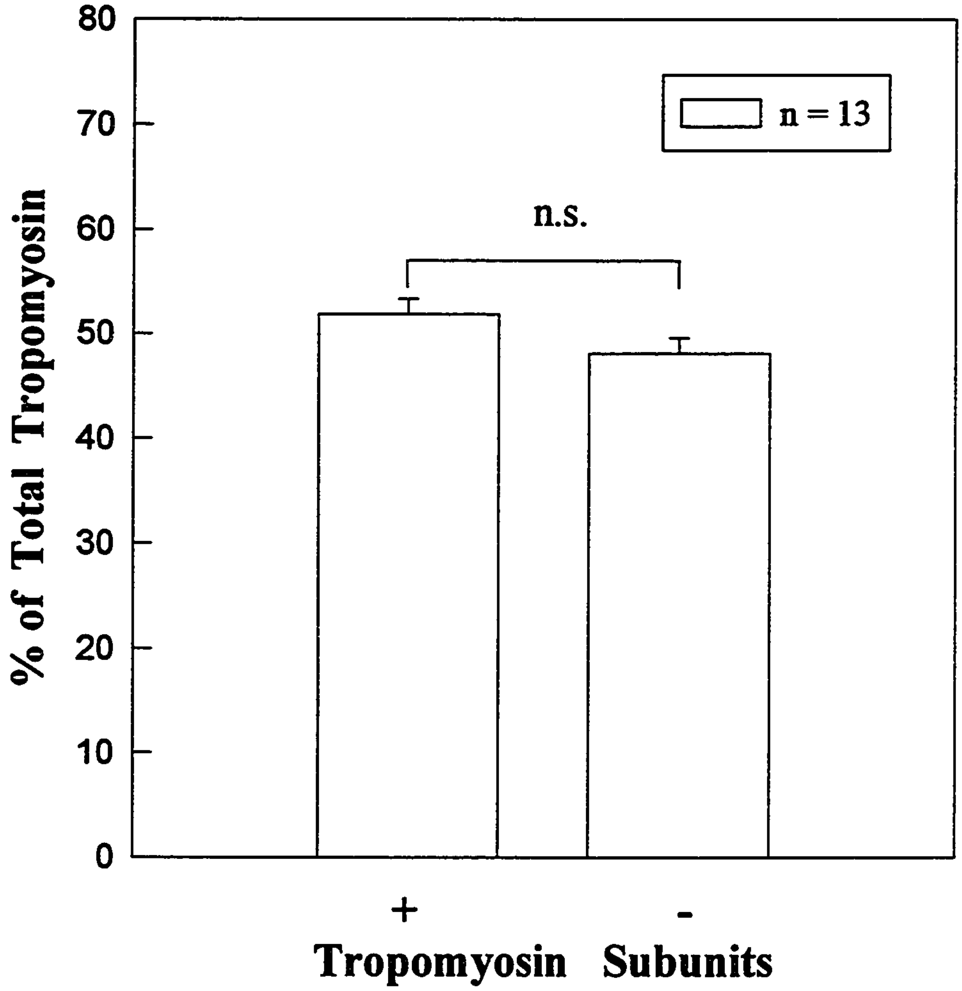

Figure 3-3. Relative abundance of tropomyosin subunits in small mesenteric arteries. As there was no apparent relationship between vessel diameter and content of a particular subunit, results are shown for the total group (n=13).

204kD (SM1), 200kD (SM2) and 198kD (NM) (Murphy, 1993). Western blot analysis using an anti-non-muscle myosin antibody showed a significant reaction with the platelet homogenates and a very faint band in the small artery samples (Figure 3-4). The band detected by the non-muscle myosin antibody in the mesenteric samples appeared to have migrated at a level equivalent to that for the platelet samples and below the coomassie blue stained bands of the 1-D gels (Figure 3-4). Thus, the small mesenteric arteries possess both muscle and non-muscle myosin heavy chains with the muscle forms being far more abundant. No significant relationship was found to exist between small mesenteric artery diameter and the relative amounts of the myosin heavy chain isoforms. Considering the mesenteric arteries as a single group, the ratio of SM1:SM2 was approximately 70:30 ($n = 18$, $p < 0.001$). Comparison of the small mesenteric arteries with samples of conduit vessels (aorta, femoral artery) from animals of similar age showed that there are site-specific differences in the proportion of SM1 and SM2 (Table 3-1). In particular, the highest proportion of SM1 was found in the femoral artery followed by the mesenteric vessels with the lowest proportion in the aorta. As a number of previously reported studies have examined myosin heavy chain expression in hog carotid artery, nine samples of this tissue were also examined. Hog carotid artery was found to contain 62% SM1 compared to 38% SM2.

Comparison of vessel segments with and without an intact endothelium indicated that the myosin heavy chain results were not significantly influenced by the presence of such cells. Separations of homogenates treated in a manner to enhance any proteolytic

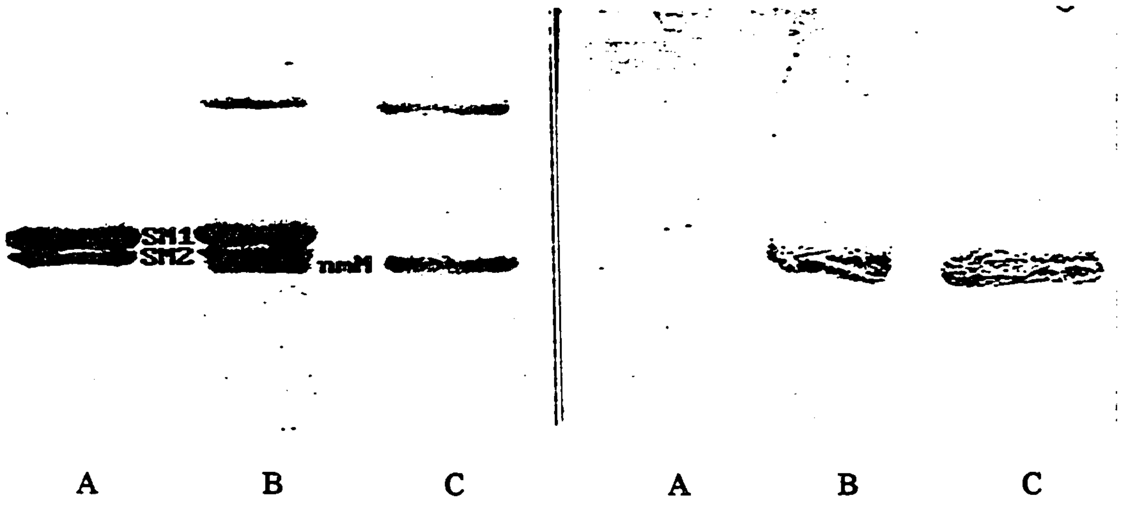

Figure 3-4: Digital image, obtained using an Image 1 analysis system (Universal Imaging, PA), showing electrophoretic separation of myosin heavy chains. In the left panel coomassie blue stained sections of acrylamide gel show separation of the heavy chains for a small mesenteric artery homogenate (lane A), a combined small mesenteric artery and platelet sample (lane B) and a platelet homogenate (lane C). It can be seen that the artery separates into two bands (SM1, SM2), the platelet into one band (NM) and the mixed sample into three bands (SM1, SM2, NM). The right panel shows a corresponding Western blot analysis using a non-muscle myosin heavy chain antibody. Marked staining is evident in the platelet and mixed samples indicating that the platelet contains only NM; while the small mesenteric vessel predominately expresses SM1 and SM2, although a very small quantity of NM is seen in the vessel (lane A right panel).

Table 3-1: Myosin SM1 Heavy Chain Content (% total SM MHC)

	RAT			HOG
	Femoral	Aorta	Small Mesenteric	Carotid
Mean	77	65*	70**	62†
SEM	1.3	2.3	2.1	1.8
n	10	11	18	9

* $p < 0.05$, femoral artery vs. aorta; ** $p < 0.01$, femoral artery vs. small mesenteric artery

† hog carotid artery contains significantly less SM1 (relative to SM2) than does rat femoral ($p < 0.001$) or small mesenteric ($p < 0.05$) arteries.

Significance determined by ANOVA in conjunction with Student-Newman-Keuls test.

degradation (e.g. prolonged room temperature storage) did not provide any evidence to suggest that the more mobile myosin heavy chain band was a breakdown product.

Discussion

The results of the study provide further evidence for diversity in contractile protein isoform expression between blood vessels. While the exact significance of these proteins variants is uncertain it is tempting to speculate that they contribute to functional variability. In particular, the correlation between α-actin content (relative to total actin) and mesenteric artery diameter, and that α-actin is more abundant in small arteries than corresponding veins may be indicative of a relationship between vascular reactivity and contractile protein composition.

Despite the present uncertainty as to the functional significance of many of the contractile protein variants, both *in vivo* and *in vitro* studies have shown that contractile protein isoform expression can be modified under a variety of situations. For example, studies performed on smooth muscles from rats indicate that there are significant developmental changes in contractile protein isoform expression (Eddinger and Murphy, 1991). In particular, there is an increase in the muscle isoforms of actin and myosin heavy chains with a concomitant decrease in the non-muscle protein forms during the first 20 days of life. Cultured vascular smooth muscle cells often undergo phenotypic modulation which results in the cell converting from a contractile to a synthetic state (Fatigati and Murphy, 1984; Owens, et al., 1986). This change in cellular character is associated with a marked decrease in α-actin expression and a compensatory increase in the β-actin isoform. Similarly cultured saphenous vein smooth muscle cells can be induced to undergo a shift in myosin heavy chain isoforms such that there is as an increase in the relative amount of the non-muscle isoforms (Seidel, et al., 1991) which is associated with a reduction in cellular contractile activity. Apparent relationships between the contractile protein isoforms expressed and mechanical function is not limited to vascular smooth muscle; for example myosin heavy chain composition of a skeletal muscle fiber correlates with both shortening velocity and maximal force generation (Caizzo, et al., 1992; Emerson and Bernstein, 1987). Thus, these examples and the data from the present study demonstrating a relationship between small artery diameter and relative α-actin content, and regional differences in the relative amounts of the myosin heavy chain isoforms, provide supportive evidence for the hypothesis that resistance artery reactivity may, in part, relate to protein isoform expression.

A potential source of error in these studies is that the arteries examined are not exclusively composed of vascular smooth muscle but also would be expected to contain, for example, endothelial cells, nerves and connective tissue. Comparison of vessels with a presumably intact endothelium with those subject to a physical denudation procedure suggest that endothelial cells were not markedly contributing to the results. In terms of the distribution of actin isoforms it would be expected that if contamination due to non-muscle tissues had been a significant problem that this would have tended to show as an increase in the non-muscle isoforms (β and γ) in the smaller arteries. As vascular smooth muscle, itself, can produce the non-muscle isoforms (β and γ) and that the contractile protein content of non-muscle cells is 1 -2 orders of magnitude less than that of smooth muscle (Murphy, 1992) the contribution of remaining cell types was probably not significant. The finding of an approximate 50:50 distribution of the tropomyosin subunits is consistent with previous studies in the literature (Gummins and Perry, 1974) and was also taken to be supportive of the reliability of our electrophoretic measurements.

Previous studies have indicated the existence of four myosin heavy chain isoforms; two muscle forms (SM1 and SM2) and two non-muscle variants (NM1 and NM2) (Rovner, Murphy and Owens, 1986). Consistent with results of the present study the major forms present in arteries appear to be SM1 and SM2, although the existence of small quantities of a non-muscle variant in small mesenteric arteries was demonstrated using a Western blotting approach. In apparent contrast to our results from small arteries, Eddinger and Murphy (1991) found that in hog (9 days of age and adult) carotid artery SM1 and SM2 to be present in approximately 77:23 and 55:45, respectively. This difference may well relate to differences in, vessel size, site within the vasculature, developmental stage or species. The data from the present study indicate that significant differences in the ratio of SM1:SM2 exist between different arterial vessels taken from the same rat. Further, as a control we examined a series of hog (21 days of age) carotid artery homogenates which were prepared and separated under the same conditions as the rat samples. Hog carotid arteries were found to have a lower percentage of SM1 relative to SM2 (62%) compared with that found in the various rat samples (65 - 77%) and this value falls in between those described by Eddinger and Murphy [76% for young (6 days) and 56% for adult]. This control value is expected from their study and gives us additional confirmation on our sample preparation and gel electrophoresis techniques.

Boels et al. (1991) reported an increased ratio of SM1:SM2 in pooled samples of guinea pig small mesenteric arteries (diameter approximately 115μm) compared to that in the main branch of the mesenteric artery (diameter approximately 600μm). These authors speculated that the functional significance may relate to increased Ca^{2+} sensitivity and hence reactivity of smaller vessels. Our results, however, did not reveal a correlation between mesenteric artery diameter and SM1:SM2 ratio; moreover, a higher ratio was found in the femoral artery. While the differences may relate to the species studied it is possible that results reflect regional differences rather than a relationship with vessel size or branch order.

The electrophoretic data from the present study, obtained under reducing conditions, do not allow conclusions to be drawn as to the composition of the intact myosin molecule. It is of interest to note, however, that Tsao and Eddinger (1993) recently reported that myosin from porcine aorta exists as three species, namely the SM1 homodimer, SM2 homodimer and the SM1-SM2 heterodimer. Further diversity in composition of the intact myosin molecule could be provided by the existence of isoforms of the myosin light chains [e.g. 17,000-dalton light chains (Helper, et al., 1988)]. While these isoforms were not examined in this dissertation, they are of potential significance for future studies.

In summary, the results of this study demonstrate the feasibility of quantitating contractile protein isoforms in small blood vessels using standard electrophoretic techniques. The data presented are, in addition, consistent with the hypothesis that differences in contractile protein function between vessels may, in part, relate to differences in contractile protein expression.

Additional studies are needed in order to examine the exact functional significance of the particular contractile protein isoforms which are expressed in resistance vessels and to determine whether such expression is developmentally and/or environmentally regulated. These studies, regarding long term regulations of contractile proteins, will require molecular biological techniques, such as RNA extraction and Northern blot. Given the feasibility of using gel electrophoresis for studying biochemical correlates of microvascular smooth muscle function, the remainder of the thesis will, however, focus on the short term regulation of arteriolar contraction. In particular, the role of MLC phosphorylation and $Ca^{2+}{}_i$ in arteriolar myogenic reactivity will be determined.

CHAPTER IV

ROLE OF CA^{2+}$_{I}$ AND MYOSIN PHOSPHORYLATION IN ARTERIOLAR BASAL TONE SETTING

Resistance vessels are typically characterized by the existence of spontaneous tone (state of partial contraction), the degree of which is dependent on the prevailing intraluminal pressure. This ability of small arterial vessels to develop spontaneous tone is a function of the vascular smooth muscle and as such represents a myogenic property of the arteriolar wall (Johnson, 1980). While the possible contribution of different contractile protein isoforms has been discussed in chapter 3, studies regarding signal transduction aspect of the myogenic reactivity will be reported in this and the following chapters.

While it has generally been assumed that a myosin light chain phosphorylation mechanism contributes to arteriolar myogenic reactivity, the evidence is based solely on studies of conduit arteries (Meininger and Davis, 1992). Further, the exact signaling pathway(s) involved in transducing an intraluminal pressure stimulus into arteriolar contraction remains uncertain. Current evidence indicates that stretch of vascular smooth muscle cells, such as would be expected to occur during an increase in intraluminal pressure, leads to activation of ion channels, increased intracellular Ca^{2+} and subsequently contraction. In addition, studies have demonstrated stretch-induced accumulation of the cellular messenger DAG, while indirect evidence has been obtained for a role for protein kinase C in myogenic vasoconstriction (Hill, et al., 1990; Laher and Bevan, 1987; Osol, et al., 1991). To understand the mechanisms which underlie myogenic reactivity and the setting of basal arteriolar tone, it is critical to determine the involvement of the Ca^{2+}-induced myosin light chain phosphorylation pathway.

The aim of the present studies was to determine, in isolated skeletal muscle arterioles the relationship between intraluminal pressure, intracellular Ca^{2+} and MLC phosphorylation. In so doing the contribution of MLC phosphorylation to setting of arteriolar basal tone was also ascertained.

Methods and Experimental Protocols

Vessel set up, $Ca^{2+}{}_i$ measurement and sample preparation were performed as described in chapter 2. Briefly, isolated rat cremaster first order arterioles were cannulated in a superfusing chamber at a transmural pressure of 70mmHg in the absence of intraluminal flow. Vessels were superfused with Krebs buffer and maintained at 34°C throughout each of the experiments. $[Ca^{2+}]_i$ was measured using fura-2 as a fluorescent indicator and fluorescence ratio $R_{340/380nm}$ was used for measurement of changes in $[Ca^{2+}]_i$. MLC isoforms were separated by two dimensional polyacrylamide gel electrophoresis. To ensure adequate loading of protein from the microvessel segments it was necessary to pool samples. The separated proteins were quantitated using a computerized image analysis system and MLC phosphorylation expressed as percent phosphorylated MLC of total 20kD MLC. As an index of reproducibility between electrophoretic separations a standard sample of homogenized rat aorta (obtained under conditions of 0 mmHg transmural pressure) was processed on each day; the extent of phosphorylation was determined to be 14.5 ± 0.8 % (mean ± SEM), n = 7 determinations.

Effect of Steady-State Intraluminal Pressure on Arteriolar Wall $Ca^{2+}{}_i$.

After equilibration and loading with Fura-2, intraluminal pressure was slowly reduced to 30 mmHg after which arteriolar wall $[Ca^{2+}]_i$ were measured as pressure was step increased to 50, 70, 100, 120, 150 and 170 mmHg. To ensure steady-state [based on pressure-induced changes in arteriolar diameter observed in earlier studies (Hill, et al., 1990; Meininger and Davis, 1992)], vessels were maintained at each pressure for a minimum of 15 minutes before collection of six 340/380 image pairs at 5 second intervals. In addition to collecting $[Ca^{2+}]_i$ data in the active state, arterioles were also examined after being rendered passive by prolonged exposure to 0 mM Ca^{2+}/2mM EGTA buffer. Diameter measurements were taken for correlation of $[Ca^{2+}]_i$ data with diameter and calculated wall tension.

Effect of Steady-State Intraluminal Pressure on Myosin Light Chain Phosphorylation

After equilibration, arterioles were exposed to one of several intraluminal pressure levels (30, 70, 120 or 150 mmHg). To ensure steady-state, vessels were maintained at their collection pressure for a minimum of 15 minutes before freezing. In addition to collecting samples in the active state, arterioles were also studied in the passive state as described above. Prior to collection of samples internal diameter measurements were taken for calculations of wall tension.

Effect of ML-7 on Arteriolar Tone

To provide additional evidence for the involvement of MLC phosphorylation in setting of basal tone and myogenic reactivity, studies were performed in the presence and absence of the myosin light chain kinase inhibitor ML-7 (1-[5-iodonaphthalene-1-sulfonyl]-1H-hexahydro-1,4-diazepine hydrochloride) (Biomol, Plymouth, PA). In the control condition (0 mM ML-7) arteriolar diameter and intracellular Ca^{2+} were collected at 30, 50, 70, 100 and 120 mmHg after which the vessel was continually superfused with either 3 or 10 µM ML-7. This agent has been reported to possess relative specificity for myosin light chain kinase and has typically been used over the concentration range employed in the present study (Nishikawa, et al., 1985; Ratz, 1993). After a 15 minutes period the Ca^{2+} and diameter measurements were repeated. Control experiments were studied to examine the effects of time and repeated pressure steps.

Drugs and Chemicals:

Unless stated all chemicals were obtained from Sigma Chemical Company (St. Louis, MO). ML-7 was prepared as a stock solution (10^{-2}M) in ethanol with subsequent dilutions in buffer as required.

Results

Consistent with previous studies (Hill and Meininger, 1994; Meininger, et al., 1991), in the presence of extracellular Ca^{2+}, isolated cremaster muscle arterioles exhibited pressure-dependent myogenic vasoconstriction over an approximate pressure range of 30 - 150 mmHg (Figure 4-1A). In the absence of Ca^{2+}, vessels responded passively to increases in intraluminal pressure (Figure 4-1A). Relative to the passive state, active pressure-dependent vasoconstriction resulted in near maintenance of a constant wall tension despite increased intraluminal pressure (Figure 4-1B).

Effect of Steady-State Intraluminal Pressure on Arteriolar Wall $Ca^{2+}{}_{i}$.

Steady-state $[Ca^{2+}]_i$, as measured by the 340/380 nm fluorescence ratio, was found to increase with increasing intraluminal pressure (Figure 4-2A). Regression analysis indicated that the relationship between pressure and intracellular Ca^{2+} approximated a linear function ($\%R_{340/380}$ at 30 mmHg = 0.32 x pressure + 91.15 ; $r^2 = 0.60$, $p < 0.001$). Over the pressure range studied estimated $[Ca^{2+}]_i$ varied from 91.4 ± 10.9 nM at 30 mmHg to 201.4 ± 27.5 nM at 150 mmHg (Fig 4-2B). In contrast to data obtained in the active state (2.5 mM Ca^{2+} superfusate), no significant pressure-induced changes in fluorescence were detected after vessels were made passive by superfusion with buffer containing 0 mM Ca^{2+}/2 mM EGTA (Figure 4-2A). For example, in the passive state estimated $[Ca^{2+}]_i$ was 37.2 ± 6.4 nM and 35.5 ± 9.0 nM at 30 and 150 mmHg (Fig. 4-2B).

Over the pressure range 30 - 120 mmHg, a significant linear correlation ($\%R_{340/380}$ at 30mmHg = 0.07 x wall tension + 87.30 ; $r^2 = 0.72$, $p < 0.001$) was obtained between intracellular Ca^{2+} and wall tension (Figure 4-2C).

Effect of Steady-State Intraluminal Pressure on Myosin Light Chain Phosphorylation

The extent of phosphorylation of the 20 kD regulatory MLC (at steady-state) was found to increase with increased intraluminal pressure (Figure 4-3). Thus, MLC phosphorylation at a pressure of 70 mmHg was 26.7 ± 2.3 % while significantly ($p < 0.001$) increasing to 39.6 ± 3.0% at a pressure of 120 mmHg. In the absence of

Figure 4-1. Relationship between arteriolar diameter, pressure and wall tension. The upper panel (A) shows the pressure-diameter relationships for cremaster muscle first order arterioles, obtained under active (2.5 mM extracellular Ca^{2+}) and passive (0 mM Ca^{2+}/2mM EGTA superfusate) conditions. The lower panel (B) illustrates the relationship between calculated wall tension (pressure x radius; dynes/cm) and intraluminal pressure for the data shown in the upper panel. The data presented in panel B were directly derived from that in panel A and as such error bars have been omitted. Results are presented as mean ± SEM.

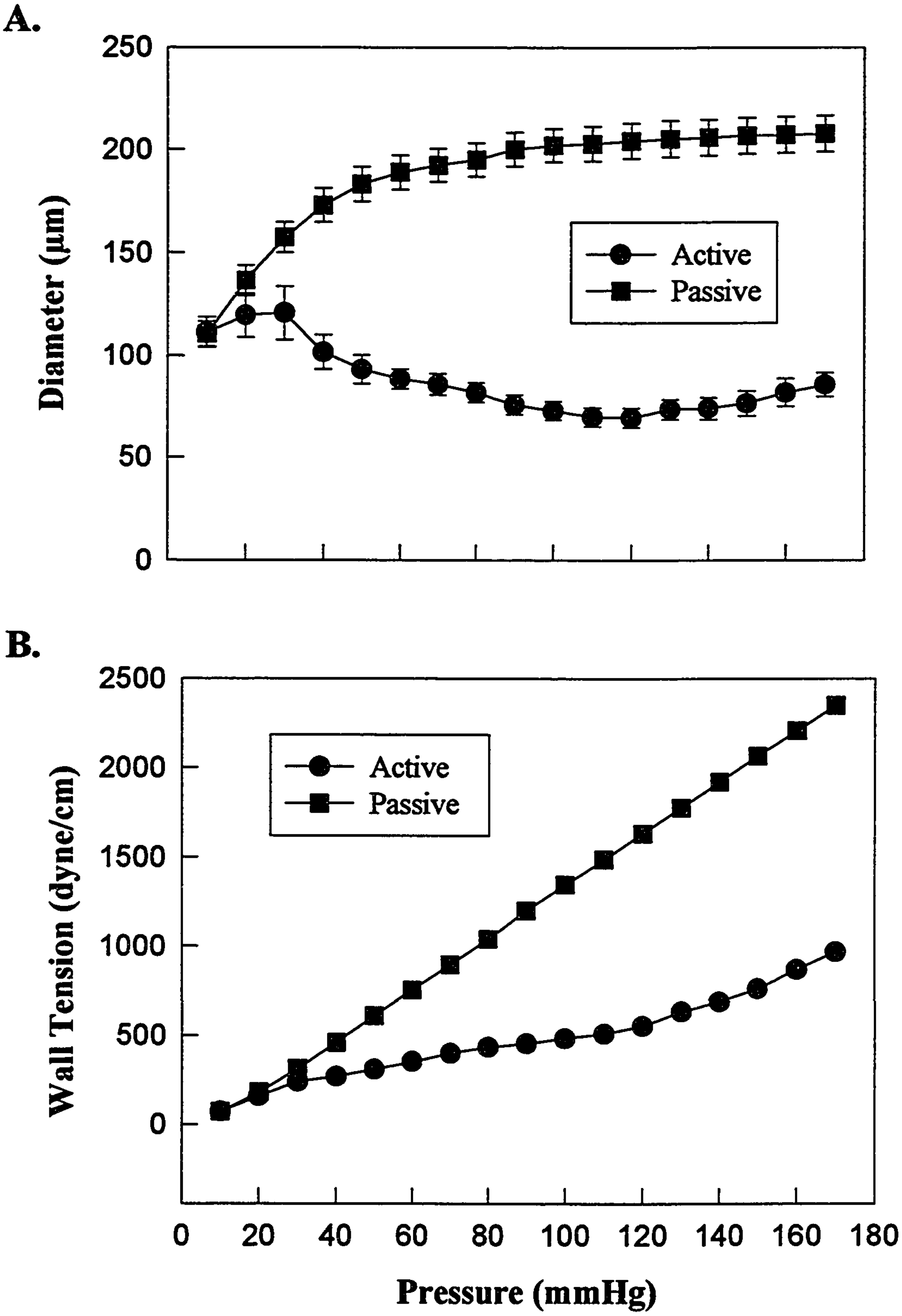
A.
250
200
150
100
50
0
Diameter (µm)
Active
Passive
B.
2500
2000
1500
1000
500
0
Wall Tension (dyne/cm)
Active
Passive
0
20
40
60
80
100
120
140
160
180
Pressure (mmHg)

Figure 4-2. Relationship between arteriolar $[Ca^{2+}]_i$, pressure and wall tension. The upper figure (A) illustrates the effect of intraluminal pressure on $[Ca^{2+}]_i$ levels expressed as the 340/380nm fluorescent ratio ($R_{340/380}$); data is shown for the active and passive states. The middle panel (B) shows the estimated $[Ca^{2+}]_i$ (nM) over the pressure range 30 - 170 mmHg. The lower figure (C) shows the relationship between calculated wall tension and $[Ca^{2+}]_i$. As described in the text a significant ($r^2 = 0.72$, $p < 0.001$) linear correlation was obtained between tension and $[Ca^{2+}]_i$.

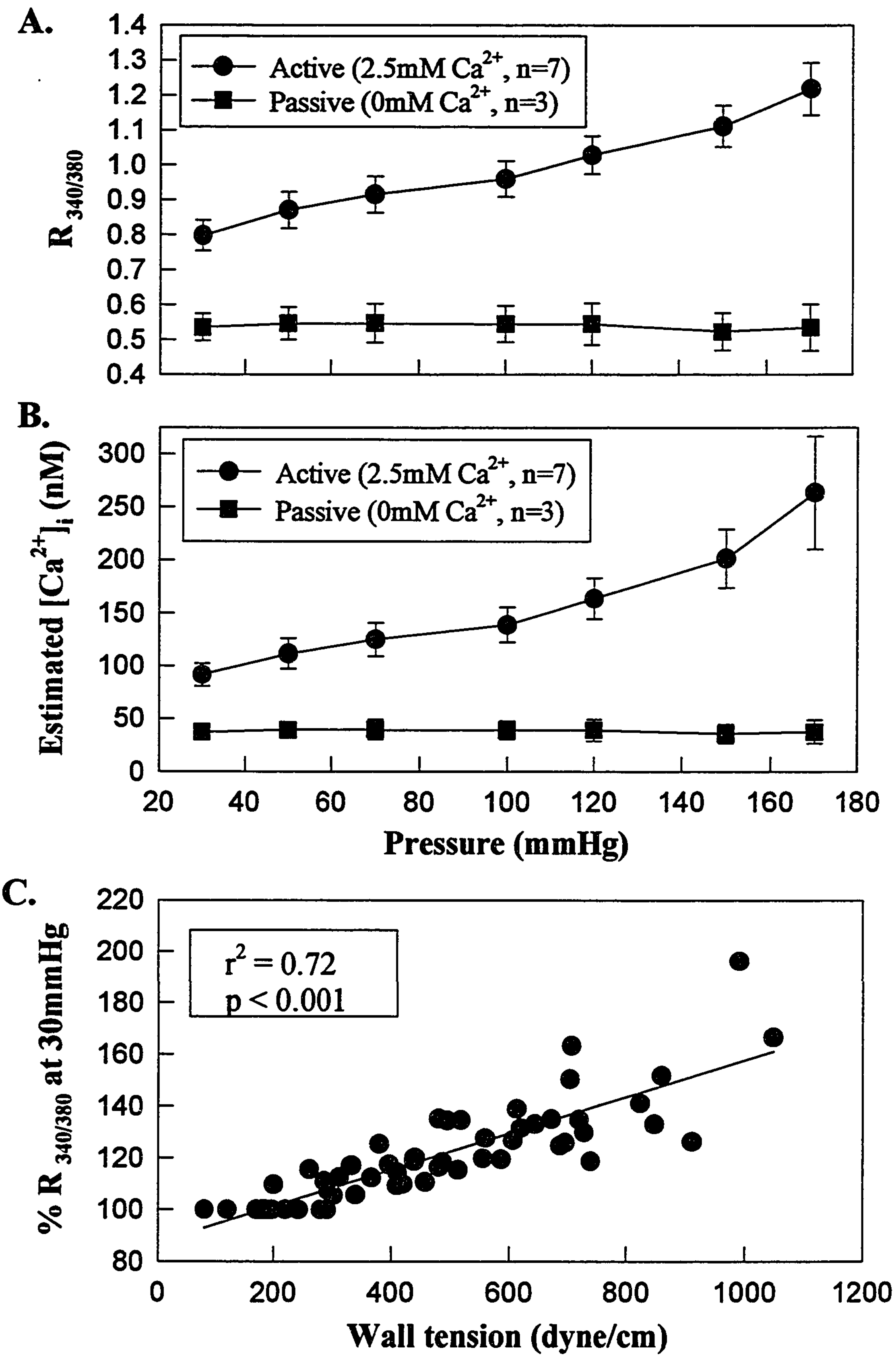
A.
1.4
1.3
1.2
1.1
1.0
0.9
0.8
0.7
0.6
0.5
0.4
$R_{340/380}$
Active (2.5mM Ca^{2+}, n=7)
Passive (0mM Ca^{2+}, n=3)
B.
300
250
200
150
100
50
0
Estimated $[Ca^{2+}]_i$ (nM)
Active (2.5mM Ca^{2+}, n=7)
Passive (0mM Ca^{2+}, n=3)
20
40
60
80
100
120
140
160
180
Pressure (mmHg)
C.
220
200
180
160
140
120
100
80
% $R_{340/380}$ at 30mmHg
$r^2 = 0.72$
$p < 0.001$
0
200
400
600
800
1000
1200
Wall tension (dyne/cm)

extracellular Ca^{2+} MLC phosphorylation was low and did not vary with pressure. As such, data obtained in the passive state was combined, resulting in a phosphorylation level of 8.5 ± 0.7 % (n = 7).

No measurable difference in the extent of phosphorylation was detected between intraluminal pressures of 30 and 70 mmHg (27.7 and 26.7 %, respectively). This could not be entirely explained by insensitivity of the electrophoretic approach, as consistently lower phosphorylation levels were obtained for the unstimulated aortic control tissues (14.5 ± 0.8 %) and samples of arterioles collected in the passive state (8.5 ± 0.7 %). No significant correlation was evident between arteriolar diameter (mean active diameter for each pooled sample) and the extent of MLC phosphorylation (Figure 4-4A); however when phosphorylation was considered in terms of wall tension (pressure x radius) a significant relationship was apparent (Figure 4-4B). Linear regression analysis of the tension (dynes/cm)/phosphorylation (% total) data resulted in a slope value of 0.026 and Y intercept of 18.35 ($r^2 = 0.61$, $n = 23$) with the slope being significantly ($p < 0.001$) different from zero.

Effect of ML-7 on Arteriolar Tone

The myosin light chain kinase inhibitor ML-7 had little effect on pressure-induced changes in intracellular Ca^{2+} (Figure 4-5A). The small inhibitory effect evident at higher pressures (100 and 120mmHg) appears to be explained by time-dependent effects as a similar response was noted in vessels subjected to three sequences of pressure steps (n=3, data not shown). Importantly, despite the presence of the higher concentrations of the inhibitor (10 μM), increases in Ca^{2+}, as assessed by both changes in the 340/380 ratio and

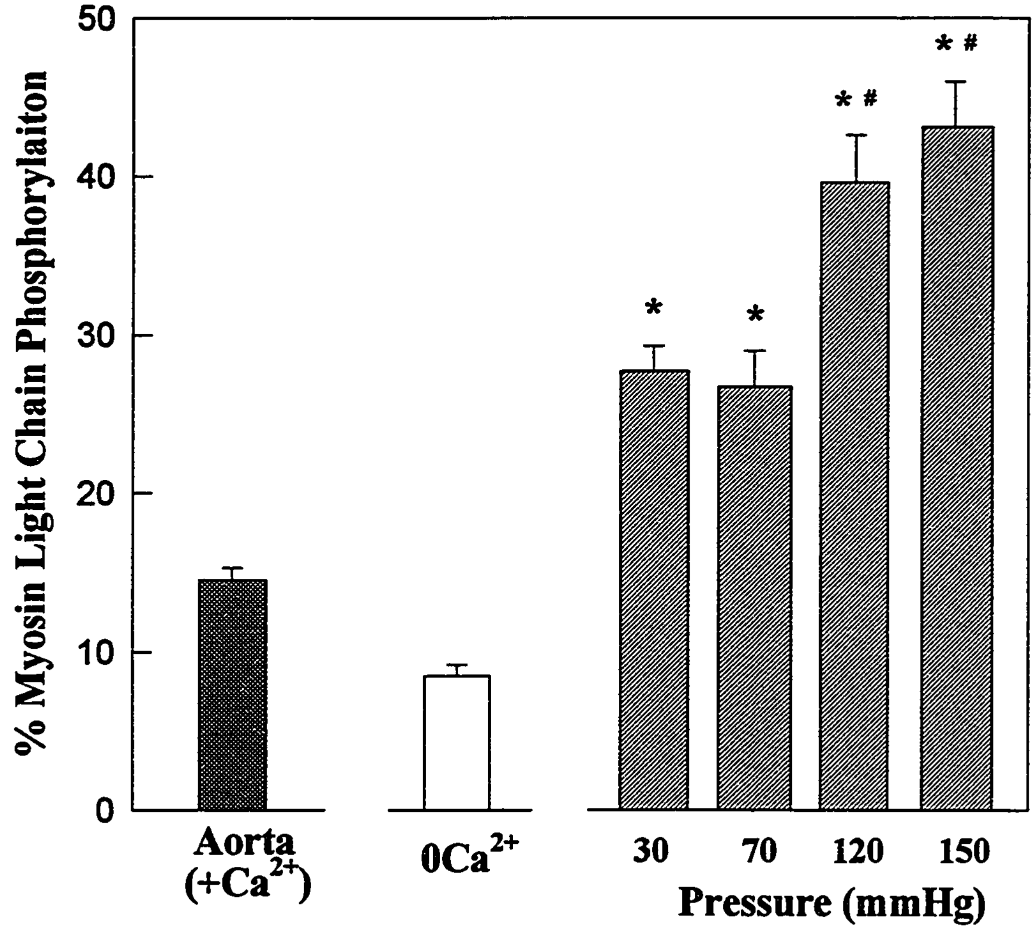

Figure 4-3. Level of myosin light chain phosphorylation expressed as a percentage of total myosin light chain. To the left of the figure results are shown for the level of phosphorylation in cremaster arterioles exposed to 0mM Ca^{2+}/2mM EGTA and the pooled aorta sample which was used as a control (see text). To the right of the figure data are shown to indicate the effect of intraluminal pressure on myosin light chain phosphorylation under active conditions. Results are expressed as mean ± SEM. $* \; p < 0.001$ vs. 0 mM Ca^{2+}; $\# \; p < 0.01$ vs. 30 mmHg.

Figure 4-4. Relationship between myosin light chain phosphorylation and diameter (A) or calculated wall tension (B). A significant linear correlation ($r^2 = 0.61$, $p < 0.001$) was obtained between tension and phosphorylation while the relationship between phosphorylation and diameter was not statistically significant ($r^2 = -0.05$, $p = 0.319$).

A.

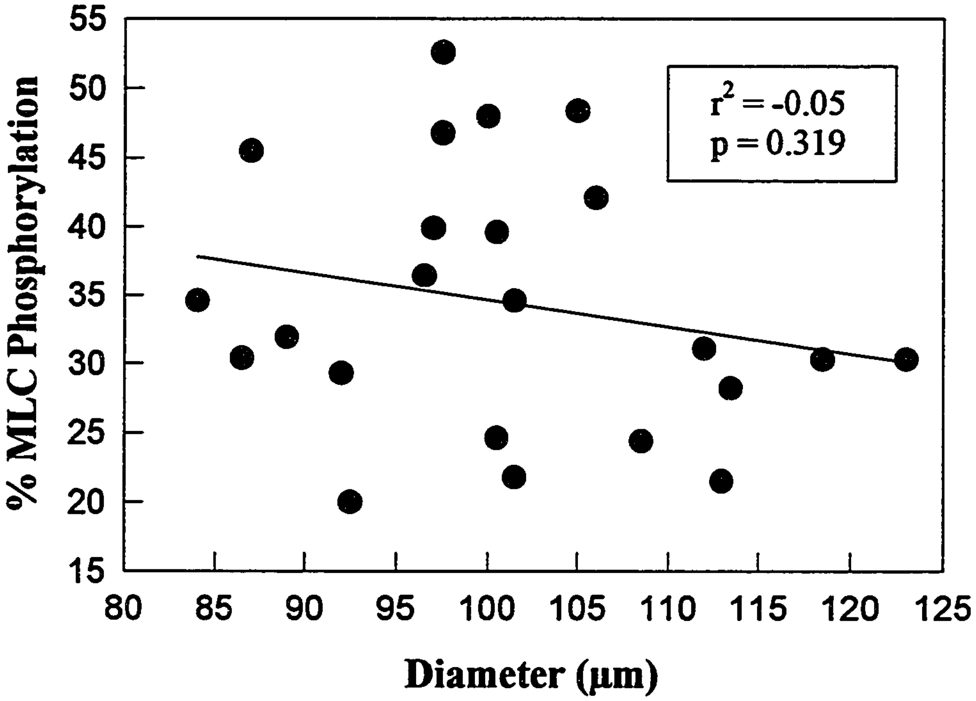
% MLC Phosphorylation
55
50
45
40
35
30
25
20
15
80
85
90
95
100
105
110
115
120
125
Diameter (µm)
$r^2 = -0.05$
$p = 0.319$

B.

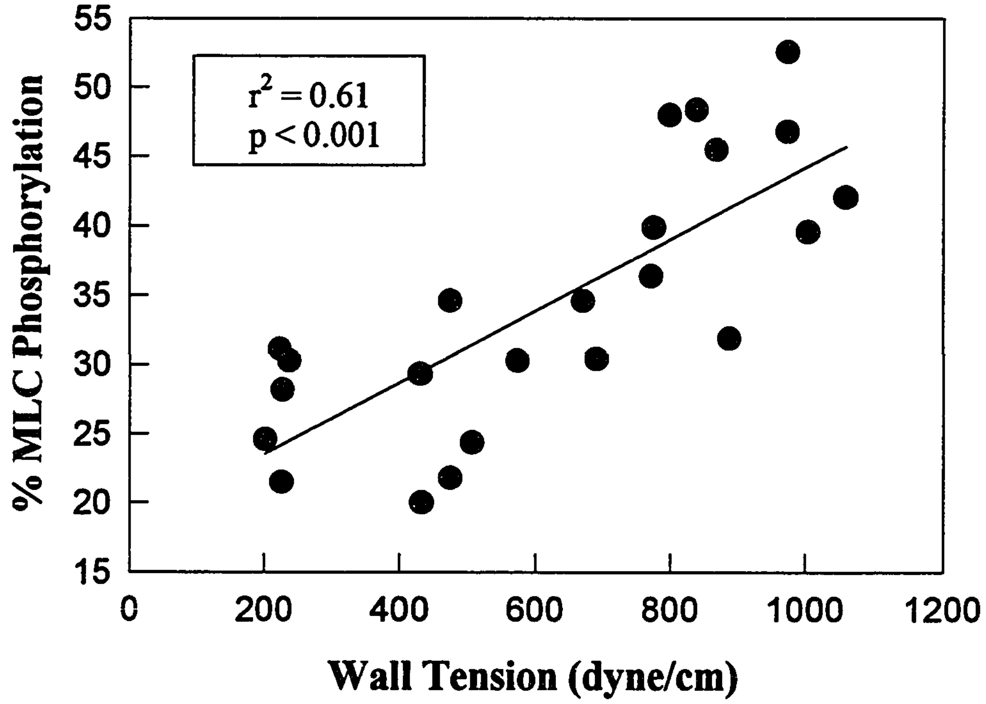
% MLC Phosphorylation
55
50
45
40
35
30
25
20
15
0
200
400
600
800
1000
1200
Wall Tension (dyne/cm)
$r^2 = 0.61$
$p < 0.001$

Figure 4-5. Effect of the myosin light chain kinase inhibitor, ML-7, on pressure-induced changes in $[Ca^{2+}]_i$ (A) and diameter (B). Ca^{2+} data are presented as percent of $[Ca^{2+}]_i$ (nM) at 30 mmHg and diameter as percent diameter at 30mmHg. Results are expressed as mean ± SEM. * $p < 0.05$ compared to control condition.

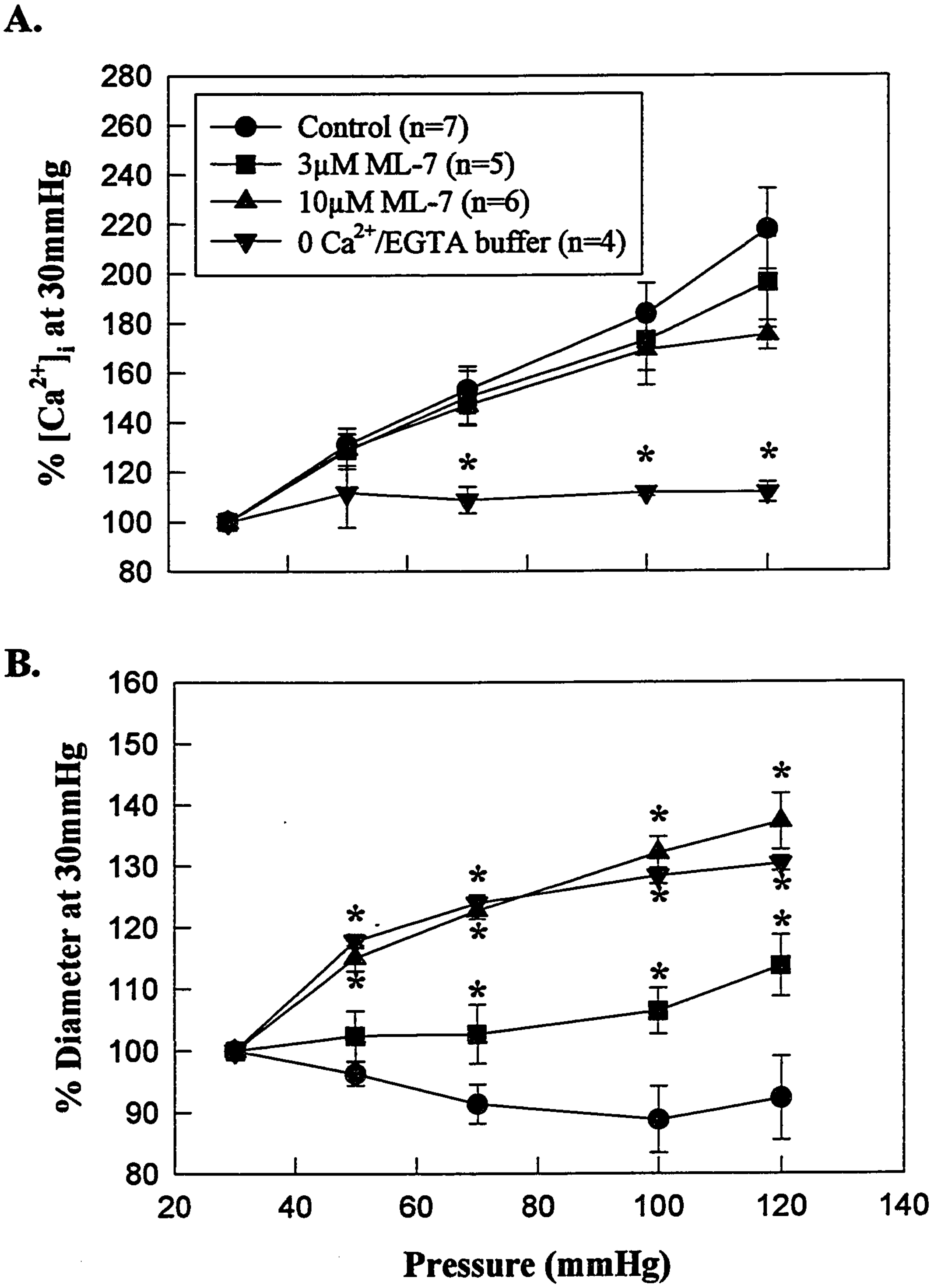
A.
% $[Ca^{2+}]_i$ at 30mmHg
280
260
240
220
200
180
160
140
120
100
80
Control (n=7)
3μM ML-7 (n=5)
10μM ML-7 (n=6)
0 Ca^{2+}/EGTA buffer (n=4)
*
B.
% Diameter at 30mmHg
160
150
140
130
120
110
100
90
80
20
40
60
80
100
120
140
Pressure (mmHg)

calculated Ca^{2+} levels, followed each pressure step. In contrast to the effect on Ca^{2+}, ML-7 caused dose-dependent inhibition of the diameter response to alterations in intravascular pressure (Figure 4-5B). At the highest ML-7 concentration examined (10μM) the response of arterioles to increases in intraluminal pressure paralleled that obtained in the passive state (0 mM Ca^{2+}/2mM EGTA), despite divergent Ca^{2+} responses (Figure 4-5B).

To confirm that ML-7 inhibited MLC phosphorylation, arterioles, at a steady-state intraluminal pressure of 120 mmHg, were exposed to 10μM ML-7 for 15 minutes and collected for gel electrophoresis. The level of 20 kD MLC phosphorylation was reduced to 21.9% (n=2) compared with 39.6% in the absence of ML-7.

Discussion

The results of this study demonstrate that arteriolar myogenic constriction is associated with elevation of intracellular Ca^{2+} and an increased level of MLC phosphorylation. Further, data obtained in the presence of the myosin light chain kinase inhibitor ML-7 suggest that an increase in the extent of phosphorylation of the myosin regulatory light chains, but not an increase in $[Ca^{2+}{}_i]$ alone, is required for development and maintenance of spontaneous basal tone. That is, in the presence of the MLCK inhibitor, arterioles failed to constrict despite pressure-induced increases in intracellular Ca^{2+}.

The results of the present study, to the best of our knowledge, represent the first report of MLC phosphorylation in true resistance vessels. Previously it has been assumed that data obtained using segments of agonist-exposed conduit vessels are applicable to events occurring in arterioles (Meininger and Davis, 1992). In an attempt to establish relationships between arterial resistance and phosphorylation, Moreland et al. (1984), using an *in situ* preparation of the canine anterior tibial artery, demonstrated that phenylephrine-induced increases in arterial resistance were associated with increased levels of MLC phosphorylation. Although not specifically examined in their study, this preparation would not be expected to possess significant spontaneous basal tone. Consistent with this suggestion, Moreland et al. (1984) reported a low level of *in vivo* basal phosphorylation (13 ± 2 %) which is comparable to *in vitro* unstimulated levels in conduit arteries and the aorta control sample used in the present study (14.5 ± 0.8 %). More recently, Laporte et al. (1994) reported MLC phosphorylation levels associated with stretch-induced tone *in vitro* ring segments of the rabbit facial vein. These authors found stretch-induced myogenic tone to be associated with increased Ca^{2+} influx and MLC phosphorylation compared to the unstretched state, however, the response to graded stretch was not determined. Similarly, Ledvora et al. (1983) demonstrated stretch-induced MLC phosphorylation in isolated segments of carotid artery. While these studies can be used to suggest a role for myosin phosphorylation in pressure/stretch phenomena they were not able to establish the relationships among intraluminal pressure, $[Ca^{2+}]_i$, phosphorylation and extent of contraction.

Of interest was the observed correlation between calculated wall tension (pressure x radius) and both intracellular Ca^{2+} and the extent of MLC phosphorylation. Although indirect, these findings are consistent with the hypothesis that wall tension (or a related variable) is the membrane signal which initiates myogenic constriction and therefore perhaps the controlled variable in myogenic responsiveness (Johnson, 1980). Despite tension being linearly correlated with Ca^{2+} and phosphorylation, total wall tension was found to be most closely regulated over an approximate physiologic pressure range (40 - 120 mmHg). This presumably is indicative that others factors, such as a tendency towards a degree of passive collapse at low distending pressures and a relative inability to contract against high distention pressure, limits the effectiveness of the control mechanism.

If wall tension is a sensed and controlled variable then an important question is, what maintains the increased levels of $[Ca^{2+}]_i$ and phosphorylation in the steady state condition - that is after pressure-induced myogenic vasoconstriction has occurred and wall tension has stabilized toward baseline? This suggests that the arteriole has shifted to a state of higher activation; a response necessary to maintain a near stable wall tension in the face of increased intraluminal pressure. Under this condition, if steady-state intracellular Ca^{2+} (and hence myosin light chain kinase activity) were to decrease, vessel distention would occur with a subsequent increase in wall tension.

Figure 4-6 shows the calculated vessel diameter at different pressures based on an ideal wall tension (vessel diameter = 0.5 x wall tension/pressure) regulation, assuming the wall tension at 70mmHg is the controlled value. We can see that the measured diameters come very close to the calculated values within a range of 30-120 mmHg, which correlates approximately to the physiological blood pressure range for arterioles. This finding possesses significance in two ways: it supports the idea that wall tension be the controlled variable for arteriolar myogenic reactivity and gives a clear view for the role of myogenic vasoregulation on local blood flow.

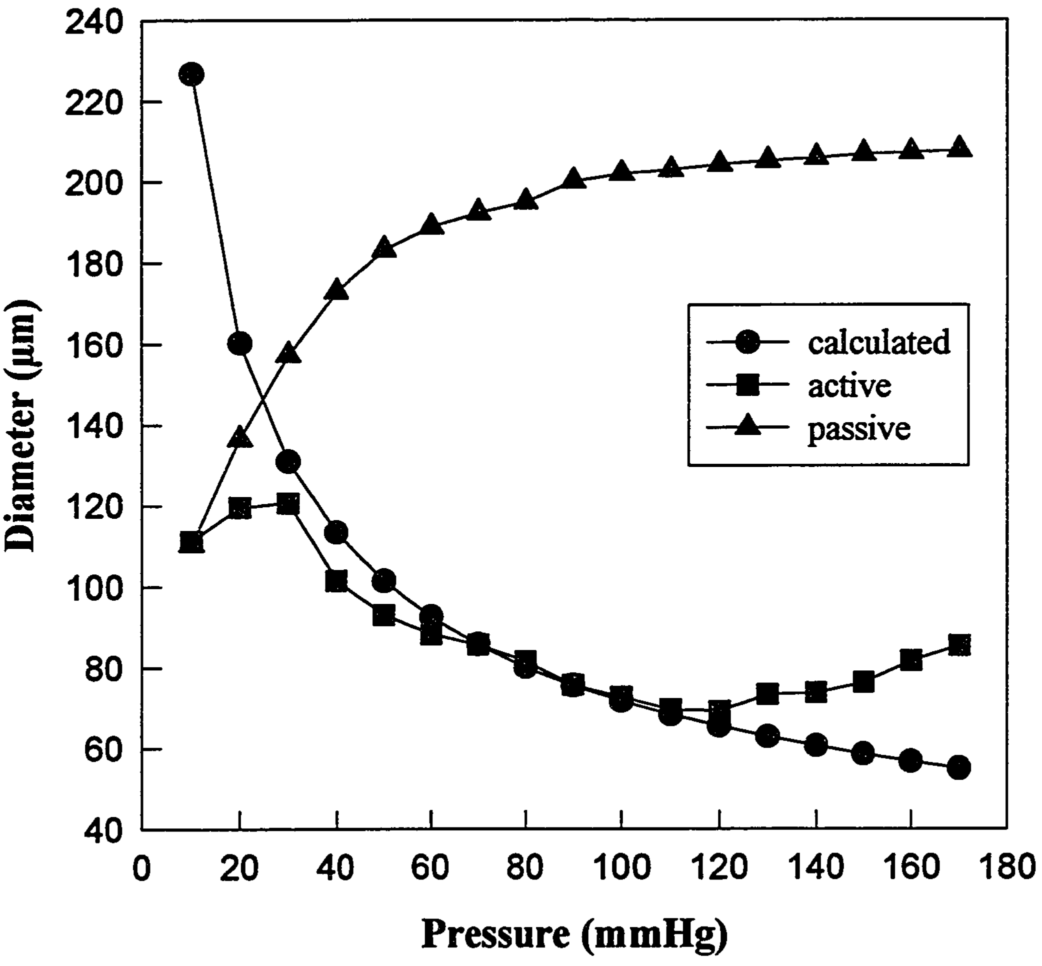

Figure 4-6. Calculated vessel diameter based on the idea that wall tension is the controlled parameter for arteriolar myogenic reactivity and do not change with pressure. Wall tension at 70mmHg is considered to be the controlled value here.

The results of the present study may be of direct relevance to previous reports of modulation of arteriolar agonist responsiveness by intraluminal pressure (Harder, 1988; Nilsson, and Sjoelbolm, 1985; VanBavel and Mulvany, 1994). As pressure is increased so is the level of $[Ca^{2+}]_i$ and MLC phosphorylation, which would be expected to place the vessel in a more activated state or on a steeper section of the Ca^{2+} (or phosphorylation)-contraction relationship. This being the case, agonist responsiveness may vary with intraluminal pressure in a manner determined by the effect of pressure/wall tension on the level of $[Ca^{2+}]_i$ and MLC phosphorylation. Further studies are required to examine the interrelationships among intravascular pressure, $[Ca^{2+}]_i$ and myosin phosphorylation in arterioles exposed to contractile agents.

In recent years several studies including our own have been used to support a role for protein kinase C in modulating basal tone and myogenic reactivity (Hill, et al., 1990; Laher and Bevan, 1987; Osol, et al., 1991). For example, the protein kinase inhibitors staurosporine and H7 were found to inhibit myogenic responsiveness of small cremaster muscle arterioles while the protein kinase C activator, (-)-indolactam potentiated myogenic vasoconstriction. Support for a possible role of protein kinase C is also provided by the observation that increased intraluminal pressure/wall tension results in increased production of DAG (Narayanan, 1994), the physiological activator of protein kinase C. These earlier studies, however, do not necessarily exclude an underlying contribution of the MLC phosphorylation pathway. Indeed at the inhibitor concentrations used basal tone was not inhibited despite marked attenuation of the constrictor response to an acute increase in intravascular pressure. In addition, studies in our laboratory have shown, in mesenteric resistance vessels, that protein kinase C-mediated contractions are dependent on a basal level of $[Ca^{2+}]_i$ and are inhibited by the myosin light chain kinase inhibitor, ML-9 (Hill, et al., 1995). As such, a contribution from multiple mechanisms may occur; however, activation of the myosin light chain kinase pathway appears obligatory.

In regard to methodological considerations the two dimensional gel electrophoretic approach used in these studies detects phosphorylation of myosin light chain by the shift in isoelectric point [the PI for phosphorylated and unphosphorylated MLC are approximately 4.97 and 5.05, respectively (Silver and Stull, 1981)]. As such, this method may not be expected to distinguish between single phosphorylations occurring at different sites. For example, MLCK results in MLC phosphorylation at serine 19 while protein kinase C causes phosphorylation at serine 1 and 2 (Murphy, 1994; Somlyo and Somlyo, 1994). However, as exposure of arterioles to the MLCK inhibitor, ML-7, resulted in an apparent dissociation between $[Ca^{2+}]_i$ levels and arteriolar diameter it appears evident that arteriolar tone and myogenic reactivity are dependent on MLCK-mediated phosphorylation. This is further supported by the observation that, in addition to inhibiting myogenic tone, ML-7 inhibited the pressure-dependent increase in MLC phosphorylation as shown by gel electrophoresis. An additional argument against the involvement of MLC phosphorylation at sites other than serine 19 is provided by *in vitro* studies demonstrating that protein kinase C-induced phosphorylation at sites serine 1 and 2 results in inhibition of smooth muscle contraction rather than activation (Parente, et al., 1992; Saitoh, et al., 1987). It would therefore be inconsistent that increased myogenic tone would be associated with increased phosphorylation at such sites. Definitive evidence for MLC serine 19 phosphorylation during myogenic vasoconstriction would require an approach such as ^{32}P-ATP labeling followed by tryptic phosphopeptide mapping. While this would be exceptionally difficult to perform on microvascular preparations it is important to note that stretch activation of carotid artery strips has been shown to be associated with [^{32}P] incorporation into MLCK phosphorylated peptides (Barany, et al., 1990). Collectively the above evidence strongly supports the methodological approach used and the proposition that basal arteriolar tone and myogenic reactivity is dependent on MLCK mediated phosphorylation of the myosin regulatory light chain.

In summary, the results of the present study demonstrate that the setting of basal arteriolar tone and myogenic reactivity is dependent on the classical Ca^{2+}-stimulated MLC phosphorylation pathway of smooth muscle contraction. Further, the data suggest that in the steady-state the effect of an intraluminal pressure increase may be detected by alterations in wall tension or a related variable.

CHAPTER V

ROLE OF CA^{2+}$_I$ AND MYOSIN PHOSPHORYLATION IN MYOGENIC AND AGONIST-INDUCED ARTERIOLAR CONTRACTIONS

Arterioles characteristically display three types of contractions: 1) basal tone - a maintained state of partial constriction; 2) myogenic contraction - constriction in response to an acute increase in vascular pressure; and 3) reactivity to circulating hormones and neurotransmitters such as norepinephrine. Arteriolar basal tone and myogenic contraction are related and sometimes addressed together as myogenic reactivity, however, the underlying cellular mechanisms may not exactly be the same (Meininger and Davis, 1992). In particular, the cellular events occurring in response to the distention phase of an acute increase in pressure may be obscured by the time steady-state myogenic constriction is achieved.

Agonist-induced smooth muscle contraction has been suggested to consist of two phases, the initial force developing phase and the following phase of sustained contraction (Aksoy, et al., 1986; Moreland, et al., 1990). MLC phosphorylation is believed to be a prerequisite for the initial tension development or contraction. While MLC phosphorylation is decreased during the second phase of contraction, the explanation for the maintained tension has been controversial. Evidence exists for both the "latch bridge" model (Hai and Murphy, 1988) and the hypothesis of thin filament regulation (for review see Walsh, 1994). Moreover, PKC mediated contractile apparatus sensitization for Ca^{2+} has been reported following agonist stimulations (Nishimura, et al., 1990; Itoh, et al., 1993). Such studies, however, are limited to smooth muscle from conduit vessels or non-vascular tissues.

The setting of arteriolar basal tone has been demonstrated to be dependent on Ca^{2+}/CaM activated MLC phosphorylation (Chapter 4). However, whether this holds true for an acute myogenic contraction and arteriolar responsiveness to agonists, such as α-adrenergic agents, has not been determined. Similarly it is unknown whether microvascular smooth muscle shows dissociation between force production (i.e. vasoconstriction) and $[Ca^{2+}]_i$ /MLC phosphorylation during the maintained phase of myogenic or agonist activation. Therefore, to elucidate temporal aspects of Ca^{2+}/MLC signaling, the aims of this study were to test the hypotheses that 1) the arteriolar contractions following acute pressure increases and agonist stimulation also depend on $[Ca^{2+}]_i$ and MLC phosphorylation; and 2) the temporal relationships between stimulus and response are different when comparing pressure- and agonist-stimulation, reflecting difference in signal transduction and Ca^{2+} handling.

Methods and Experimental Protocols

Vessel cannulation, $[Ca^{2+}]_i$ measurement and MLC sample preparation were performed as described in chapter 2. Briefly, isolated rat cremaster first order arterioles were cannulated in a superfusion chamber and initially set at a transmural pressure of 70mmHg in the absence of intraluminal flow. Vessels were superfused with Krebs buffer and maintained at 34°C throughout each of the experiments. $[Ca^{2+}]_i$ was measured using fura-2 as a fluorescent indicator and fluorescence ratio $R_{340/380nm}$ was used for measurement of changes in $[Ca^{2+}]_i$. MLC isoforms were separated by two dimensional polyacrylamide gel electrophoresis. To ensure adequate loading of protein from the microvessel segments it was necessary to pool samples. The separated proteins were quantitated using a computerized image analysis system and MLC phosphorylation expressed as percent phosphorylated MLC of total 20kD MLC. As an index of reproducibility between electrophoretic separations a standard sample of homogenized rat aorta (obtained under conditions of 0 mmHg transmural pressure while superfused with a buffer containing 2.5mM Ca^{2+}) was processed on each day; the extent of phosphorylation was determined to be 14.9 ± 0.5% (mean ± SEM), n = 12 determinations.

Time Course of Ca^{2+} Measurements

The following general time course for $[Ca^{2+}]_i$ measurements was used for both pressure and agonist-stimulations: immediately prior to the increase of pressure or application of NE, six (6) pairs of fluorescence images from 340nm and 380nm excitation were collected at 10 second intervals. Following the stimulation, twelve (12) image pairs were collected at 2 second intervals, then four (4) pairs were taken at 10 second intervals followed by eight (8) pairs at 30 second intervals. A total of thirty (30) pairs of images were taken for each stimulation which covered a 5 minute period post stimulation. For extended monitoring, such as following some of the larger pressure steps, measurements were taken at 30 second or 120 second intervals after the initial 5 minute period.

Sample Collection for MLC Phosphorylation

To avoid time delay and diffusion errors during NE stimulation, applications of the agonist were carried out by a complete bath change when preparing samples for MLC phosphorylation. With the superfusion pump stopped, buffer in the cannulating chamber was rapidly drained with an electric vacuum and quickly replaced with pre-warmed buffer containing an appropriate concentration of NE. The enzymatic reactions were promptly stopped by freezing the vessel segment with acetone/dry ice at the desired time points (~4 seconds, 10~15 seconds and 5 minutes) after the stimulation (application of NE, or pressure step).

The whole procedure was video taped for quick collections (< 15 seconds) and an electronic time generator was used to post time stamps on the tape which allows the confirmation of reaction time before freezing upon replay. For collection of samples at 5 minutes, an electronic caliper coupled to a chart recorder was used for monitoring vessel diameter changes.

Results

Arteriolar diameter and $Ca^{2+}{}_i$ response to acute increase in intraluminal pressure

To determine the time necessary to ensure that steady-state arteriolar diameter and intracellular Ca^{2+} levels had been achieved, following an acute increase in intravascular pressure, the response to a pressure change from 70 - 100 mmHg was followed in a time-dependent fashion (Figure 5-1). The acute pressure step resulted in an initial arteriolar

Figure 5-1. Arteriolar diameter and Ca^{2+} responses to an increase in intraluminal pressure from 70 to 100 mmHg. Absolute arteriolar diameter at 70 mmHg was 85.6 ± 5.8 μm. Data are normalized to account for differences in control diameter and $[Ca^{2+}]_i$ values, respectively. Panel A illustrates that the acute pressure step results in an initial distention of the arterioles followed by vasoconstriction to a diameter significantly smaller than control diameter. $[Ca^{2+}]_i$ (panels B) is seen to increase as the arteriole is distended. Steady-state diameter and Ca^{2+} values are obtained within a 5 minute period. Results are presented as mean ± SEM; * indicates significant different from basal, $p < 0.05$.

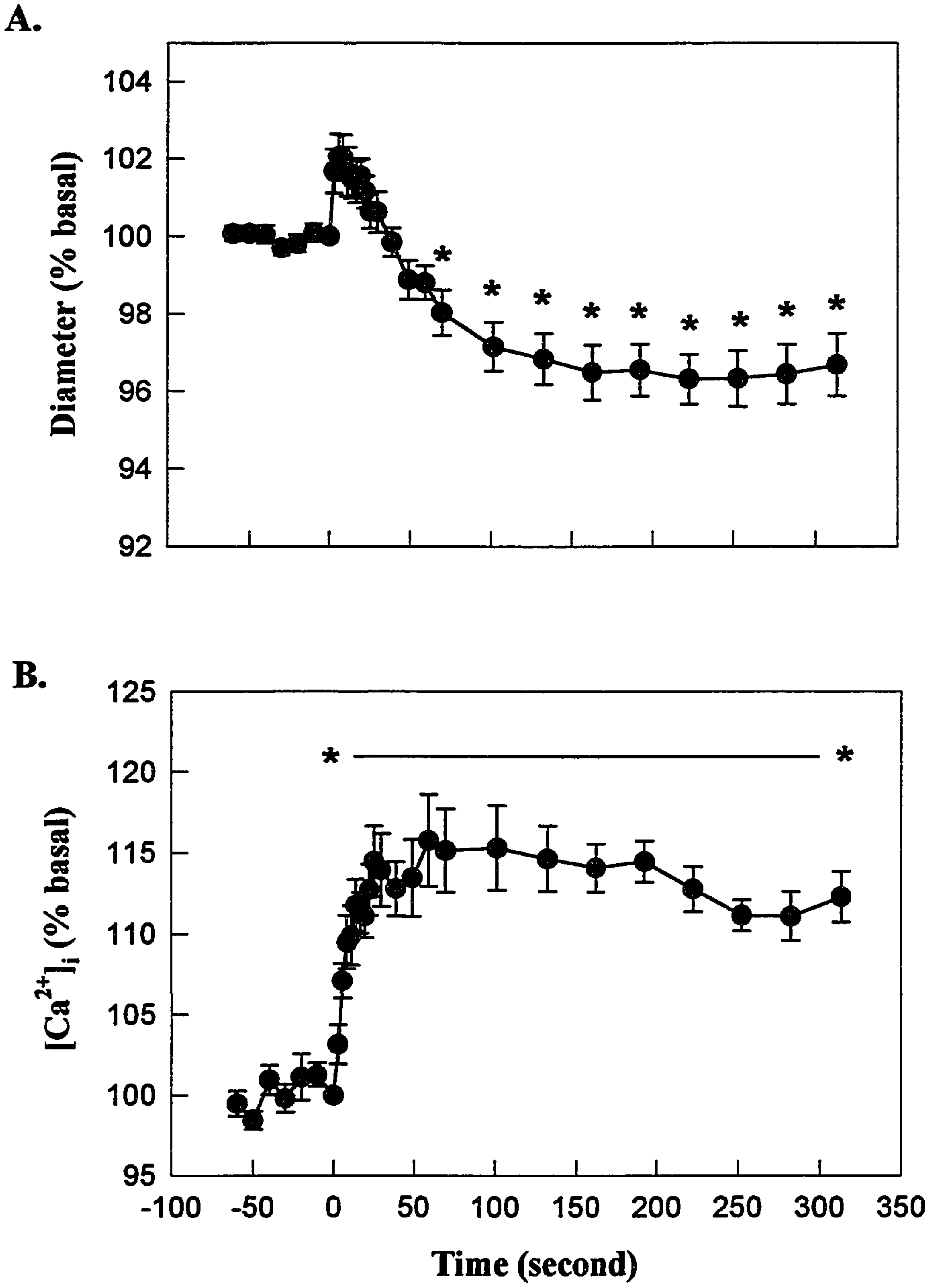
A.
Diameter (% basal)
104
102
100
98
96
94
92
*
*
*
*
*
*
*
*
*
B.
[Ca2+]i (% basal)
125
120
115
110
105
100
95
*
*
-100
-50
0
50
100
150
200
250
300
350
Time (second)

distention followed by vasoconstriction to a diameter significantly ($p < 0.05$) smaller than the control diameter. Intracellular Ca^{2+} showed a monophasic response to the 30 mmHg pressure step, increasing as the vessel was distended and remaining elevated for the duration of the pressure increase. Stable arteriolar diameters and intracellular Ca^{2+} levels were reached within a five minute period.

Similar responses were seen when the same size pressure step increase (30mmHg) was applied to the vessels from different starting (baseline) pressures (Figure 5-2). Vessels have less tone at 30mmHg compared with vessels at 120mmHg, and hence the same stimulus stretches the vessels out further (109.6 ± 0.9% compared with 101.9 ± 0.5%, n = 10 and 9, respectively; $p < 0.001$). A greater Ca^{2+} rise was seen to the pressure increase of 30 to 60mmHg (120.0 ± 2.6 % compared with 110.0 ± 1.3% corresponding to pressure increasing from 120 to 150mmHg). If the response to 70-100mmHg is plotted, it falls in between the curves for 30 to 60mmHg and 120 to 150mmHg and located somewhat closer to the latter one. A comparison of vessel responses to 30 to 60mmHg vs. 120 to 150mmHg is summarized in Table 5-1. Arteriolar diameter and Ca^{2+} responses were also examined when vessels were subjected to greater stretches - pressure step-increased from 50 to 120mmHg and from 30 to 150mmHg (Figures 5-3 and 5-4, respectively). The vessels were forced out further to 112.5 ± 1.5 % and 124.3 ± 2.9% of basal diameters, respectively, and the corresponding maximum Ca^{2+} increase were 129.8 ± 4.1 % and 201.6 ± 12.0 %. The responses to 30-150mmHg were monitored for a longer period of time, 30 minutes after the pressure step, because it was apparent that

Figure 5-2. Arteriolar diameter (A) and Ca^{2+} (B) responses to pressure step increases from 30mmHg to 60mmHg and 120mmHg to 150mmHg. Data are presented as mean ± SEM and normalized to the basal conditions.

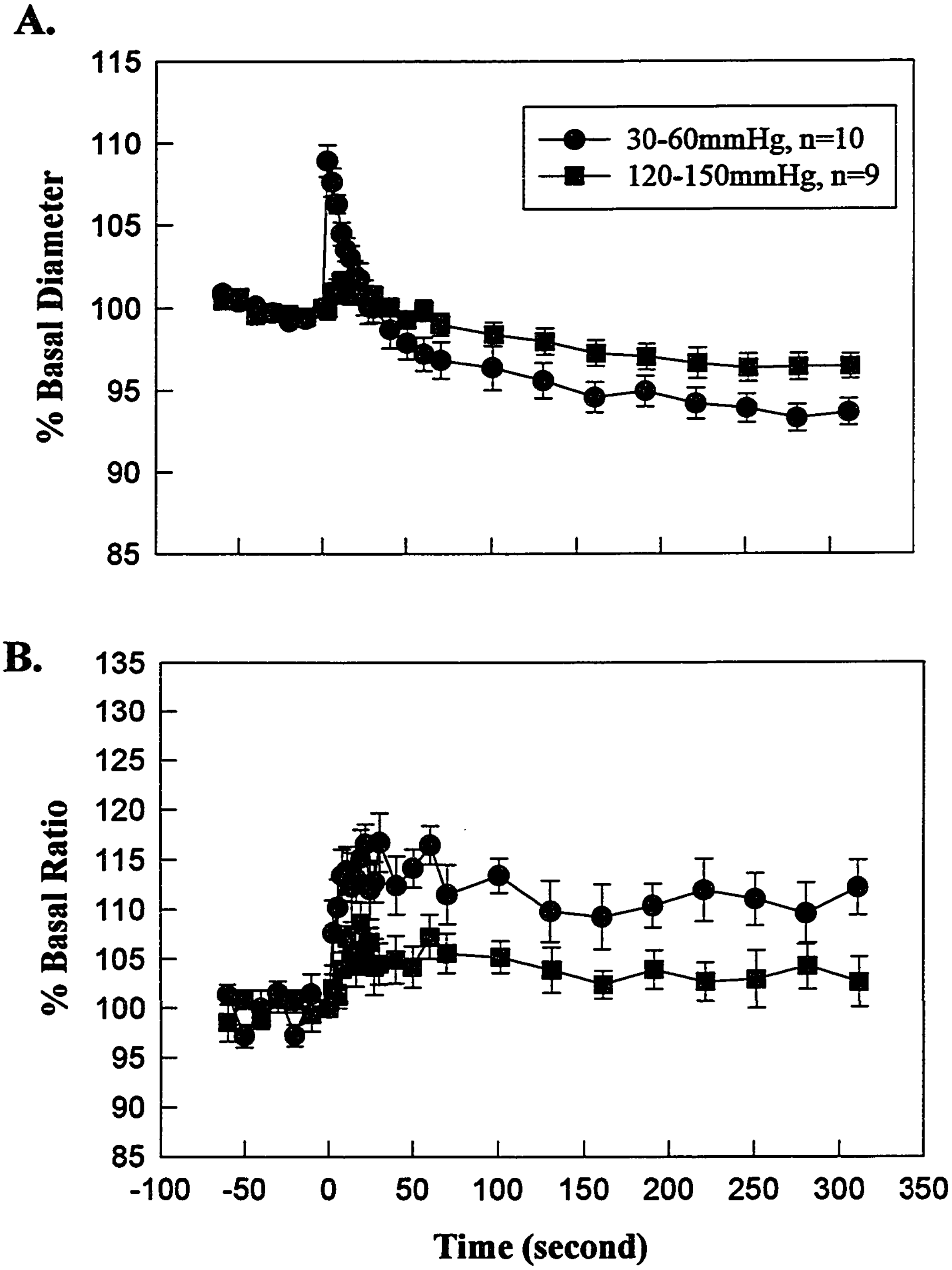
A.
115
110
105
100
95
90
85
% Basal Diameter
30-60mmHg, n=10
120-150mmHg, n=9
B.
135
130
125
120
115
110
105
100
95
90
85
% Basal Ratio
-100
-50
0
50
100
150
200
250
300
350
Time (second)

Table 5-1. Comparison of arteriolar responses to 30mm Hg pressure increase starting at 30 and 120mm Hg.

	Diameter	Tension	peak $[Ca^{2+}]_i$	steady state $[Ca^{2+}]_i$	contraction
30-60mmHg	110%	219%	120%	111%#	93.6%
120-150mmHg	102%*	128%*	110%*	104%*#	96.4%*

All data are presented as changes normalized to the basal conditions (before the pressure step). * indicates significantly different from the corresponding response starting at 30mmHg; # indicates significantly different from peak value of the same pressure step; $p < 0.05$.

despite the large increase in $[Ca^{2+}]_i$ it takes a much longer time period for the vessels to contract following such an extensive stretch.

Linear regressions were fitted between maximum distention (% basal diameter), maximum wall tension increase (% basal wall tension) and maximum Ca^{2+} increase (% basal $[Ca^{2+}]_i$) of the vessels (Figure 5-5). Wall tension was calculated using the Laplace relationship (pressure x radius), here the radius value was taken from the pixel measurement from a region covering vessel diameter in the fluorescent ratio image. Points in the diagrams represent each individual vessel from all of the pressure steps (n=50). A slightly better linear correlation was obtained in the relationship between tension increase and $[Ca^{2+}]_i$ increase ($y = 0.23\ x + 72.9$, $p < 0.001$, $r^2 = 0.83$) than between stretch and $[Ca^{2+}]_i$ increase ($y = 4.07\ x - 313.5$, $p < 0.001$, $r^2 = 0.72$), which further suggests the role of wall tension in regulating myogenic reactivity.

MLC phosphorylation levels following an acute pressure step

MLC phosphorylation levels were examined following a 70-100mmHg pressure increase. From a basal level of 26.7 ± 2.3 % (n=6), MLC phosphorylation increased to 37.0 ± 2.1% ($p<0.05$, n=6) in 10 to 15 seconds after the pressure step while decreasing to 31.9 ± 1.1% (n=5) at 5 minutes. Corresponding to 10-15 seconds after pressure increase from 70 to 100mmHg is the time when $[Ca^{2+}]_i$ reaches the maximum level and the vessels start to contract (refer to Figure 5-1).

Figure 5-3. Arteriolar diameter (A) and Ca^{2+} (B) responses to pressure step increase from 50mmHg to 120mmHg and followed by return to 50mmHg. The vessels were monitored for 10 minutes after each pressure change to ensure the steady state had been reached. By relaxing the vessels, the arteriolar myogenic reactivity also exhibited its function following pressure reduction. Data are presented as mean ± SEM and normalized to the basal conditions (n=5).

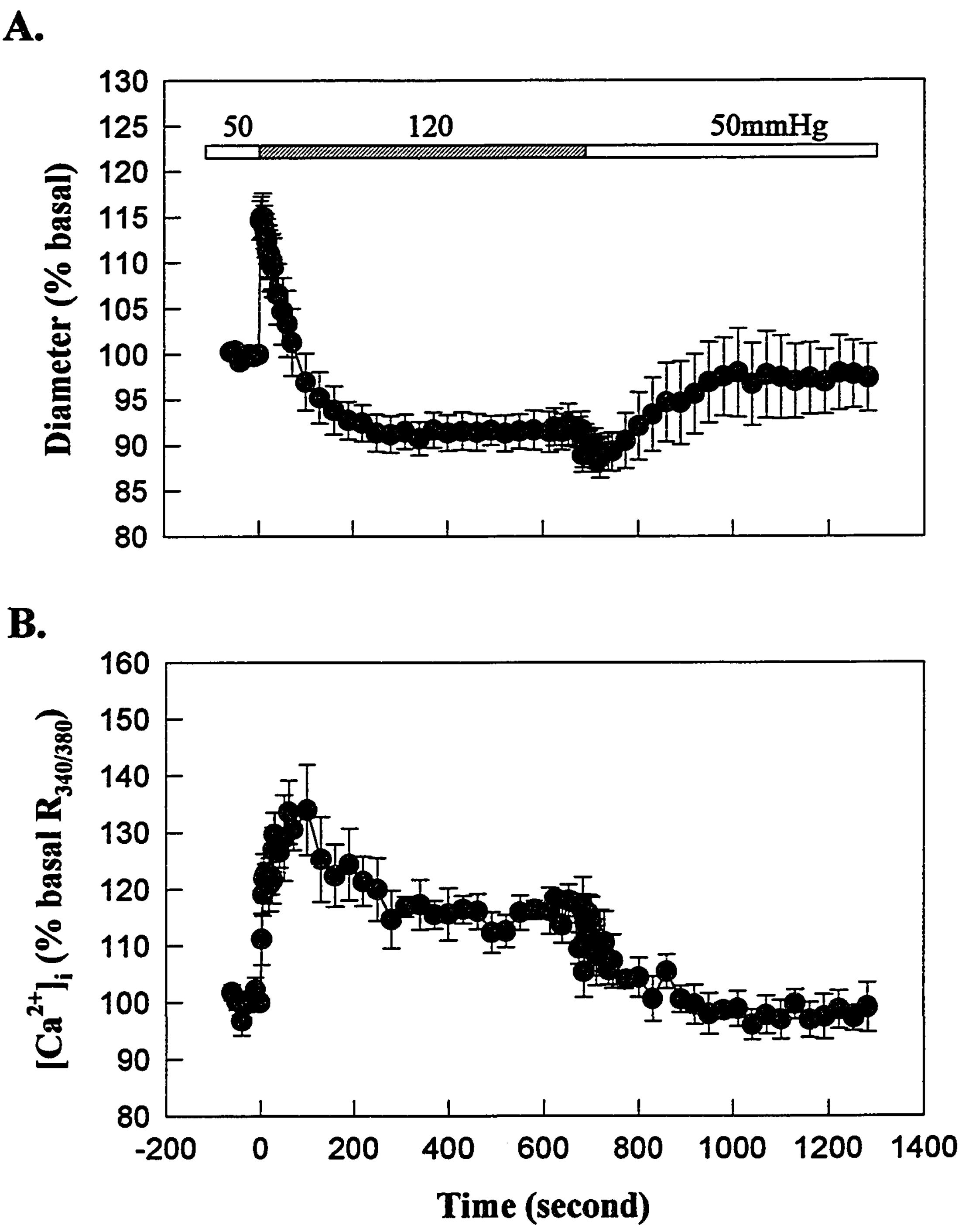
A.
50
120
50mmHg
Diameter (% basal)
130
125
120
115
110
105
100
95
90
85
80
B.
[Ca2+]i (% basal R340/380)
160
150
140
130
120
110
100
90
80
-200
0
200
400
600
800
1000
1200
1400
Time (second)

Figure 5-4. Arteriolar diameter (A) and Ca^{2+} (B) responses to an acute 30-150mmHg pressure step. $[Ca^{2+}]_i$ showed a biphasic increase, however, this was exaggerated by extending the monitoring time to 30 minutes. No significant contraction or $[Ca^{2+}]_i$ decrease was observed at 5 minute, which is the time period usually used for monitoring a arteriolar response. Data are presented as mean ± SEM and normalized to the basal conditions(n=5).

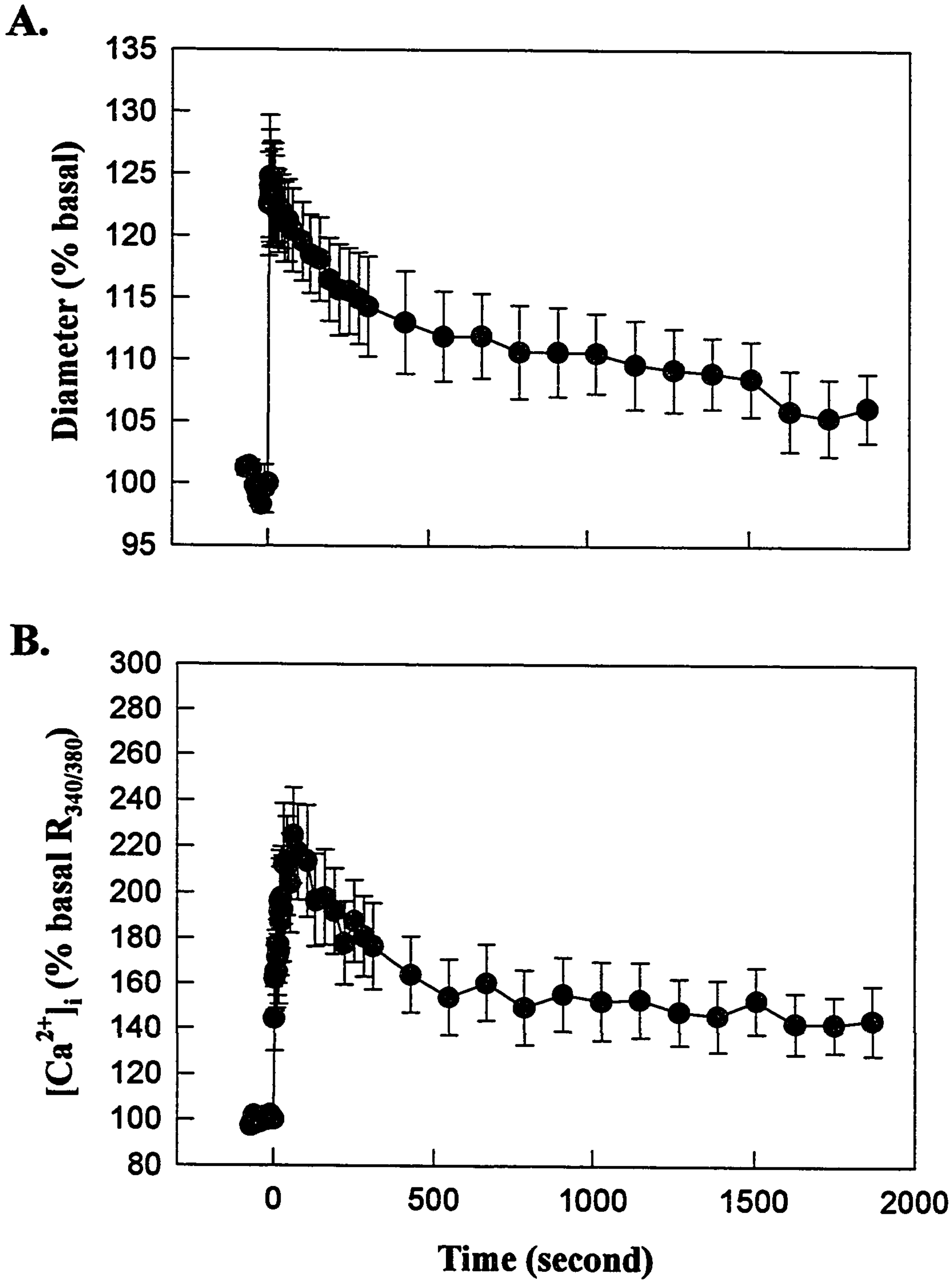
A.
Diameter (% basal)
135
130
125
120
115
110
105
100
95
B.
$[Ca^{2+}]_i$ (% basal $R_{340/380}$)
300
280
260
240
220
200
180
160
140
120
100
80
0
500
1000
1500
2000
Time (second)

Figure 5-5. Relationship between pressure step-induced stretch and $[Ca^{2+}]_i$ increases (A), and increase in wall tension and $[Ca^{2+}]_i$ increase (B). Data came from all the pressure step experiments, n=50.

A.

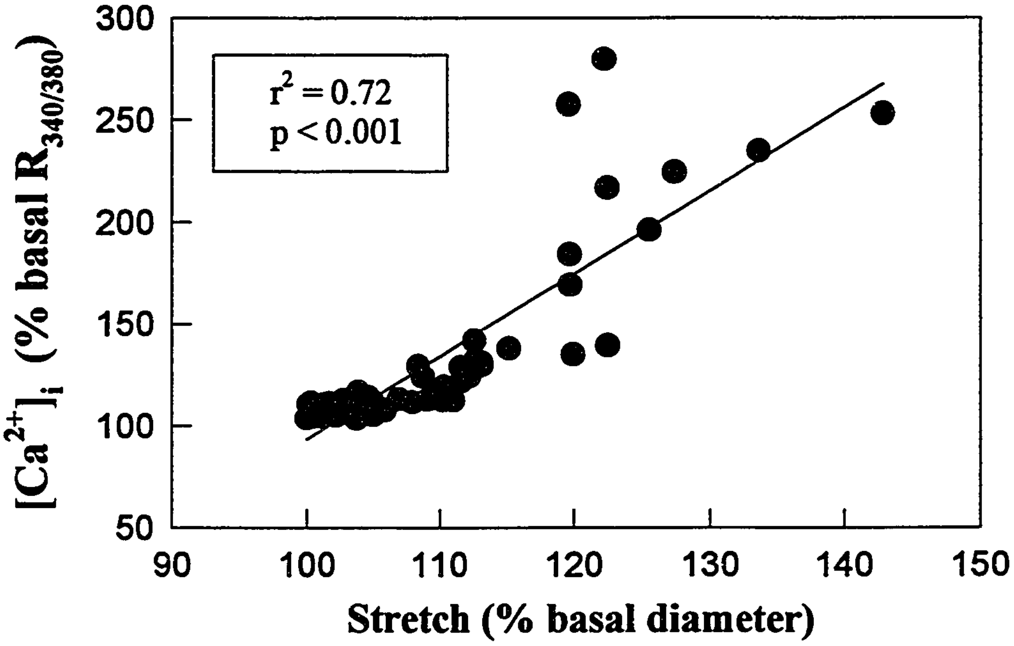
$r^2 = 0.72$
$p < 0.001$
$[Ca^{2+}]_i$ (% basal $R_{340/380}$)
300
250
200
150
100
50
90
100
110
120
130
140
150
Stretch (% basal diameter)

B.

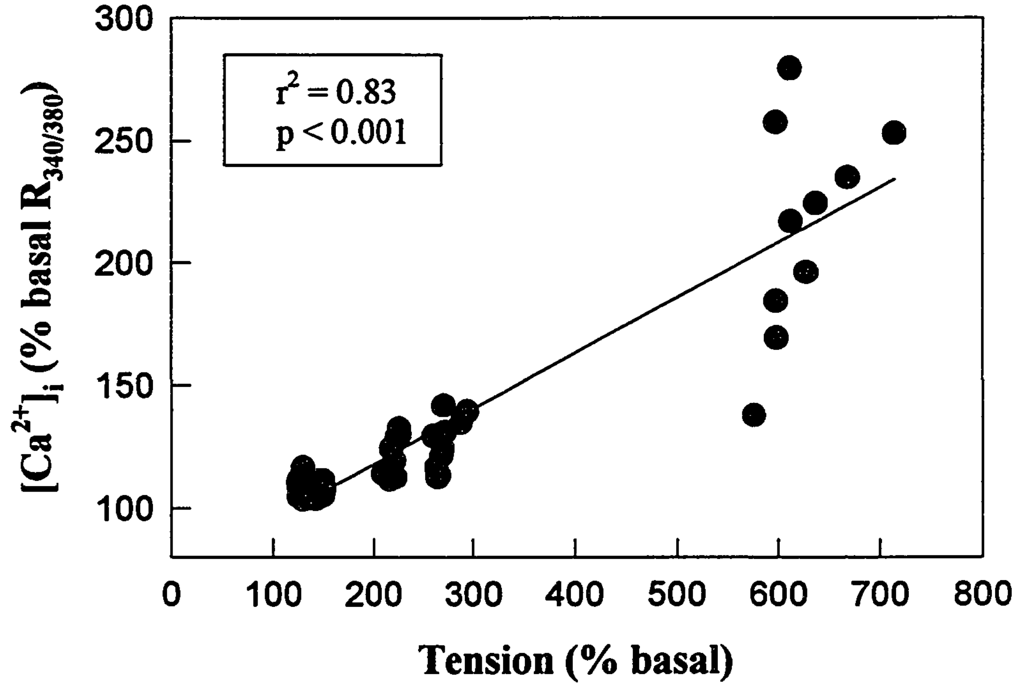
$r^2 = 0.83$
$p < 0.001$
$[Ca^{2+}]_i$ (% basal $R_{340/380}$)
300
250
200
150
100
0
100
200
300
400
500
600
700
800
Tension (% basal)

Arteriolar diameter and $Ca^{2+}{}_i$ response to agonist stimulation

Arteriolar diameter and Ca^{2+} responses to the α-adrenergic agonist, NE, were also examined. Vessels constricted rapidly to NE, 0.1, 1 and 5μM, in a dose dependent manner and the contractions were maintained in presence of agonist (Figure 5-6A). For instance, in response to 0.1, 1 and 5 μM NE, the vessels maximally constricted to 89.2 ± 2.3 %, 77.4 ± 1.6 % and 76.0 ± 1.5 % of the basal diameter, respectively. However, $[Ca^{2+}]_i$ showed more biphasic responses with a rapid spike followed by a plateau phase which remained a significantly increased level at higher concentrations of agonist (Figure 5-6B). The magnitude of both the peak values and the maintained levels at steady states were NE dose dependent. For example, the peak values of $[Ca^{2+}]_i$ increase are 120.5 ± 3.7 %, 191.3 ± 11%, and 257.0 ± 21.0 % corresponding to 0.1, 1, and 5 μM NE stimulation.

MLC phosphorylation levels following an agonist stimulation

MLC phosphorylation levels following 5μM NE stimulation were measured (Figure 5-7). Corresponding with the rapid increase in $[Ca^{2+}]_i$ and vessel contraction, MLC phosphorylation increased to a level of 48.3 ± 2.1% (n=6) within 3~5 second of agonist stimulation. This level decreased to 36.6 ± 2.5 % (n=5) in 10~15 seconds and maintained at 34.1 ± 2.1% (n=5) at 5 minutes. 3~5 seconds approximates the time when $[Ca^{2+}]_i$ reaches the peak level. The MLC phosphorylation levels remained significantly increased during the entire agonist stimulation period.

Comparison of myogenic and agonist-induced contractions

A comparison of arteriolar myogenic constriction (50-120mmHg pressure step) and a comparable contraction to agonist (0.1μM NE) is shown in figure 5-8. In response to the

Figure 5-6. Arteriolar diameter (A) and Ca^{2+} (B) responses to 0.1μM, 1μM, and 5μM NE stimulations. Data are normalized to the basal conditions.

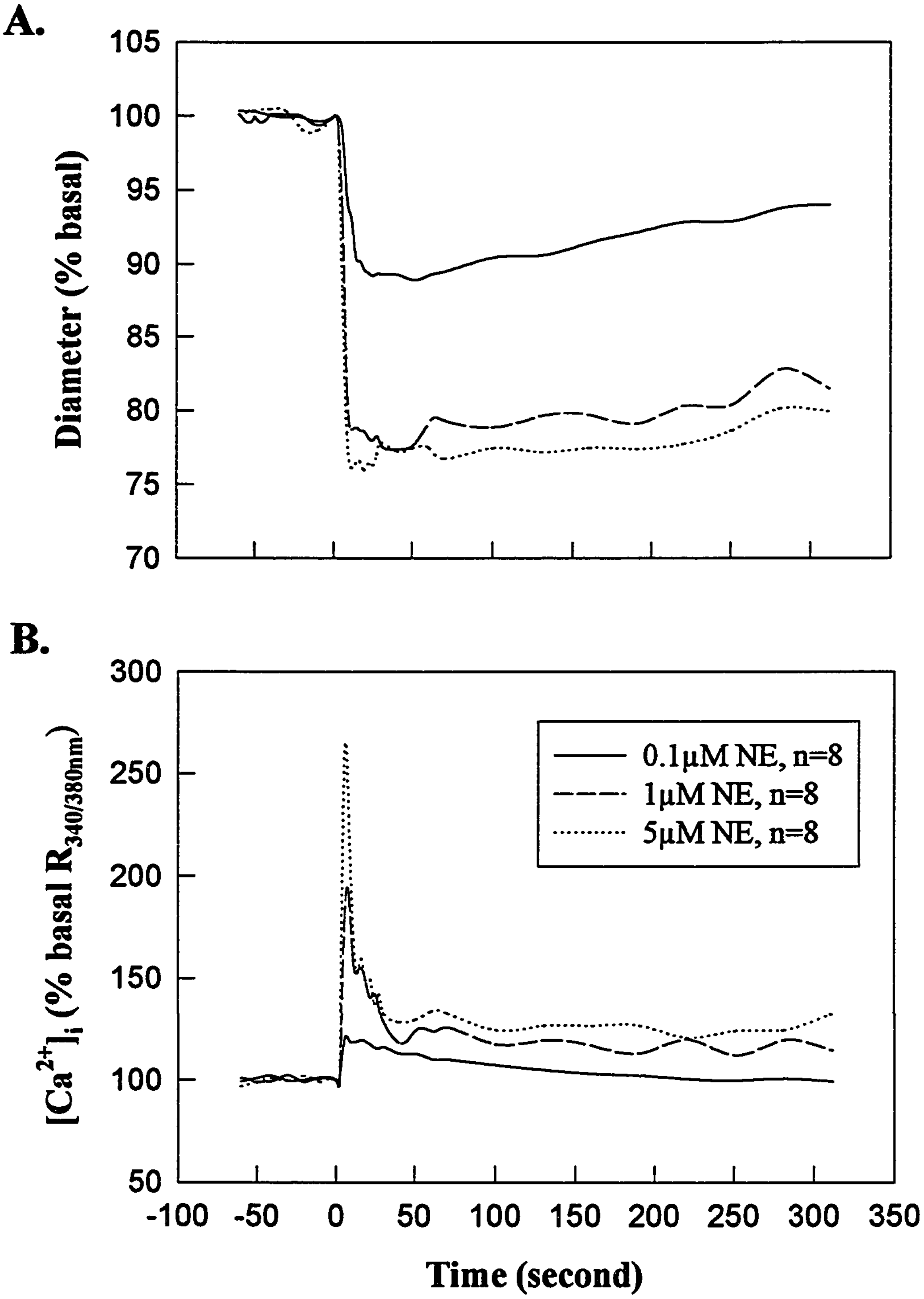
A.
Diameter (% basal)
105
100
95
90
85
80
75
70
B.
[Ca^{2+}]$_i$ (% basal R$_{340/380nm}$)
300
250
200
150
100
50
-100
-50
0
50
100
150
200
250
300
350
Time (second)
0.1μM NE, n=8
1μM NE, n=8
5μM NE, n=8

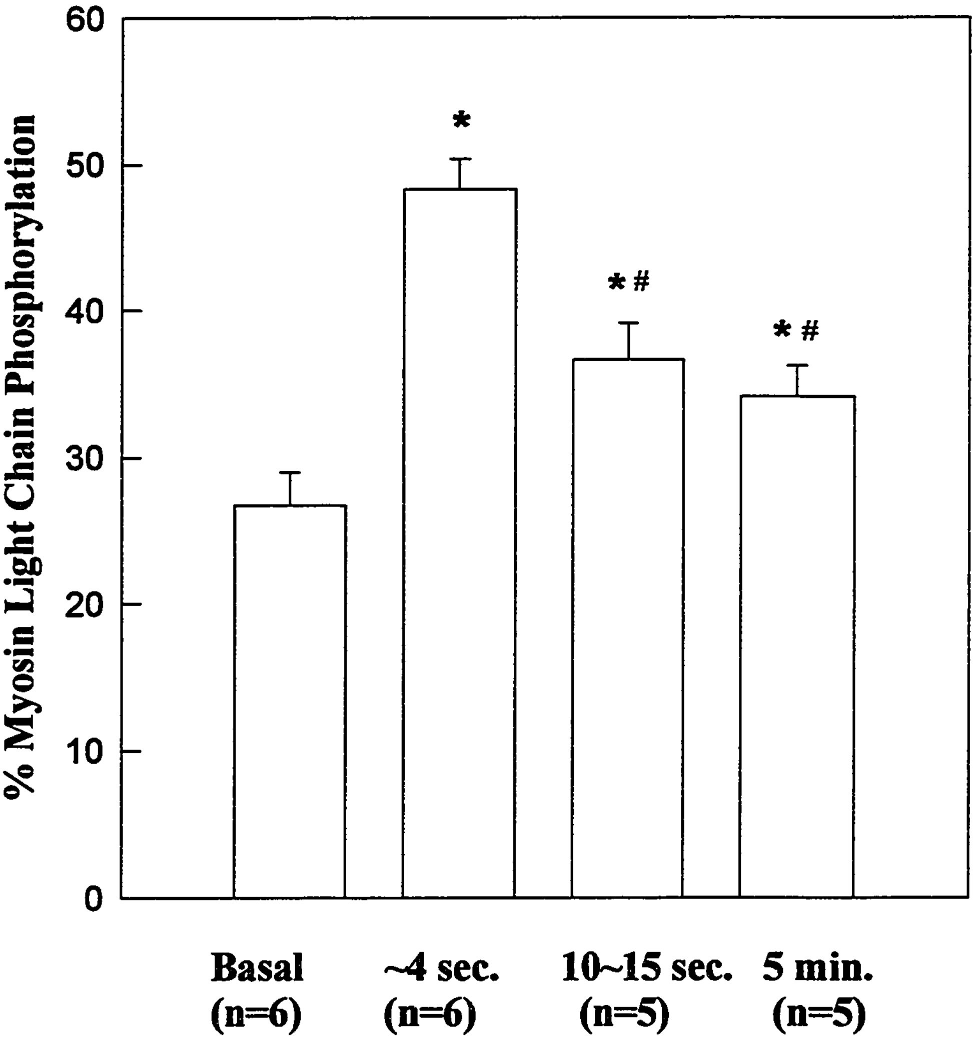

Figure 5-7. MLC phosphorylation following NE stimulation. Data are presented as mean ± SEM. * indicates significant different from basal, # indicated significant from maximum; $p < 0.05$.

Figure 5-8. Comparison of arteriolar diameter (A) and Ca^{2+} (B) responses to an acute pressure increase and a comparable NE stimulation. Data are presented as mean ± SEM and normalized to the basal conditions. * indicates significant different from basal, $p < 0.05$.

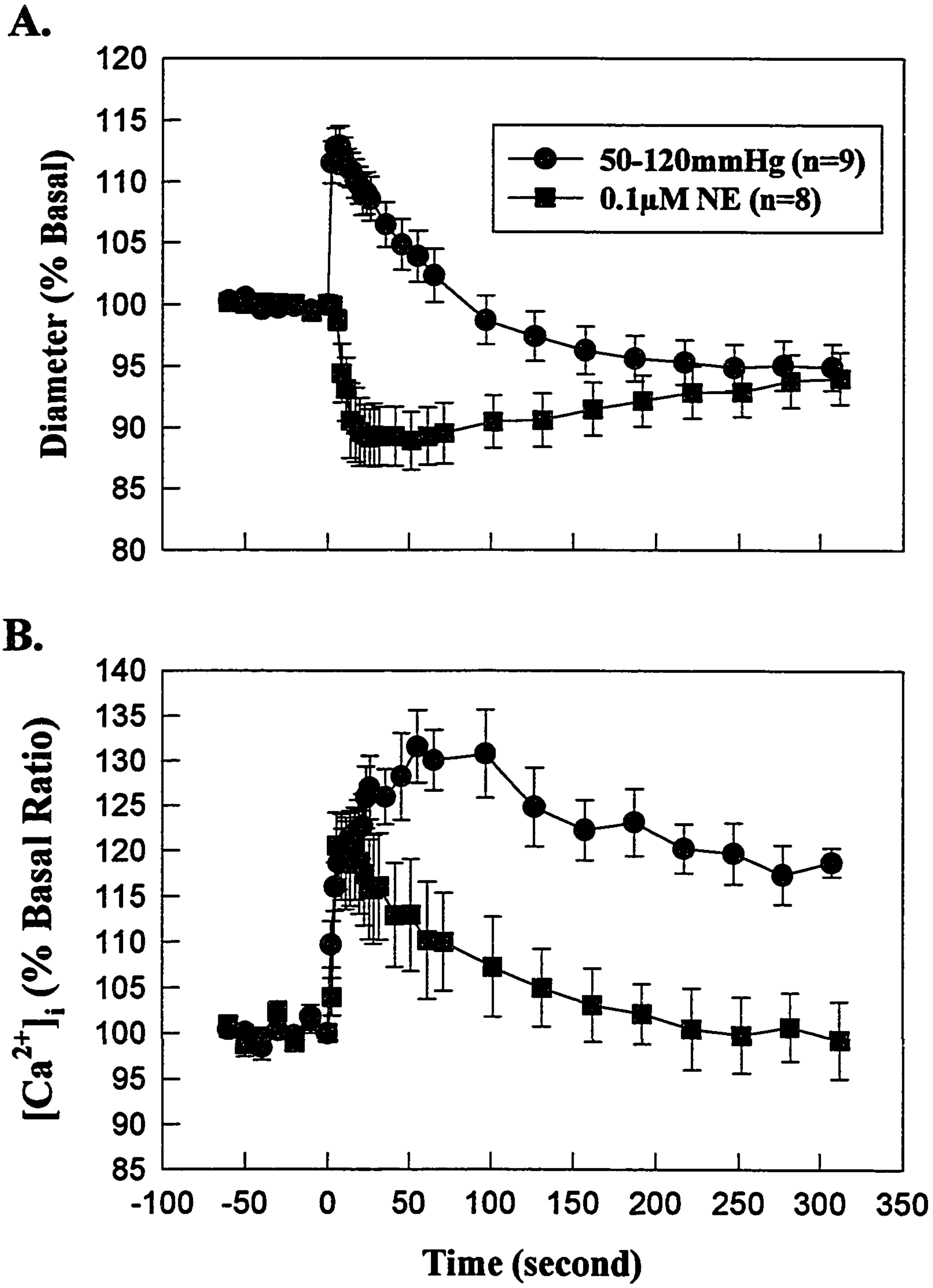
A.
B.
Diameter (% Basal)
120
115
110
105
100
95
90
85
80
50-120mmHg (n=9)
0.1μM NE (n=8)
[Ca^{2+}]$_i$ (% Basal Ratio)
140
135
130
125
120
115
110
105
100
95
90
85
-100
-50
0
50
100
150
200
250
300
350
Time (second)

acute pressure increase, vessels (n = 9) were first distended then slowly contracted to and maintained at smaller diameter while the agonist caused a rapid constriction (at 50 mmHg, n = 8). Although the vessels from both groups constricted to about the same level at steady states (94.9 ± 1.9 % and 94.1 ± 2.1% of basal, respectively), the patterns of contraction were completely different. Further, Ca^{2+} responses were also distinct, for example, at the end of the 5 minute stimulation, $[Ca^{2+}]_i$ remained significantly elevated in the pressure increased vessels (118.7 ± 1.6 %, $p < 0.01$) while declining towards the base line level in agonist-challenged vessels (99.3 ± 4.2%).

Discussion

The results from this study demonstrate that both arteriolar myogenic and agonist induced contractions are associated with increases in $[Ca^{2+}]_i$ and myosin phosphorylation. Further, the increase in vessel wall tension following an acute pressure step correlates linearly ($r^2 = 0.83$) to the resultant peak increase in $[Ca^{2+}]_i$. Higher concentrations of agonist, as well as larger steps of pressure increase, induced Ca^{2+}_i response shows two phases: a transient rapid increase followed by a sustained elevation. Agonist could constrict arterioles to a similar extent as myogenic contraction but at much lower $[Ca^{2+}]_i$, suggesting that the arteriolar contractile apparatus is more sensitive to Ca^{2+}_i during agonist induced contraction than during pressure-induced contraction and implying the possible involvement of additional regulatory mechanisms.

It is currently generally accepted that smooth muscle contraction is caused by Ca^{2+}/CaM activated MLC phosphorylation by MLCK. However, this mechanism has not been tested in resistance vessels probably because of the technical difficulties involved in and the enormous time and patience required for the subject. As far as we know, this study is the first to demonstrate the levels of MLC phosphorylation in arteriolar contraction occurring in response to either pressure or agonist stimulations. Our knowledge on smooth muscle contractions has, thus far, come largely from studies performed on large vessels or non-vascular smooth muscles. Several studies have demonstrated that physical stretch of smooth muscles will cause an increase in $[Ca^{2+}]_i$ and this has been confirmed both at single cell level (Davis, Meininger and Zawieja, 1992; Wellner and Isenberg, 1994) and in smooth muscle tissues from different vascular sites (Laher and Bevan, 1989; Meininger, et al., 1990). There are also reports to show that stretch of both vascular and non-vascular smooth muscles can activate MLCK and increase MLC phosphorylation (Barany, et al., 1990; Csabina, et al., 1986; Ledvora, et al., 1983). However, the experimental approaches involved in these studies may not be physiological. For example, in the studies of Barany et al. and Ledvora et al., MLC phosphorylation levels were measured when porcine carotid arterial smooth muscle strips were stretch to 1.7 times their resting lengths which would not be expected to occur in a *in vivo* situation. Although the MLC phosphorylation levels from the studies of Csabina et al. were found to be increased upon stretch and decayed with time, $[Ca^{2+}]_i$ was not monitored in their study and therefore, the correlation between $[Ca^{2+}]_i$ and MLC phosphorylation was not provided. Experimental methodologies employed in the present study, i.e. changing of intraluminal pressure within a physiological range in cannulated arterioles which demonstrate spontaneous tone, enables us to provide results of close physiological relevance. The dependency of arteriolar myogenic and agonist-induced contraction on Ca^{2+}_i and MLC phosphorylation, as demonstrated in the present study, further confirmed their obligatory roles in smooth muscle contraction, in general.

Decreases in MLC phosphorylation during the prolonged, sustained phase of arteriolar contractions to pressure increases and agonist stimulation were observed in the present study. The decrease in MLC phosphorylation was accompanied by a decline in $[Ca^{2+}]_i$, for example, the $[Ca^{2+}]_i$ increase at 5 minutes after 5μM NE stimulation was 127.1 ± 5.4% compared with 257.0 ± 21.0 % at the maximum increase during the earlier phase. This phenomenon is consistent with the reported observations from other studies (Csabina, et al., 1986; Moreland, et al., 1992). In the studies of Csabina et al., they found that stretch-induced MLC phosphorylation of rat uterus smooth muscle decreased from a maximum value of 83% (within 1 minute of stimulation) to 22% in 30 minutes. It can possibly be explained by the 'latch-bridge" hypothesis put forward by Hai and Murphy (1988) that the actomyosin interaction has changed from a state of active cross-bridge cycling to a state of dephosphorylated, non-cycling attachment of myosin heads to actin filaments. In the case of cannulated arterioles this may translate to the tendency for the vessel to hold its diameter rather than further constricting. The transient increase in MLC phosphorylation observed by Moreland et al. (1992) was under a Ca2+ clamped condition may suggest a novel regulatory mechanism. However, this may or may not be involved in our studies because the increase in MLC phosphorylation was accompanied by an increase in $[Ca^{2+}]_i$. Thin filament regulation is a possible alternative explanation to this situation. It is also possible that caldesmon or calponin, as suggested by other investigators (Katruyama, et al., 1992; Walsh, 1994), come in to play during this latter phase, however, studies of thin filament regulation in intact vessels are lacking. Further biochemical studies will be needed to address the involvement of these possibilities in arteriolar smooth muscle contraction.

From the previous chapter, we know that steady state $[Ca^{2+}]_i$ at 120mmHg is significantly higher than that at 30mmHg, and this increased $[Ca^{2+}]_i$ may indicate a more activated state of the vessel at higher pressures. Therefore, comparison of the vessels' response to the same pressure/stretch stimulation (i.e. 30mmHg pressure step) at different starting pressure will allow us to examine the modulatory effect of varied levels of basal activation. While 70mmHg is considered the *in vivo* pressure for rat cremaster first order arterioles, 30mmHg and 120mmHg corresponds to the two pressures within which the myogenic regulation appears to be most effective (refer to Figure 4-1). Vessels were found to be distended further by the same pressure step at lower pressures due to the decreased level of tone possessed at those pressures, however, the patterns of responses are similar. Notice that the contraction to 120-150mmHg pressure increase is less than that to 30-60mmHg; one may argue that at higher pressures the vessels are desensitized to pressure increase/stretch. However, this is unlikely because a larger increase in both stretch and tension occurred at the lower pressure, although the applied pressure step was the same (Table 5-1). In other words, the level of stimulation that vessels faced at lower pressure was actually greater than that at higher pressure which, together with the accompanied greater $Ca2+_i$ response, could explain the differences between the contractions. Moreover, the responses between the two appeared closer if data was shown in the forms of absolute change because arteriolar $[Ca2+]_i$ was higher and vessels were maintaining smaller diameters at the higher pressure (data not shown).

Presenting the data in relative changes was to eliminate the variations between basal condition of each vessels and as such to provide a clearer display of the results.

In response to greater stretches (e.g. pressure step from 50 to 120mmHg or from 30 to 150mmHg) vessels showed definite biphasic $[Ca^{2+}]_i$ increases which may indicate a two-component $Ca^{2+}{}_i$ mobilization with each component having different 'stretch sensitivity'. This biphasic $[Ca^{2+}]_i$ increase actually also existed in the responses to 30mmHg pressure step (as shown in Table 5-1), however, it was less apparent and obscured in the group data by variations in the time course of the $[Ca^{2+}]_i$ increase for individual vessels (Figure 5-2). The possible mechanisms for the $[Ca^{2+}]_i$ increase during arteriolar myogenic and agonist-induced contractions are discussed in the next chapter. An observation that remains very interesting was that, after the transmural pressure increased from 30 to 150mmHg, the vessels did not constrict as quickly as they did in responding to other pressure steps although the increase in $[Ca^{2+}]_i$ was much higher. It is possible that the vessels have been damaged by the vigorous stretch (about 124% of basal). But, this seems unlikely, or at least the damage is readily reversible, since upon returning pressure to 70mmHg vessels still exhibited a level of spontaneous tone comparable to that occurring prior to the large pressure step (data not shown). Further, similar amount of stretch (i.e. approximately 25%) have been applied to vascular smooth muscle cells without apparent damage (Davis, Donovitz and Hood, 1992). Another explanation is that the vessels have been stretched out so far that the overlap of thick and thin filament is compromised and the smooth muscle enters the descending limb of its length-tension relationship and therefore the force generation appeared to be slow. Such being the case, one would expect a faster shortening velocity once the vessel started to contract. However, this is still not true in our situation. For example, vessels contracted about 2.1 % between 3 and 5 minute after the pressure step while about 0.1 % between 13 and 15 minute and 0.4 % between 23 and 25 minute. An additional argument against a marked shift to a less favorable position on the length-tension curve is that despite the large magnitude of the pressure step absolute pressures remained within the normal myogenic range. Measurement of MLC phosphorylation levels may help to further interpret this data and will provide an interesting direction for future studies.

Wall tension has been proposed to be the controlled variable in myogenic reactivity (Johnson, 1980), and the studies presented in the previous chapter have shown that steady state $[Ca^{2+}]_i$ is approximately linearly related to the arteriolar wall tension. It is exciting to notice from the present study that the increase in $[Ca^{2+}]_i$ following an acute pressure step increase is better correlated with the increase in wall tension than the degree of stretch. This, again, suggests that wall tension may be vitally important in regulation of arteriolar myogenic reactivity. When intraluminal pressure increases vessels are distended and tension increases, the amount of stretch (change in diameter) is related to the tension change because tension is the product of pressure and vessel radius. As vessels constrict to the increased pressure, their diameter decreases and therefore the stimulation is removed (if the stretch is considered the stimulus). One would then expect the $[Ca^{2+}]_i$ would come back to the basal level; however, this is not what the data indicated. In contrast, if we consider tension as the stimulus and the parameter to control, we would still expect an increased $[Ca^{2+}]_i$ because the contraction does not fully compensate for the pressure increase and therefore tension is still elevated (i.e. an error signal remains). The relative roles of stretch and tension will be further investigated in future studies in which the rate of application of the pressure stimulus will be varied (e.g. slow ramp increase).

Using single smooth muscle cells freshly isolated from pig coronary artery, Davis, Meininger and Zawieja (1992) found that progressive stretch is associated with graded, sigmoidal increase in $[Ca^{2+}]_i$ although they did not provide a correlation coefficient between the two variables. Tension was not measured in their study either, it would be very difficult to do so in their system, but, the stretch caused increases in cell length which would be expected to lead to increases in tension. However, the relationship between tension and $[Ca^{2+}]_i$ may not be necessarily linear, although a significant correlation has been found in the present study. It is possible that a linear relationship is approximated only within the range we tested while this range is but a small portion of the whole relationship, e.g. when stimulation (stretch) is beyond an appropriate physiological range the tension-$[Ca^{2+}]_i$ curve may become exponential. In fact, our data appeared to show this trend when vessels were subjected to a pressure increase from 30 to 150mmHg [as shown in Figure 5-6 (B) represented by the group of points on the right most part of the curve]. More data with greater variation in stimulation magnitude will be needed to define such a relationship.

Another finding in the present studies is that when different stimuli are matched for a similar extent of arteriolar contraction at steady state, the pressure step (50-120mmHg) generated a greater $[Ca^{2+}]_i$ increase than the agonist (0.1μM NE) stimulation (as shown in Figure 5-10). Therefore, smooth muscle cells appear more sensitive to the effects of Ca^{2+}_i in the presence of the agonist. Similar results showing smooth muscle sensitization during agonist stimulated contractions have been reported by other investigators and many studies have suggested that this sensitization is due to the PKC activated MLC phosphatase inhibition (Katruyama and Morgan, 1993; Kitazawa, et al., 1991; Nishimura, et al., 1990). For example, using α-toxin permeabilized rabbit portal veins pre-stimulated with Ca^{2+} (pCa 5), Kitazawa et al. (1991) showed that phenylephrine and GTPγS decreased the rate of MLC dephosphorylation in presence of a MLCK inhibitor, ML-9. Further, they demonstrated that under Ca^{2+}-clamped conditions, addition of GTPγS increased the force generation without any effect on MLCK activity. Experiments from our own laboratory (Hill, et al., 1996) have shown that in α-toxin permeabilized rat small mesenteric artery preparations the PKC activator, indolactam, induces contraction at constant $[Ca^{2+}]_i$ and that this contraction is associated with an increased MLC phosphorylation (e.g. in pCa 7 buffer, 1μM indolactam contracted the vessel to approximately 60% of maximal diameter and the MLC phosphorylation level increased from 7.5 ± 1.8 % to 29.5 ± 6.6 %). This, again, supports the hypothetical role of PKC in sensitizing smooth muscle cells by inhibiting MLC phosphatase and demonstrates that such mechanisms are active in small arterial vessels.

In summary, the present study further supports the hypothesis that intracellular calcium and myosin light chain phosphorylation play obligatory roles in arteriolar myogenic reactivity. Vascular wall tension may be a factor of great significance in regulating acute myogenic responses. Agonist (norepinephrine) induced arteriolar contractions are also dependent on the Ca^{2+}/CaM activated MLC phosphorylation pathway. However, the differences in temporal responses between myogenic and agonist-induced contractions indicate that different signal transduction pathways are present. The data also suggest that other regulatory mechanisms, such as the sensitization of the contractile elements perhaps by pathways involving PKC, may contribute to the agonist-induced response.

CHAPTER VI

INVOLVEMENT OF EXTRACELLULAR AND INTRACELLULAR CA^{2+} IN ARTERIOLAR MYOGENIC AND AGONIST-INDUCED CONTRACTIONS

Cytosolic Ca^{2+} may come from two distinct sources: either the extracellular space via influx through various Ca^{2+} channels or the intracellular stores by different release mechanisms. The Ca^{2+} concentration gradient across the plasma membrane as well as the membrane of intracellular stores (presumable SR) is approximately 10,000 fold with a cytosolic concentration about 100nM under resting conditions. This much lower [Ca^{2+}]$_i$ is maintained, mostly, by the Ca^{2+}-ATPase and Na^{+}-Ca^{2+} exchanger on plasma membrane working together with the Ca^{2+}-ATPase on intracellular store membrane. While there is evidence to show that the voltage operated Ca^{2+} channels on smooth muscle cell membrane account for the Ca^{2+} influx to maintain arteriolar basal tone (Harder, et al., 1987; Jackson and Duling, 1989), stretch activated cation channels, recently found in both vascular and visceral smooth muscle cells, have also been reported to contribute to the Ca^{2+} influx upon stretch (Kirber, et al., 1988; Davis, Donovitz and Hood, 1992). Although the role of SACs has been speculated to be responsible for causing smooth muscle cell depolarization, to date, there is no direct evidence for their involvement during the pressure induced arteriolar myogenic response (Meininger and Davis, 1992). Receptor operated Ca^{2+} channels, which have been demonstrated in other cell types (Felder, et al., 1992; Llopis, et al., 1992), remain putative and need to be further characterized in smooth muscle cells. Two principal types of intracellular Ca^{2+} stores have been implicated in smooth muscle contraction: the IP_3 sensitive stores and the ryanodine sensitive stores (Iino, 1990), however, the relationship between these stores is still a subject of dispute. Despite a number of studies have demonstrated stretch-induced Ca^{2+} release from these stores, evidence for the intracellular Ca^{2+} mobilization during arteriolar myogenic contractions is still lacking.

In previous chapters, the role of Ca^{2+} and MLC phosphorylation in arteriolar myogenic and agonist-induced contractions has been discussed and the findings support an obligatory role for Ca^{2+}/CaM activated MLC phosphorylation in microvascular smooth muscle contraction. However, the question as to the exact source, or sources, of Ca^{2+} which are required for activation of the contractile process in microvascular smooth muscle during myogenic activation remain uncertain.

The aim of this chapter was to determine, in isolated skeletal muscle arterioles, the pathways by which $[Ca^{2+}]_i$ is increased to initiate arteriolar myogenic and agonist-induced contractions. Comparisons between myogenic and adrenergic agonist-induced contractions were performed as the Ca^{2+} requirements of the latter mode of smooth muscle activation has been more widely studied. Further, the experimental approach was designed to provide insight into the relative contribution of voltage-gated Ca^{2+} entry, intracellular release and Ca^{2+} sensitization to these two distinct modes of activation of microvascular smooth muscle.

Methods and Experimental Protocols

The methods for vessel isolation, cannulation and $Ca^{2+}{}_i$ measurement were described in detailed in chapter 2. Briefly, isolated rat cremaster first order arterioles were cannulated in a superfusion chamber and initially set at a transmural pressure of 70mmHg in the absence of intraluminal flow. Vessels were superfused with Kreb's buffer and maintained at 34°C throughout each of the experiments. $[Ca^{2+}]_i$ was measured using fura-2 as a fluorescent indicator and fluorescence ratio $R_{340/380nm}$ was used as a measurement of change in $[Ca^{2+}]_i$. Vessel diameter was measured both using electronic caliper system and the pixel counting technique.

Time Course for Ca^{2+} Measurements

The following general time course for $Ca^{2+}{}_i$ measurements was used for both pressure and agonist stimulations: immediately prior to the increase of pressure or application of NE, six (6) pairs of fluorescence images from 340nm and 380nm excitation were collected at 10 second intervals. Following stimulation, twelve (12) image pairs were taken at 2 second intervals, then four (4) pairs were collected at 10 second intervals followed by eight (8) pairs at 30 second intervals. A total of thirty (30) pairs of images were taken for each stimulation which covers an approximately 5 minute period post stimulation.

Effect of Ca^{2+} Entry Blockade on Arteriolar Basal Tone and Response to an Acute Increase in Intraluminal Pressure

To determine the role of voltage-gated Ca^{2+} entry in myogenic vasoconstriction, changes in intracellular Ca^{2+} and vessel diameter were monitored during an acute pressure step from 50 - 120 mmHg in the absence and presence of a VOC blocker, verapamil. Verapamil, at a final concentration of 1 and 10μM, was added to the superfusate reservoir and the arterioles were pre-treated for a period of 20 minutes. Verapamil was used in preference to the dihydropyridine antagonist, nifedipine, as preliminary studies found this latter agent to be adversely affected by the illumination conditions resulting in unstable levels of arteriolar basal tone and fluorescence emission. This problem was not encountered with verapamil. Images were collected according to the general time course described above. Gd^{3+} was added along with 10μM of verapamil to further eliminate Ca^{2+} entry, particularly via SACs (Yang and Sachs, 1989).

Effect of Ca^{2+} Entry Blockade on Adrenergic Agonist-Induced Arteriolar Contraction

Changes in intracellular Ca^{2+} and vessel diameter were monitored during exposure to either norepinephrine at final concentrations of 0.1, 1 and 5 μM. Images were collected using the general time course described above. While the intracellular Ca^{2+} release has been suggested to be involved in agonist-induced contractions, contribution of Ca^{2+} influx to the intracellular $[Ca^{2+}]_i$ is less studied. Ca^{2+} channel blockers, Verapamil and Gd^{3+}, were added to the superfusate as above to determine the role of Ca^{2+} entry in the agonist-induced constriction.

Relationship Between Arteriolar Intracellular Ca^{2+} Stores Accessed by Caffeine and α-Agonist

To demonstrate whether overlap existed between the arteriolar caffeine and agonist-accessible Ca^{2+} pools studies were conducted after swapping from Ca^{2+} containing extracellular buffer to a Kreb's solution with 0mM Ca^{2+} and 2mM EGTA. The superfusion bath was rapidly exchanged (x2) with the 0 Ca^{2+} solution immediately followed by an exposure to caffeine (20 mM), and after the 340/380nm fluorescence signal declined a 5µM concentration of phenylephrine (PE) was applied. Following this, vessels were superfused with Ca^{2+} containing solution and allowed to re-develop the initial level of spontaneous tone. The experiments were then repeated with the exception the response to phenylephrine was examined before the exposure to caffeine.

Effect of Ryanodine on Arteriolar Tone and Acute Myogenic Reactivity

To further study the contribution of intracellular Ca^{2+} stores to myogenic tone, experiments were conducted using the following protocol:

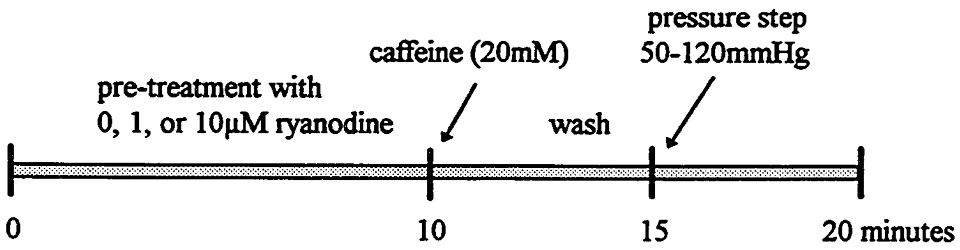

arterioles were pretreated (10 minutes) with ryanodine (1 or 10µM) and then briefly exposed to caffeine (20mM). The exposure of the vessels to caffeine served two aims: 1. test the effectiveness of ryanodine on emptying caffeine accessible stores by inducing a release and 2. further facilitate the action of ryanodine by opening the Ca^{2+} release channels because ryanodine functions better when the channels are in an open state (Meissner, 1986). Following the wash out of caffeine (5 minutes), the [Ca^{2+}]$_i$ and diameter responses to an acute 50 - 120 mmHg pressure step was monitored. Experiments were performed in the standard Kreb's solution containing 2.5 mM Ca^{2+}.

Effect of Steady-State Intraluminal Pressure on Caffeine-Induced $[Ca^{2+}]_i$ *Changes*

After collection of the baseline diameter and 340/380 nm fluorescence ratio measurements, arteriolar segments were exposed to caffeine at a final concentration of 20mM in the presence of the standard Kreb's buffer containing 2.5mM Ca^{2+}. The response to caffeine was measured with the vessels set to an intraluminal pressure of either 50 or 120 mmHg after which the vessel was washed with fresh buffer (20 minutes) and the response repeated at the other pressure. The pressure at which the first measurement was taken did not affect, in itself, the subsequent response to caffeine at the other pressure. After completion of the above, vessels were again washed and the responses to caffeine were repeated in the presence of 1μM verapamil to assess the effect of pressure on Ca^{2+} entry blockade mediated alteration of caffeine accessible stores.

Mn^{2+} Quench Studies

To provide evidence for Ca^{2+} influx and intracellular release during pressure and agonist-induced stimulation the superfusate bathing fura-2 loaded arterioles was rapidly changed from the standard Kreb's solution to a similar buffer containing 1mM Mn^{2+} and lacking added Ca^{2+}. As shown in the protocol diagram below, within 10~15 seconds of changing the bath the appropriate stimulus was applied to the vessel. Changes in intracellular fluorescence were monitored with excitation at 340nm and 360nm. The rationale behind this approach was Mn^{2+} would enter the vessel via the same Ca^{2+} influx pathways mediating basal tone and quench the fluorescence signals emitted following excitation at both 340 and 360 nm. Further, the Mn^{2+} would dilute the effects of any residual extracellular Ca^{2+}: removal of Ca^{2+} would normally require exposure to a buffer containing 0mM Ca^{2+} with EGTA, a procedure which rapidly results in depletion of arteriolar intracellular Ca^{2+} stores. If, in the presence of the Mn^{2+} containing buffer, either a pressure stimulus or agonist released intracellular Ca^{2+} this would be evident as an increase in intensity of the 340nm fluorescence signal while little change should be observed for the isobestic 360nm wavelength.

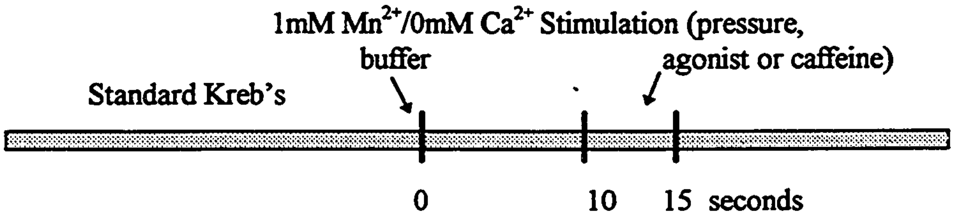

Results

Effect of Ca^{2+} Entry Blockade on Arteriolar Basal Tone and Response to an Acute Increase in Intraluminal Pressure

Application of the L-type voltage-operated calcium channel blocker, verapamil, resulted in a dose dependent inhibition of arteriolar basal tone and an accompanying decrease in $[Ca^{2+}]_i$ (Figure 6-1, measurements were taken under steady states conditions at intraluminal pressures of 50 and 120mmHg in presence of 0, 1, and 10μM verapamil). For example, at 50mmHg, $R_{340/348nm}$ were 0.83 ± 0.03% and 0.78 ± 0.01% under conditions of control and pre-treatment with 1μM verapamil corresponding to diameters of 98.9 ± 7.3% and 136.3 ± 8.1%, respectively. Although vessels were almost maximally dilated in

Figure 6-1. Effect of Ca^{2+} entry blockade on arteriolar steady state basal tone (A) and $[Ca^{2+}]_i$ (B). * indicates significant from basal; $p < 0.05$. Data are presented as mean ± SEM.

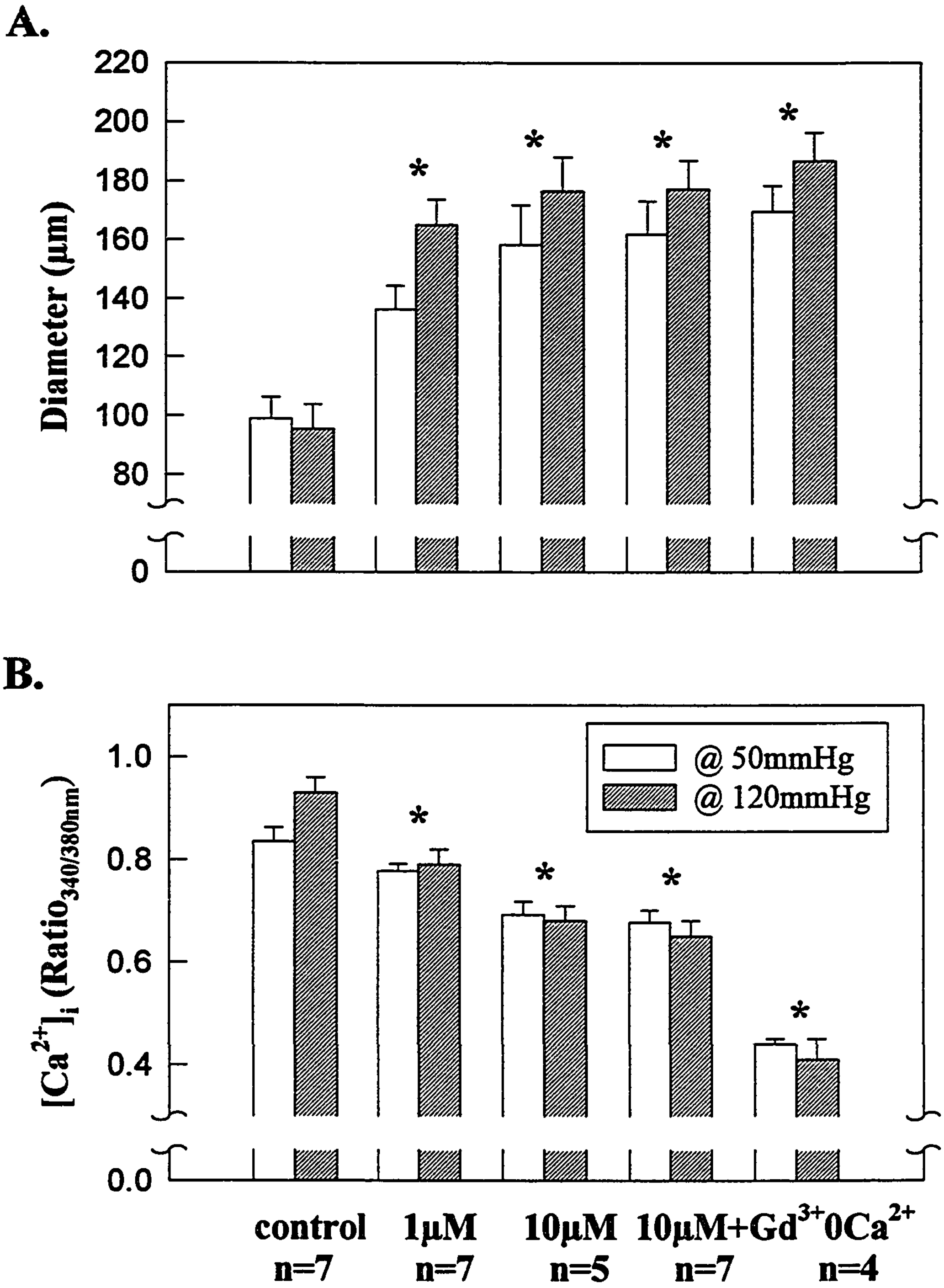
A.
Diameter (µm)
220
200
180
160
140
120
100
80
0
*
*
*
*
B.
$[Ca^{2+}]_i$ (Ratio$_{340/380nm}$)
1.0
0.8
0.6
0.4
0.0
*
*
*
*
▭ @ 50mmHg
▨ @ 120mmHg
control n=7
1µM n=7
10µM n=5
10µM+Gd^{3+} n=7
0Ca^{2+} n=4

presence of 10μM verapamil (compared with in 0mM Ca^{2+}/EGTA solution; e.g. 158.2 ± 13.5μm vs. 169.5 ± 8.7μm at 50mmHg), steady-state $[Ca^{2+}]_i$ was still significantly higher ($p < 0.05$) than when vessels had been superfused with 0mM Ca^{2+}/EGTA solution ($R_{340/348nm}$ were 0.68 ± 0.03 vs. 0.44 ± 0.1 at 50mmHg, Figure 6-1).

Under control conditions, as shown in the previous chapter, following an acute 50 -120mmHg increase in intraluminal pressure the arterioles showed an initial phase of distention which was paralleled by a rapid increase in $[Ca^{2+}]_i$. This phase was followed by active contraction of the arterioles during which $[Ca^{2+}]_i$ remained significantly greater than that in the basal period (Figure 6-2). The calcium channel blocker verapamil (1 or 10μM) abolished the pressure-induced vasoconstriction in response to the 50-120 mmHg pressure step. In apparent contrast to the diameter response $[Ca^{2+}]_i$ increased significantly from the basal of each condition, albeit transiently, in response to the pressure stimulus both following 1 and 10μM verapamil treatment (Figures 6-2 and 6-3). Addition of Gd^{3+} (10μM in presence of 10μM verapamil) did not show further inhibition of the arteriolar responses (Figures 6-1, 6-2 and 6-3).

Effect of Ca^{2+} Entry Blockade on Adrenergic Agonist-Induced Contraction

Arterioles showed dose-dependent increases in $[Ca^{2+}]_i$ and extent of vasoconstriction to norepinephrine (0.1, 1.0 and 5μM; Figures 6-4, 6-5 and 6-6). The change in intracellular Ca^{2+} was typically biphasic with a marked early transient increase followed by a decline to a steady-state level; while the vasoconstriction was largely monophasic being maintained despite the decline in Ca^{2+} from peak levels (also refer to chapter 5 for another set of similar experiment under control conditions). The effect of Ca^{2+} entry blockade appeared to have a stronger effect on steady-state $[Ca^{2+}]_i$ and this

Figure 6-2. Effect of Ca^{2+} entry blockade on arteriolar diameter (A) and Ca^{2+} (B) response to an acute 50-120mmHg pressure increase.

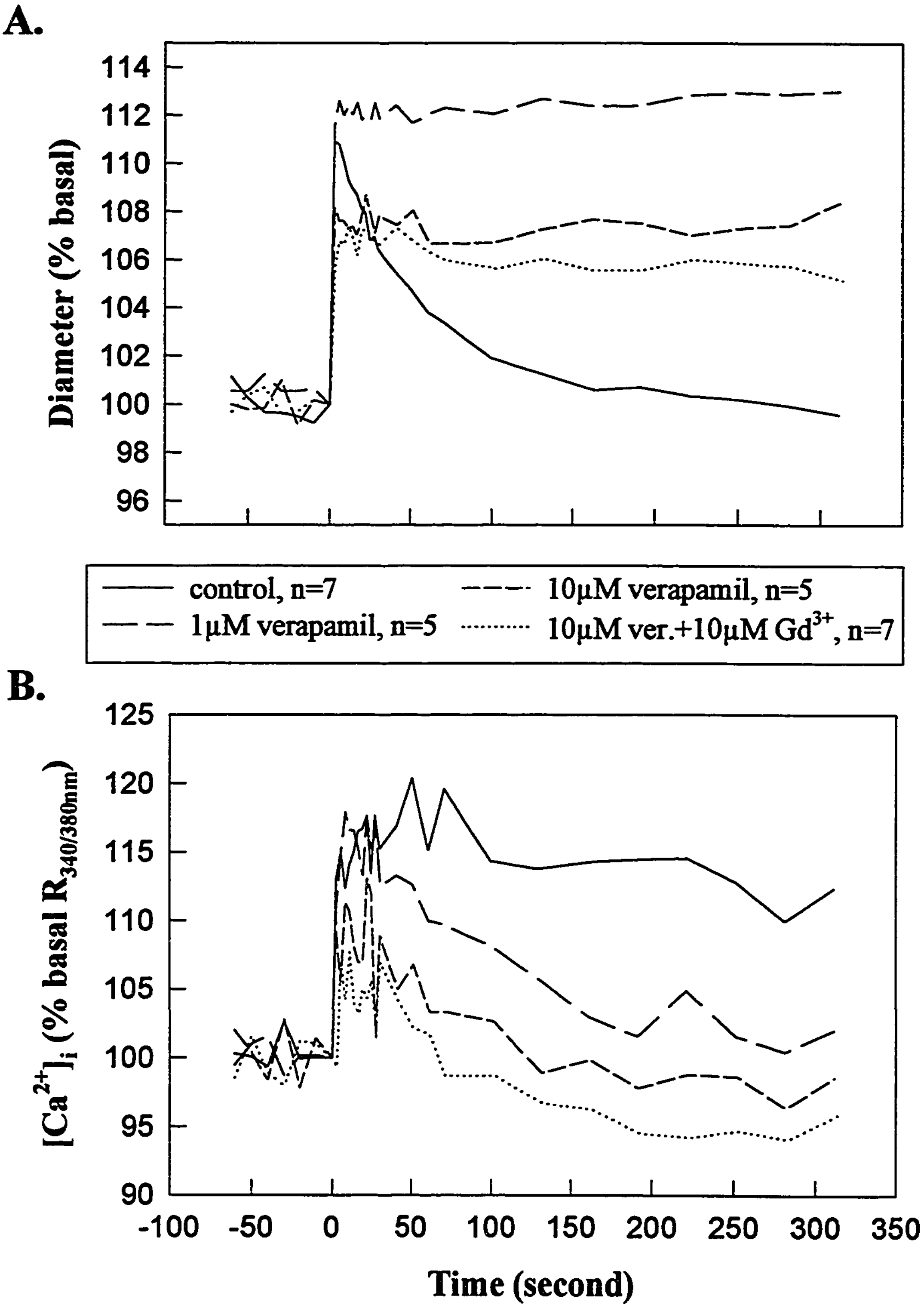
A.
Diameter (% basal)
114
112
110
108
106
104
102
100
98
96
control, n=7
10μM verapamil, n=5
1μM verapamil, n=5
10μM ver.+10μM Gd3+, n=7
B.
[Ca2+]i (% basal R340/380nm)
125
120
115
110
105
100
95
90
-100
-50
0
50
100
150
200
250
300
350
Time (second)

Figure 6-3. Effect of Ca^{2+} entry blockade on arteriolar basal, maximal and steady state $[Ca^{2+}]_i$ in response to an acute 50-120mmHg pressure increase. Responses are normalized to the basal under control (A) and each treatment (B) conditions. * indicates significant from basal; $p < 0.05$. Data are presented as mean ± SEM.

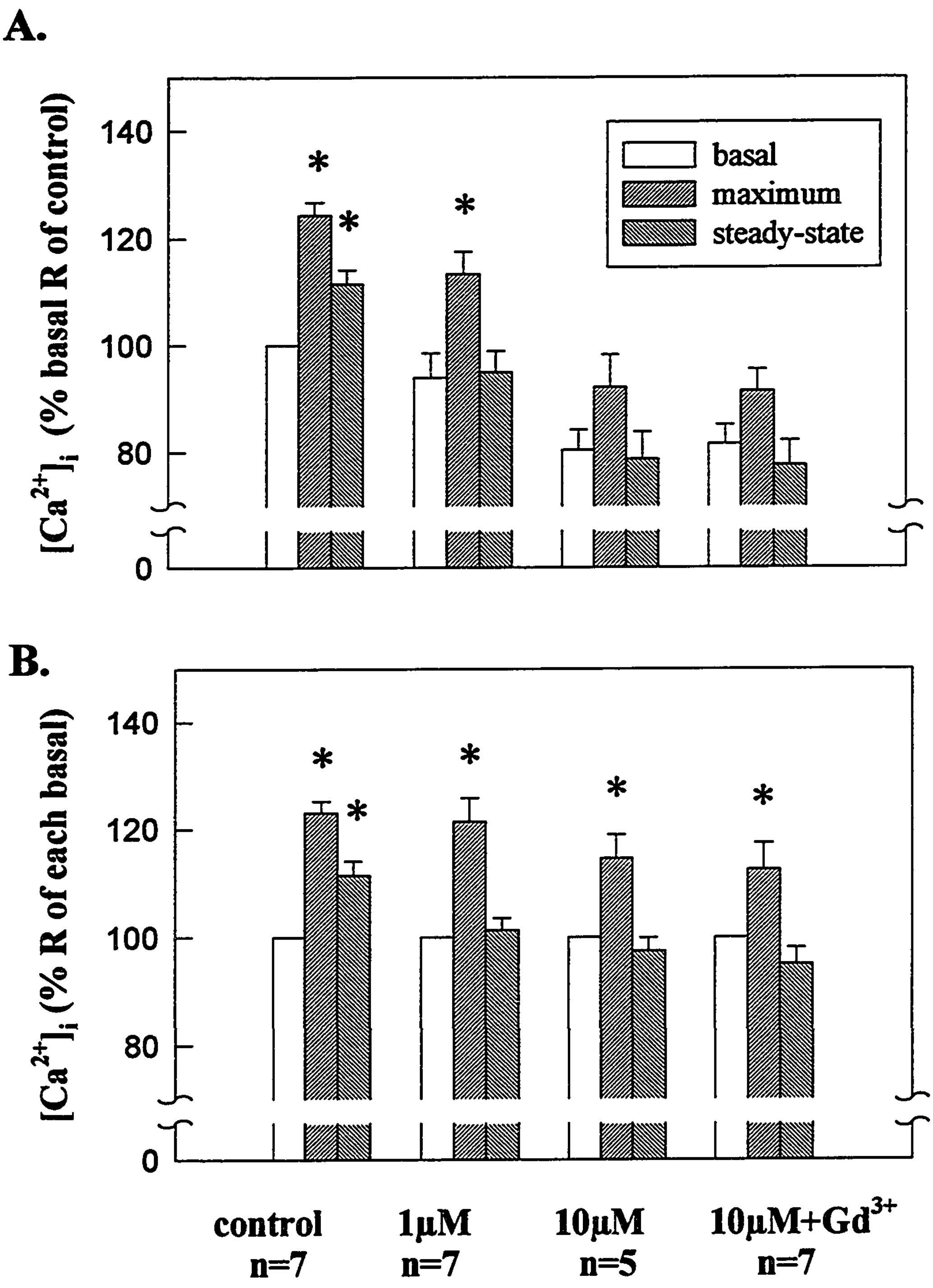
A.
[Ca^{2+}]$_i$ (% basal R of control)
140
120
100
80
0
basal
maximum
steady-state
*
*
*
B.
[Ca^{2+}]$_i$ (% R of each basal)
140
120
100
80
0
*
*
*
*
*
control
n=7
1μM
n=7
10μM
n=5
10μM+Gd^{3+}
n=7

Figure 6-4. Effect of Ca^{2+} entry blockade on arteriolar diameter (A) and Ca^{2+} (B) response to 0.1μM norepinephrine stimulation. The effect of Gd^{3+} was tested in the presence of 10μM verapamil. Data are normalized to each basal conditions, n = 5.

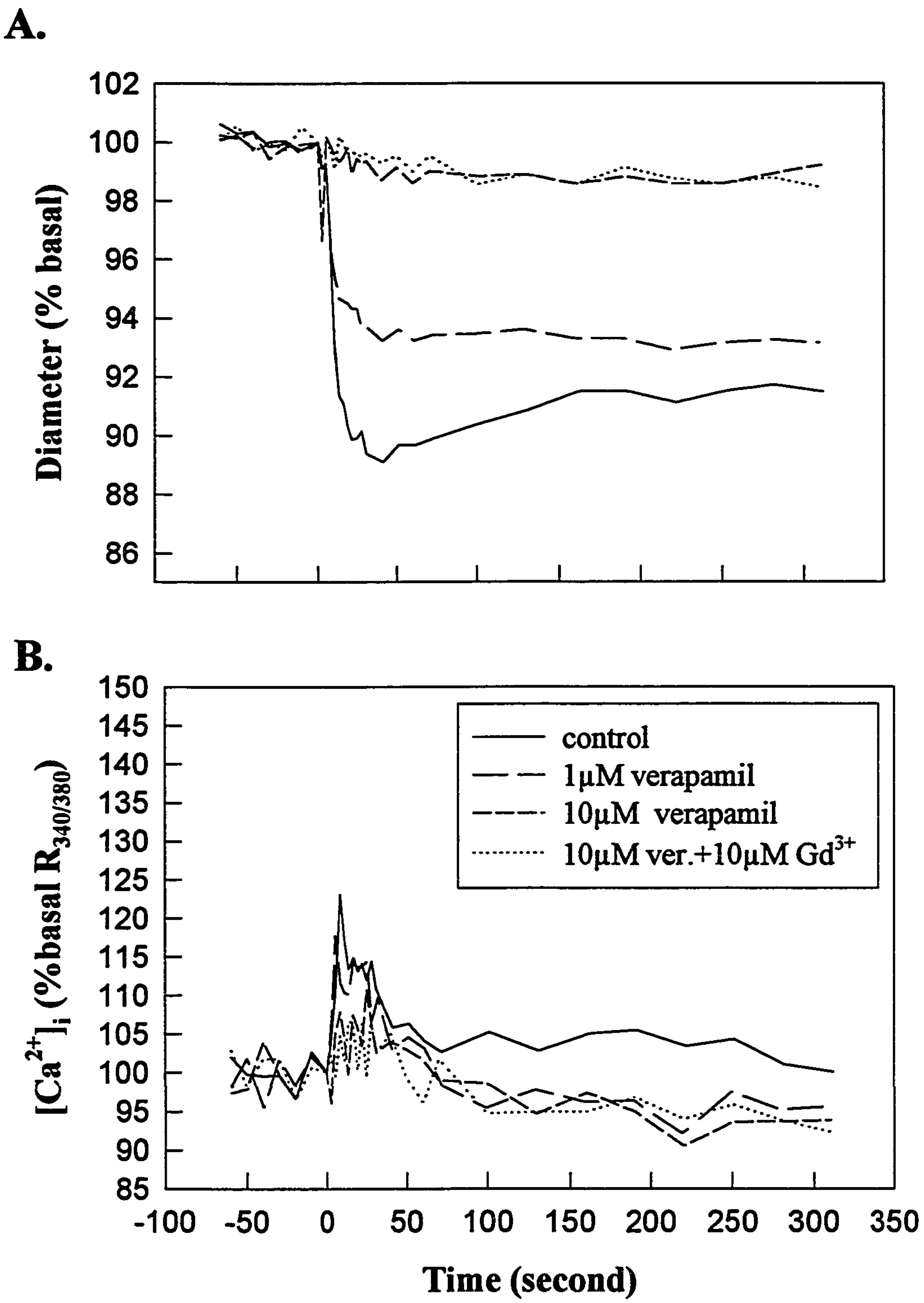
A.
102
100
98
96
94
92
90
88
86
Diameter (% basal)
B.
150
145
140
135
130
125
120
115
110
105
100
95
90
85
$[Ca^{2+}]_i$ (%basal $R_{340/380}$)
control
1μM verapamil
10μM verapamil
10μM ver.+10μM Gd^{3+}
-100
-50
0
50
100
150
200
250
300
350
Time (second)

Figure 6-5. Effect of Ca^{2+} entry blockade on arteriolar diameter (A) and Ca^{2+} (B) response to 1μM norepinephrine stimulation. The effect of Gd^{3+} was tested in the presence of 10μM verapamil. Data are normalized to each basal conditions, n = 5.

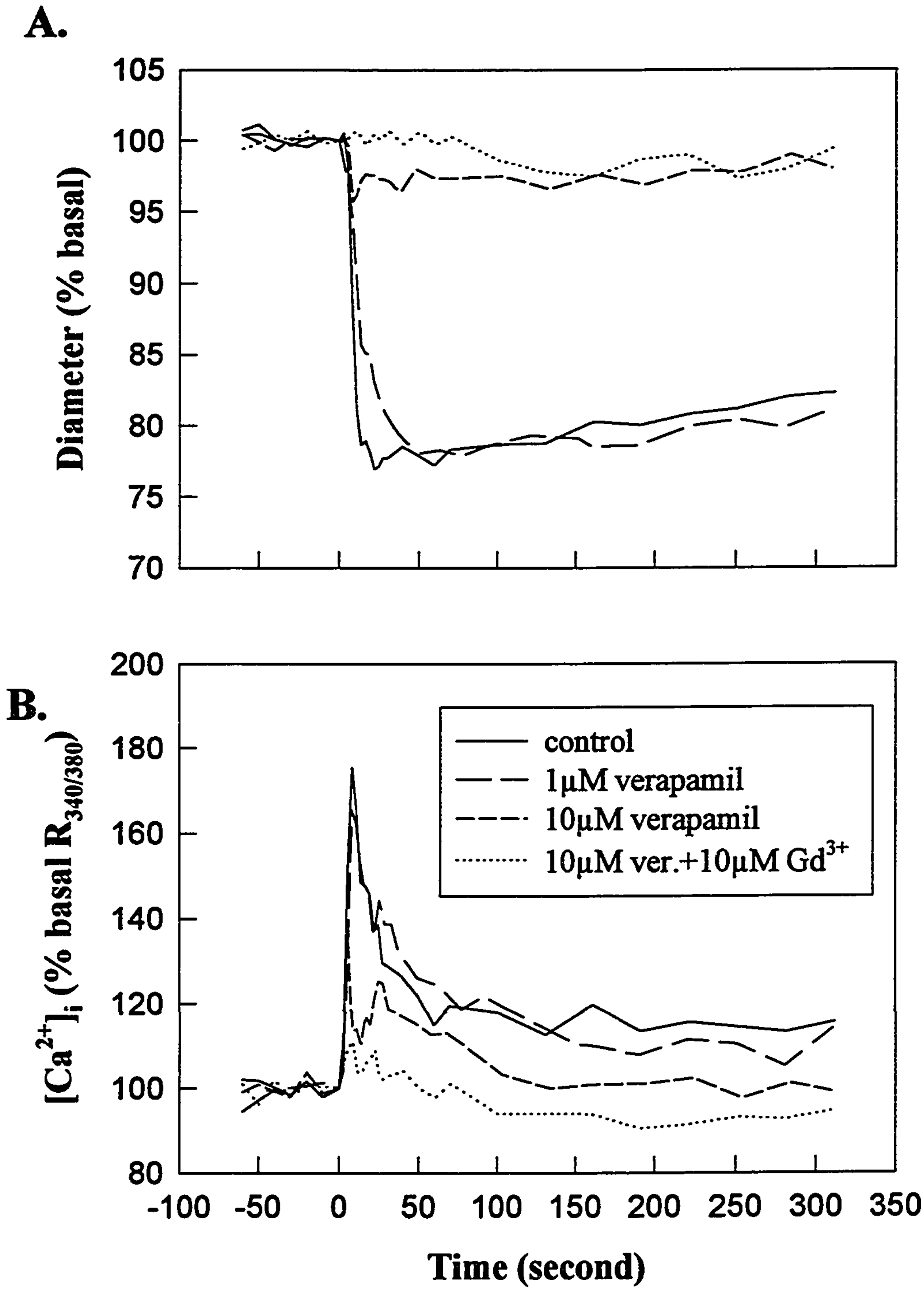
A.
105
100
95
90
85
80
75
70
Diameter (% basal)
B.
200
180
160
140
120
100
80
$[Ca^{2+}]_i$ (% basal $R_{340/380}$)
control
1μM verapamil
10μM verapamil
10μM ver.+10μM Gd^{3+}
-100
-50
0
50
100
150
200
250
300
350
Time (second)

Figure 6-6. Effect of Ca^{2+} entry blockade on arteriolar diameter (A) and Ca^{2+} (B) response to 5μM norepinephrine stimulation. The effect of Gd^{3+} was tested in the presence of 10μM verapamil. Data are normalized to each basal conditions, n = 5.

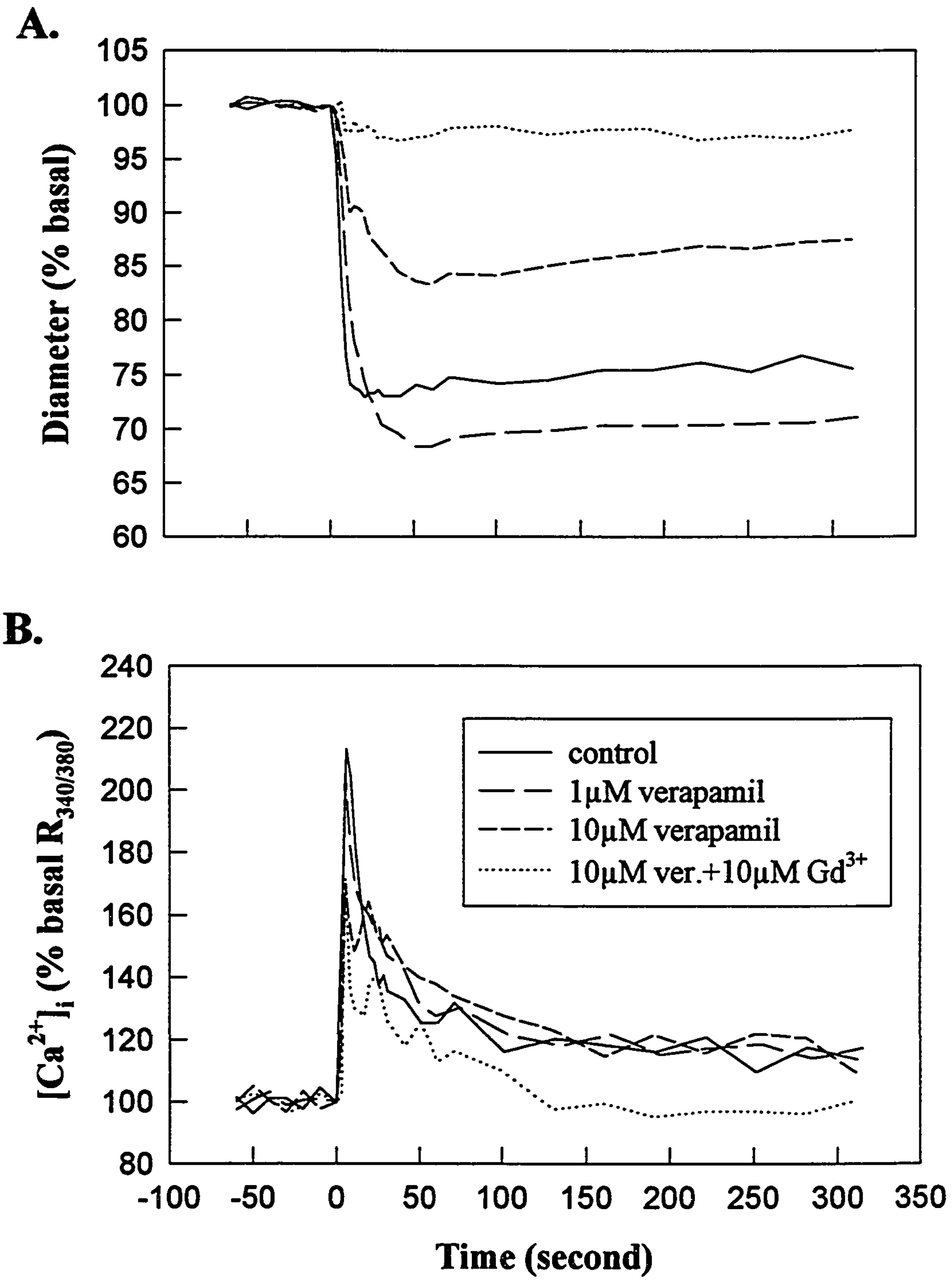
A.
Diameter (% basal)
105
100
95
90
85
80
75
70
65
60
B.
$[Ca^{2+}]_i$ (% basal $R_{340/380}$)
240
220
200
180
160
140
120
100
80
control
1μM verapamil
10μM verapamil
10μM ver.+10μM Gd^{3+}
-100
-50
0
50
100
150
200
250
300
350
Time (second)

effect is more obvious in the responses to low concentrations of agonist stimulation (Figure 6-7). Despite the verapamil dose-dependent arteriolar tone inhibition, in 10μM verapamil, 5μM NE still caused a significant contraction but this contraction was abolished by the further addition of 10μM Gd^{3+} to the superfusate (Figure 6-8) which decreased the basal $[Ca^{2+}]_i$ to a lower level ($R_{340/380nm}$ were 0.65 ± 0.05 vs. 0.60 ± 0.06, respectively; $p < 0.05$).

Relationship Between Arteriolar Intracellular Ca^{2+} Stores Accessed by Caffeine and α-Agonist

In the absence of extracellular Ca^{2+}, both caffeine (20mM) and PE (5μM) induced Ca^{2+} releases from intracellular stores as demonstrated by the rapid increases in the fluorescence ratio $R_{340/380nm}$ (Figures 6-9 and 6-10), and further the caffeine mediated release was substantial even when PE induced Ca^{2+} mobilization was diminished with repeated challenges (Figure 6-9) or as a result of prolonged exposure to $0Ca^{2+}$/EGTA solution (Figure 6-10). However, PE failed to demonstrate further Ca^{2+} increases following a caffeine stimulation (Figure 6-9). The decreases in magnitude of fluorescence ratio for both caffeine and PE stimulations, with the superfusion time in 0 Ca^{2+}/EGTA buffer, suggests a gradual depletion of the intracellular Ca^{2+} store occurs when arterioles are subjected to 0mM extracellular Ca^{2+} (Figure 6-10).

Effect of Ryanodine on Arteriolar Tone and Acute Myogenic Reactivity

Consistent with the notion that ryanodine activates Ca^{2+} release channels on intracellular stores and locks them in an open position, caffeine induced Ca^{2+} release was attenuated following ryanodine pre-treatment of the arterioles (peak values for

Figure 6-7. Effect of Ca^{2+} entry blockade on arteriolar maximal and steady-state Ca^{2+} response to 0.1μM (A), 1μM (B) and 5μM (C) norepinephrine stimulation. The effect of Gd^{3+} was tested in the presence of 10μM verapamil. Data are normalized to the basal under each conditions and presented as mean ± SEM, n = 5. * indicates significant from basal; $p < 0.05$.

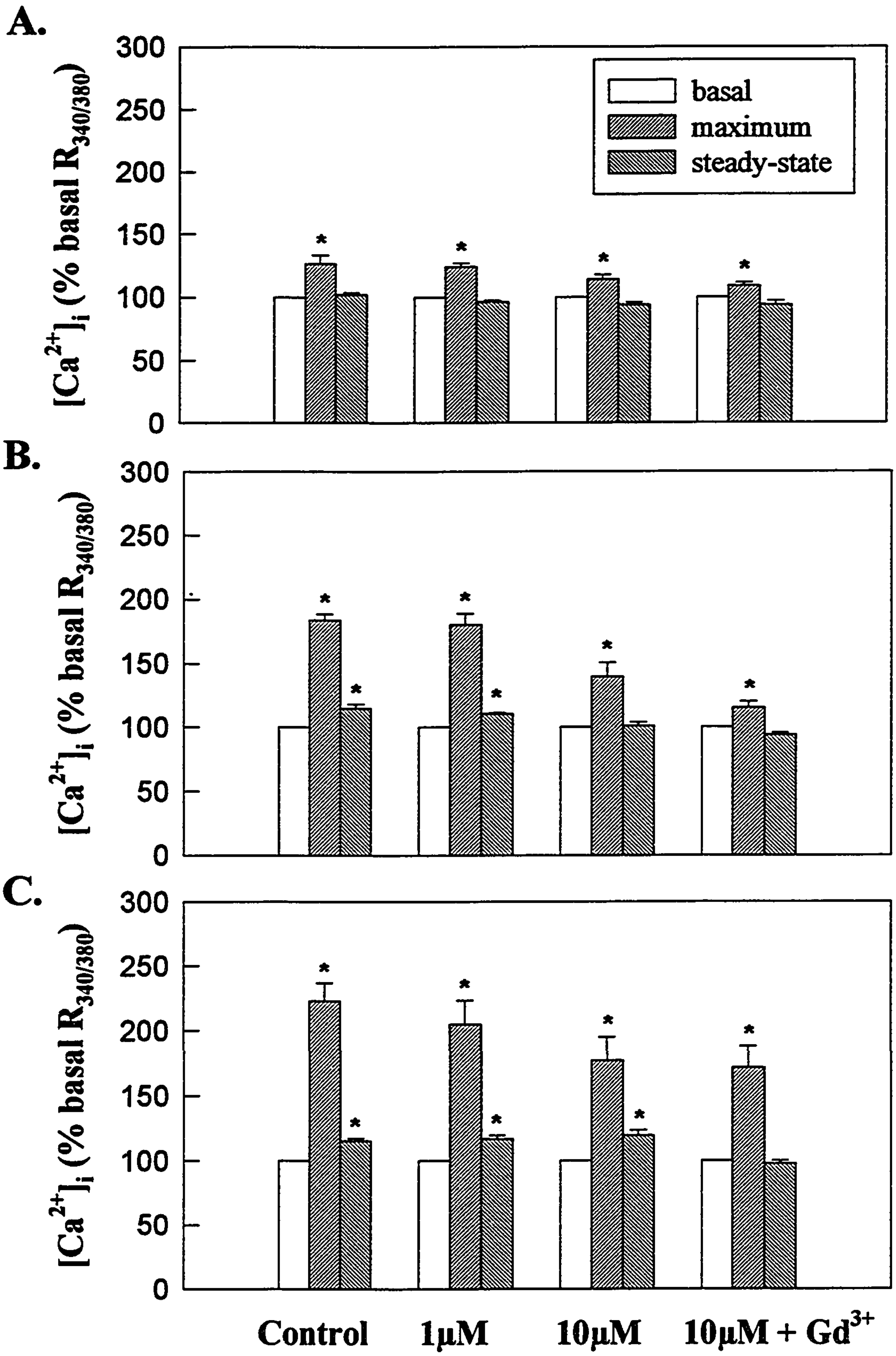
A.
B.
C.
$[Ca^{2+}]_i$ (% basal $R_{340/380}$)
0
50
100
150
200
250
300
basal
maximum
steady-state
*
Control
1μM
10μM
10μM + Gd^{3+}

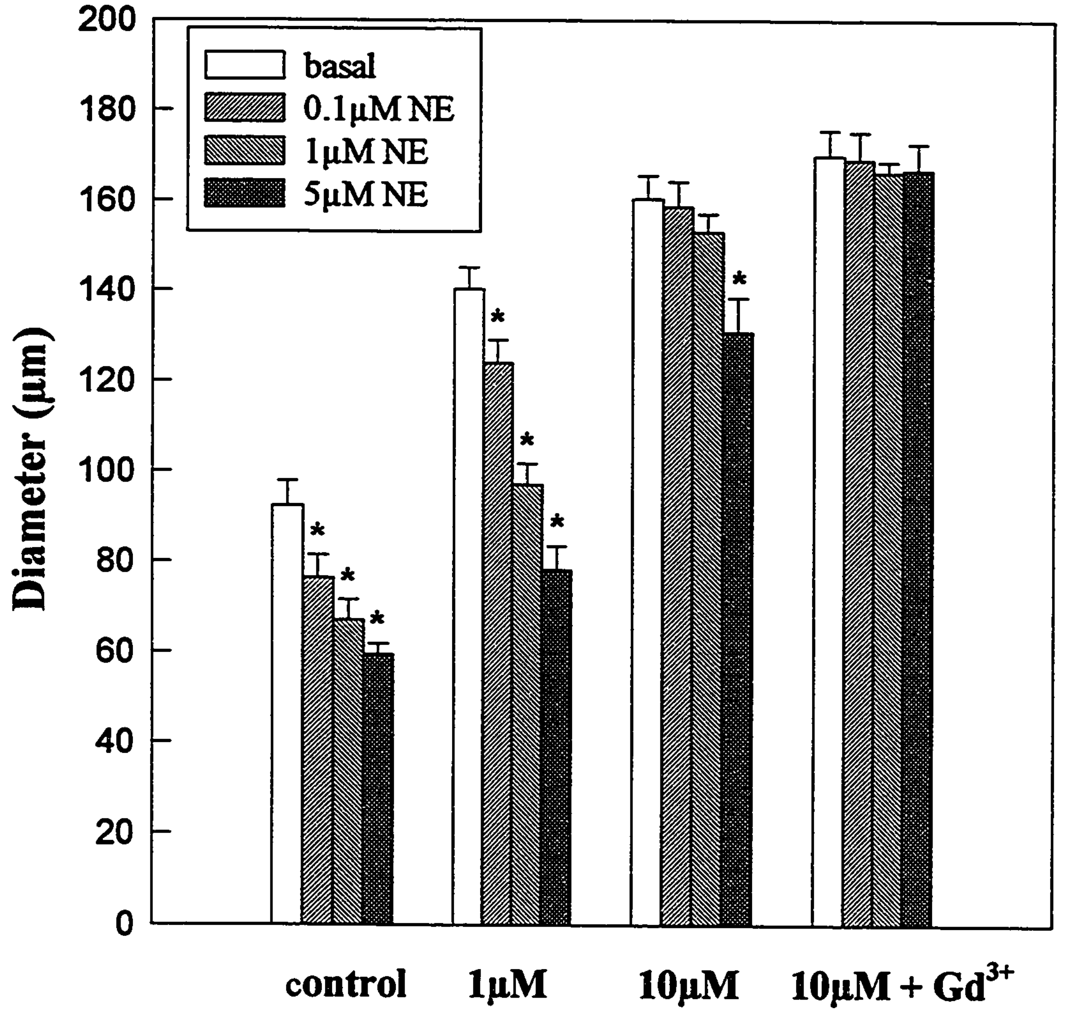

Figure 6-8. Effect of Ca^{2+} entry blockade on steady-state arteriolar constriction to 0.1, 1 and 5μM norepinephrine. Data are presented as mean ± SEM, n = 5. * indicates significant from basal; $p < 0.05$.

Figure 6-9. Representative tracings of Ca^{2+} response revealing the relationship between caffeine and agonist-released Ca^{2+} pools. Top panel shows the stored Ca^{2+} mobilizations performed in the absence of extracellular Ca^{2+} with 20mM caffeine followed by 5μM phenylephrine. Bottom panel shows the stored Ca^{2+} mobilizations performed in the absence of extracellular Ca^{2+} with 5μM phenylephrine followed by another 5μM phenylephrine then 20mM caffeine. Dotted line in the bottom panel indicates the level of $[Ca^{2+}]_i$ rise caused by caffeine releasing of intracellular stores as shown in the top panel.

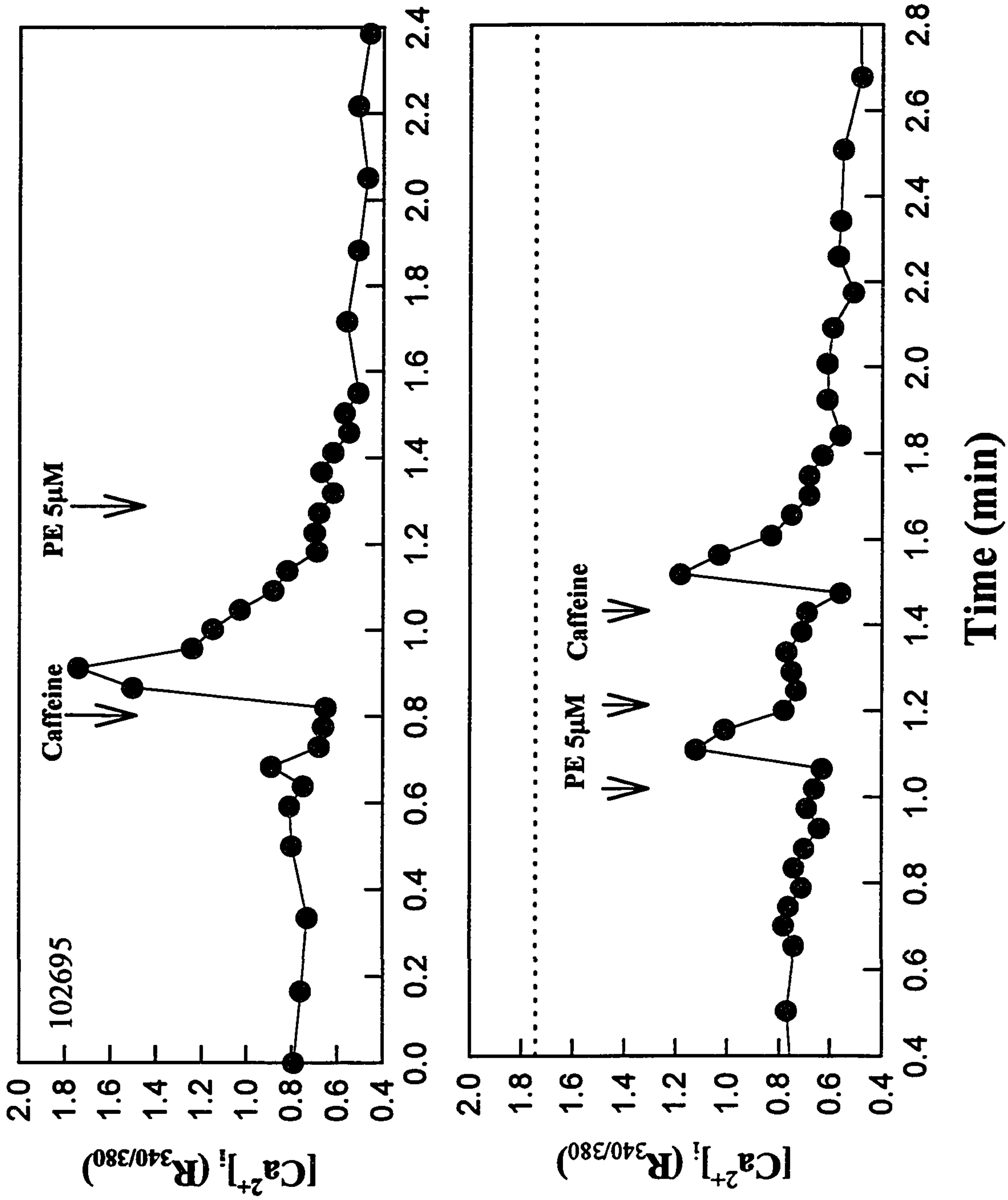
102695
Caffeine
PE 5µM
$[Ca^{2+}]_i$ ($R_{340/380}$)
2.0
1.8
1.6
1.4
1.2
1.0
0.8
0.6
0.4
0.0
0.2
0.4
0.6
0.8
1.0
1.2
1.4
1.6
1.8
2.0
2.2
2.4
PE 5µM
Caffeine
$[Ca^{2+}]_i$ ($R_{340/380}$)
2.0
1.8
1.6
1.4
1.2
1.0
0.8
0.6
0.4
0.4
0.6
0.8
1.0
1.2
1.4
1.6
1.8
2.0
2.2
2.4
2.6
2.8
Time (min)

Figure 6-10. Representative tracings showing the time course for the depletion of intracellular Ca^{2+} stores accessed by agonist and caffeine in the absence of extracellular Ca^{2+}. Vessels were challenged by 5μM PE at 1, 2, 3, 4, and 5 minutes after changing the superfusate from normal Kreb's buffer (with 2.5mM Ca^{2+}) into a buffer containing 0mM Ca^{2+} and 2mM EGTA. Caffeine were applied following the PE stimulation at 3 and 5 minutes. Dotted line indicates the time extracellular Ca^{2+} was changed.

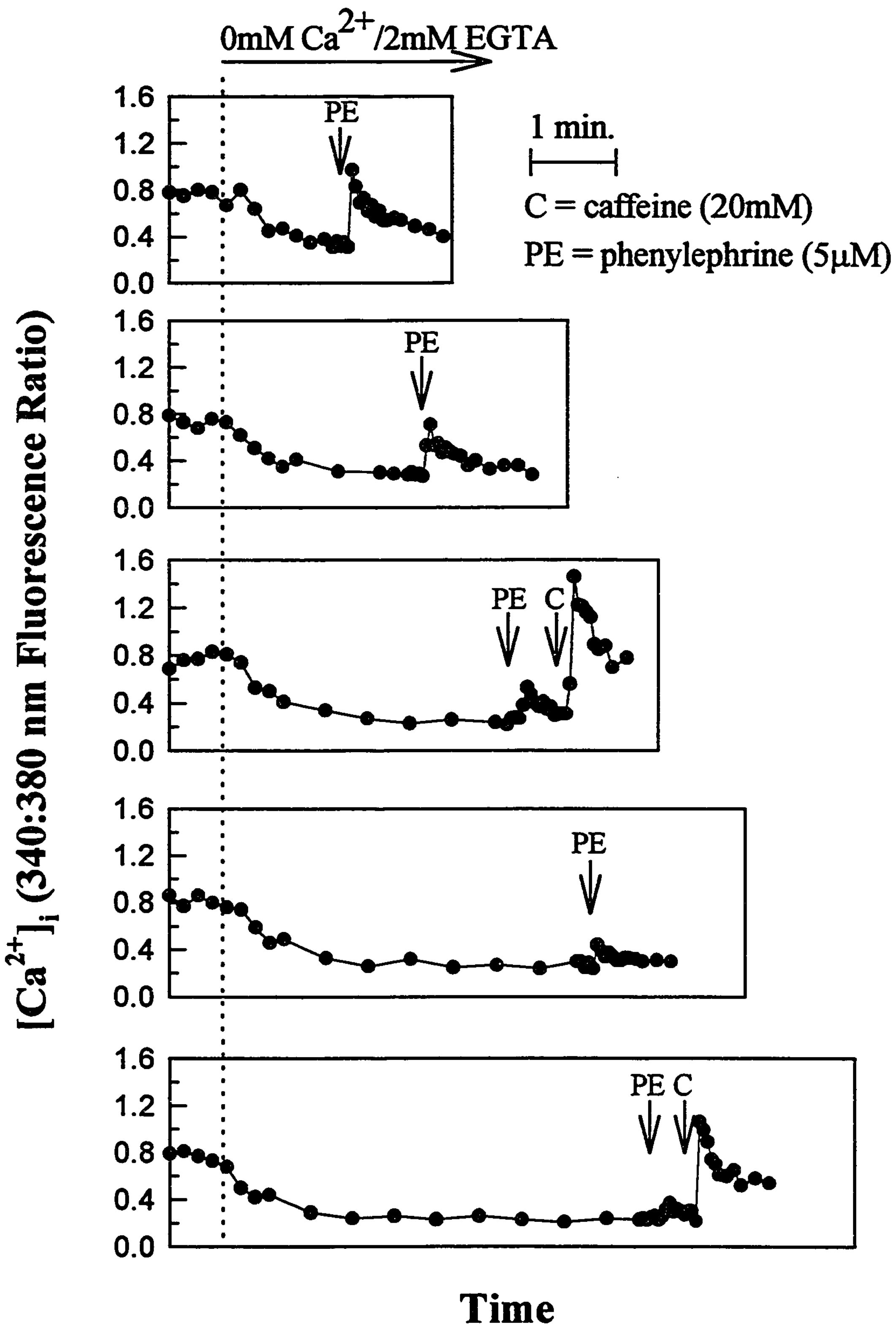
0mM Ca2+/2mM EGTA
1 min.
C = caffeine (20mM)
PE = phenylephrine (5µM)
[Ca2+]i (340:380 nm Fluorescence Ratio)
1.6
1.2
0.8
0.4
0.0
PE
C
Time

fluorescence ratio were 2.41 ± 0.19 vs. 1.82 ± 0.24; $n = 4$, $p < 0.05$). The rate of $[Ca^{2+}]_i$ increase following an acute 50-120mmHg pressure step was slower in vessels subjected to ryanodine pre-treatment (time required to reach half-maximum level were 8.5 ± 0.1 and 14.8 ± 2.0 seconds respectively, $p < 0.05$), however, the arteriolar basal tone was potentiated ($p = 0.02$) and vessels still exhibited myogenic contractions (Figure 6-11). While 1μM ryanodine caused a maintained constriction of the vessel higher concentrations (10μM) did not appear to have further effect on vessel diameter and, similarly to the lower concentration, did not prevent the pressure-induced vasoconstriction.

Effect of Steady-State Intraluminal Pressure on Caffeine-Induced $[Ca^{2+}]_i$ Changes

Under control conditions, caffeine (20mM) caused comparable $[Ca^{2+}]_i$ increases at 50 and 120mmHg, however, the vessels demonstrated a significantly greater contraction at the lower pressure of 50mmHg (figure 6-12). In the presence of VOC blocker, verapamil (1μM), the rise in $[Ca^{2+}]_i$ was significantly decreased at 120mmHg ($p < 0.02$) compared with that occurring at 50mmHg which remained similar to that under control condition, while the arteriolar contraction to caffeine continued to be significantly less ($p < 0.001$) at 120mmHg than that at 50mmHg (Figure 6-12). The latter data suggests that in the presence of verapamil the higher pressure (120mmHg) may partially deplete the caffeine-accessible Ca^{2+} store.

Mn^{2+} Quench Studies

Following replacing the normal superfusate with a buffer containing 0mM Ca^{2+}/1mM Mn^{2+}, a dilation of the arterioles was observed with a rapid decrease in

Figure 6-11. Representative tracings showing the effect of ryanodine on arteriolar Ca^{2+} and diameter responses to an acute 50-120mmHg pressure increase.

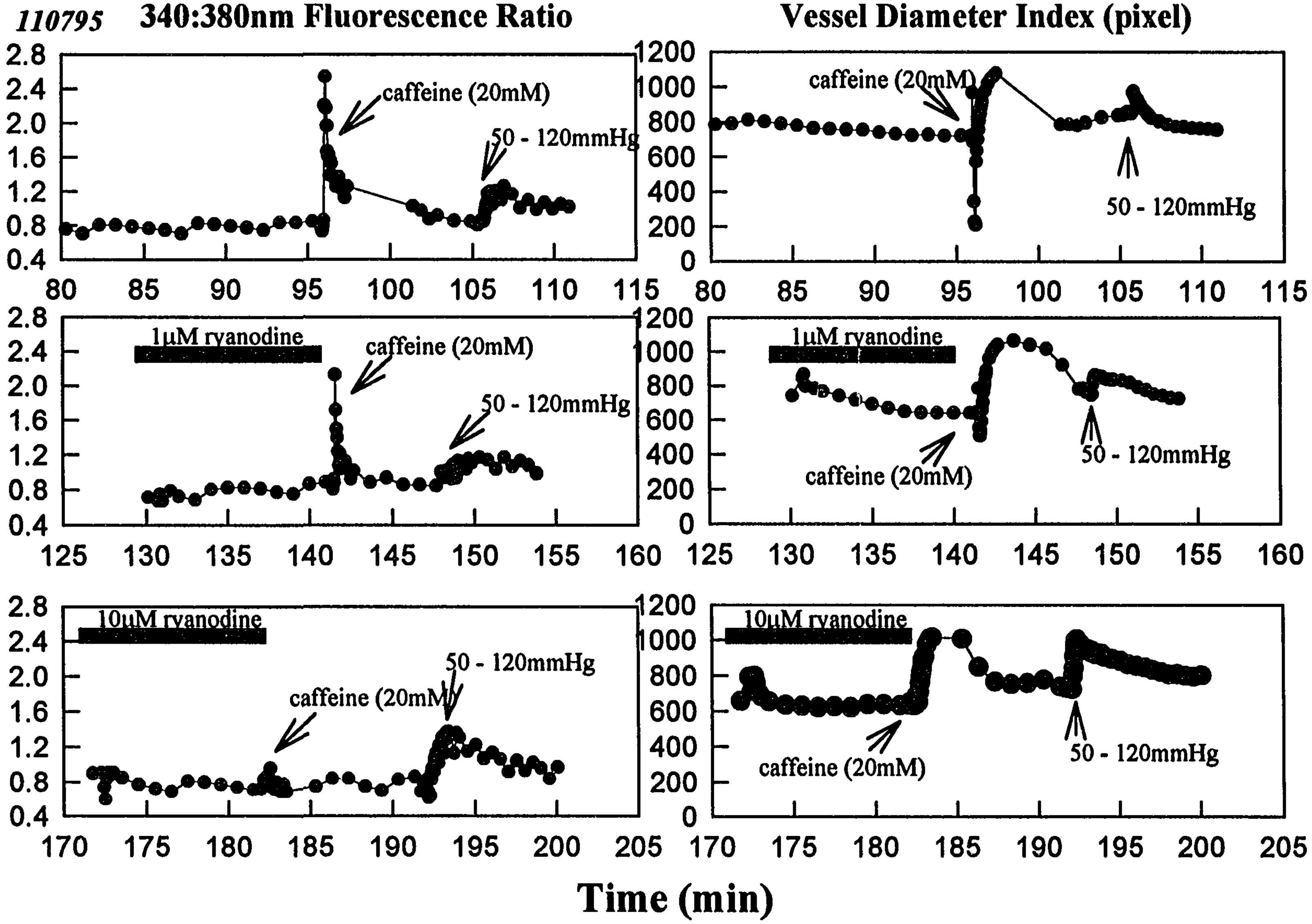
110795
340:380nm Fluorescence Ratio
Vessel Diameter Index (pixel)
2.8
2.4
2.0
1.6
1.2
0.8
0.4
1200
1000
800
600
400
200
0
80
85
90
95
100
105
110
115
125
130
135
140
145
150
155
160
170
175
180
185
190
195
200
205
caffeine (20mM)
50 - 120mmHg
1µM ryanodine
10µM ryanodine
Time (min)

Figure 6-12. Effect of intracellular pressure on arteriolar diameter and Ca^{2+} responses to caffeine (20mM) under conditions of control and verapamil pre-treatment. Data are presented as mean ± SEM.

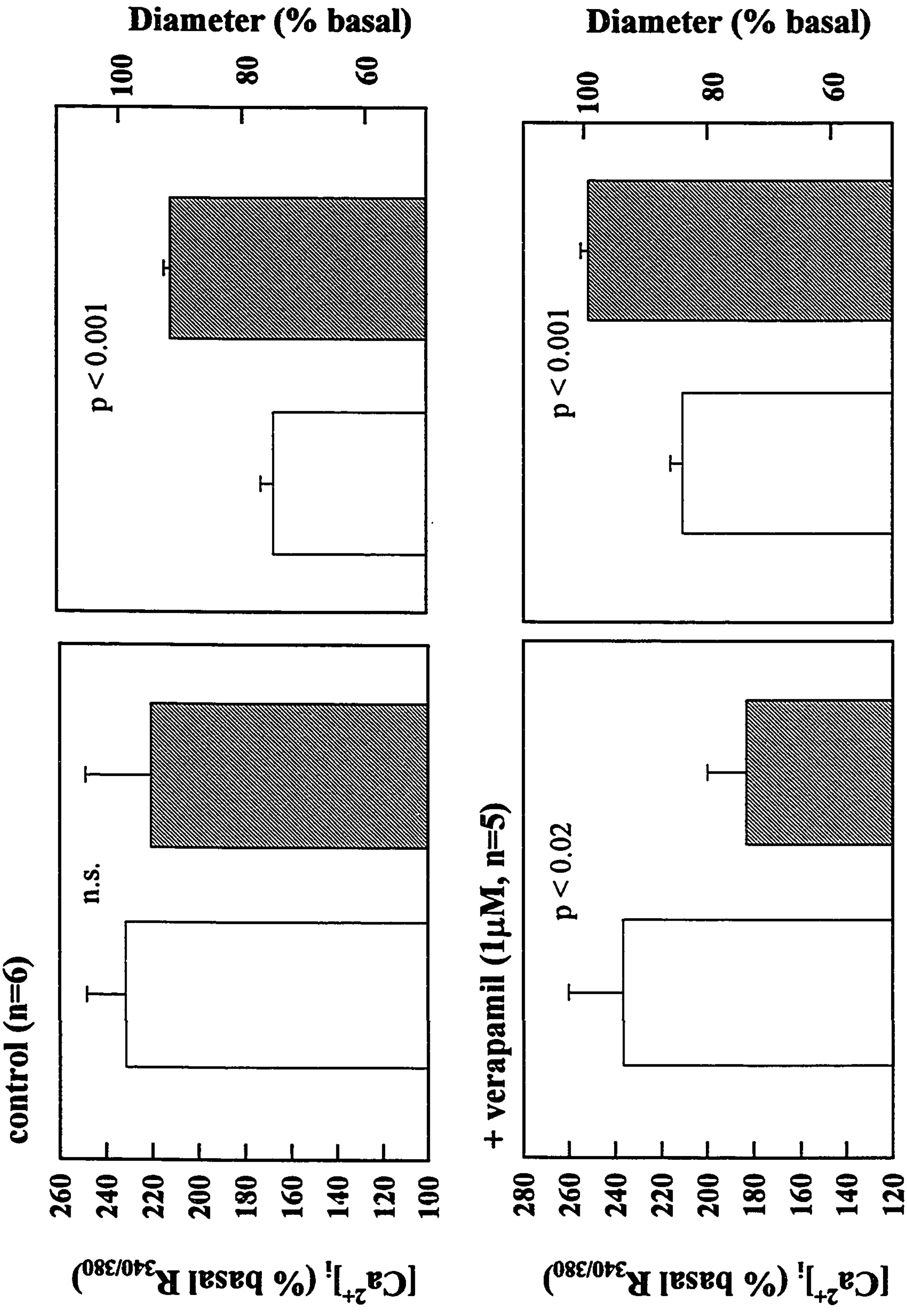
control (n=6)
+ verapamil (1µM, n=5)
Diameter (% basal)
100
80
60
Diameter (% basal)
100
80
60
p < 0.001
p < 0.001
n.s.
p < 0.02
[Ca2+]i (% basal R340/380)
260
240
220
200
180
160
140
120
100
[Ca2+]i (% basal R340/380)
280
260
240
220
200
180
160
140
120

fluorescence intensities indicating a decrease in $[Ca^{2+}]_i$ (by 340nm excitation) and a Mn^{2+} influx (by 340nm and 360nm excitations; Figure 6-13). 10~15 seconds after swapping into the 0mM Ca^{2+}/1mM Mn^{2+} buffer, a pressure step increase from 50 to 120mmHg did not cause a detectable increase in fluorescence intensity of the 340nm image (Figures 6-13 and 6-14) while a subsequent caffeine (20mM) stimulation demonstrated a rapid increase that decayed with time (Figure 6-13). Similarly, at the time point (10~15 seconds following buffer change) when pressure increase did not affect the fluorescence intensity of 340nm image, 5μM PE was capable of generating a transient increase in intensity of 340nm signal indicating Ca^{2+} release (Figure 6-14).

Discussion

By showing a decreased level of $[Ca^{2+}]_i$ in the presence of a L-type voltage-operated Ca^{2+} channel blocker, verapamil, results from the present study, besides giving supportive evidence to the notion that Ca^{2+} influx through plasma membrane is required for the maintenance of arteriolar basal tone, further demonstrated that myogenic contraction to transmural pressure increase depends on an extracellular Ca^{2+} source. While intracellular Ca^{2+} release may also be involved in these events, it does not appear to be mandatory. On the other hand, NE induced vessel contraction showed less of a dependency on Ca^{2+} entry and further implicated the involvement of a Ca^{2+} sensitizing mechanism. The ryanodine sensitive intracellular Ca^{2+} store appears to be larger than the agonist-sensitive (presumably IP_3 stimulated) Ca^{2+} store in rat cremaster first order arterioles.

The presence of extracellular Ca^{2+} as a necessity for the maintenance of arteriolar tone has been demonstrated by a number of investigators using in vivo preparations (Harder, et al.,

Figure 6-13. Representative tracings detecting arteriolar intracellular Ca^{2+} release during pressure step-increase and a following caffeine stimulation. Upper panel shows the time course of arteriolar diameter response while the fluorescence intensity of 340nm and 360nm excitations are plotted in the lower panel.

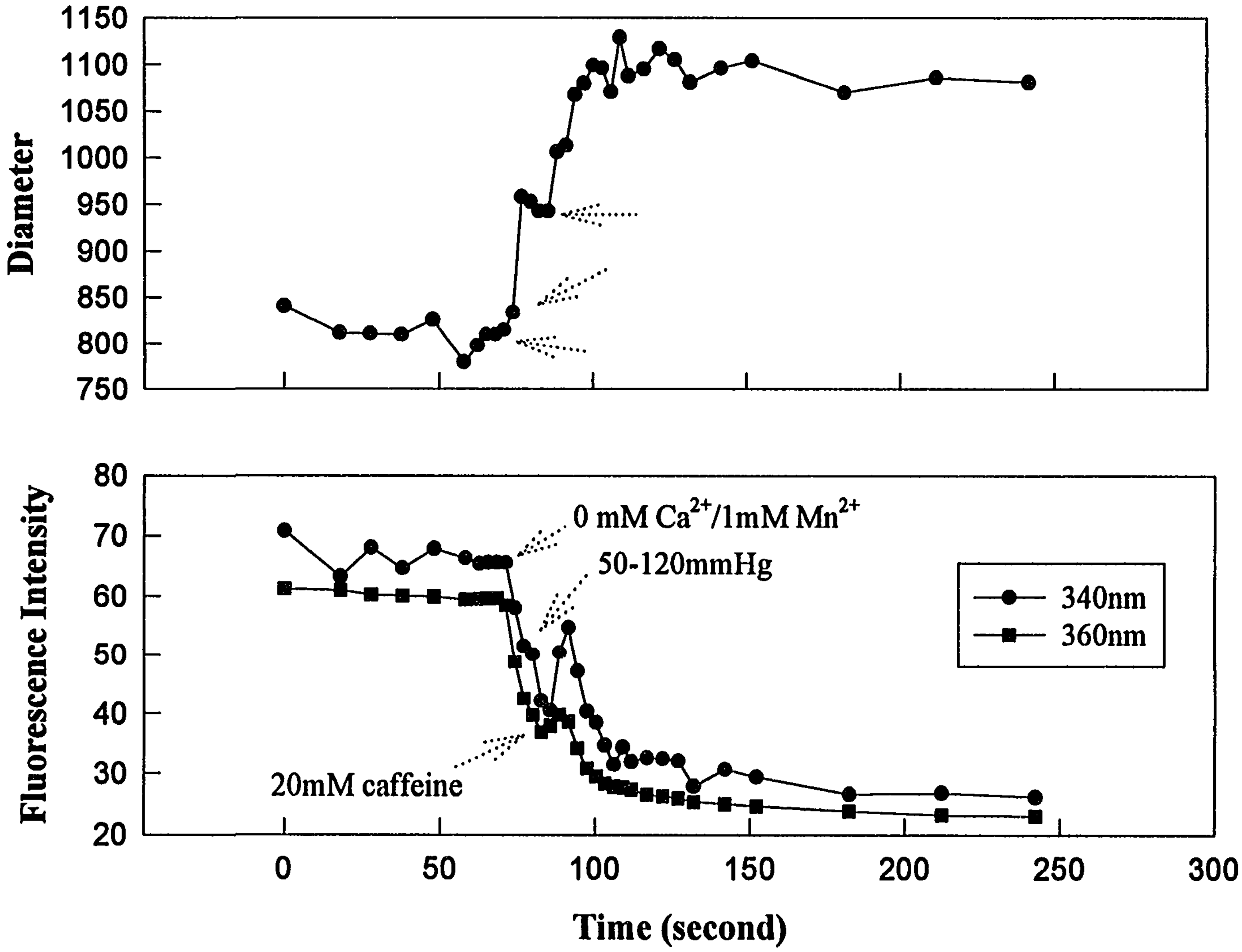
Diameter
1150
1100
1050
1000
950
900
850
800
750
Fluorescence Intensity
80
70
60
50
40
30
20
0 mM Ca^{2+}/1mM Mn^{2+}
50-120mmHg
20mM caffeine
340nm
360nm
0
50
100
150
200
250
300
Time (second)

Figure 6-14. Representative tracings of fluorescence intensities of 340nm and 360nm excitation detecting intracellular Ca^{2+} release during pressure increase and NE stimulation.

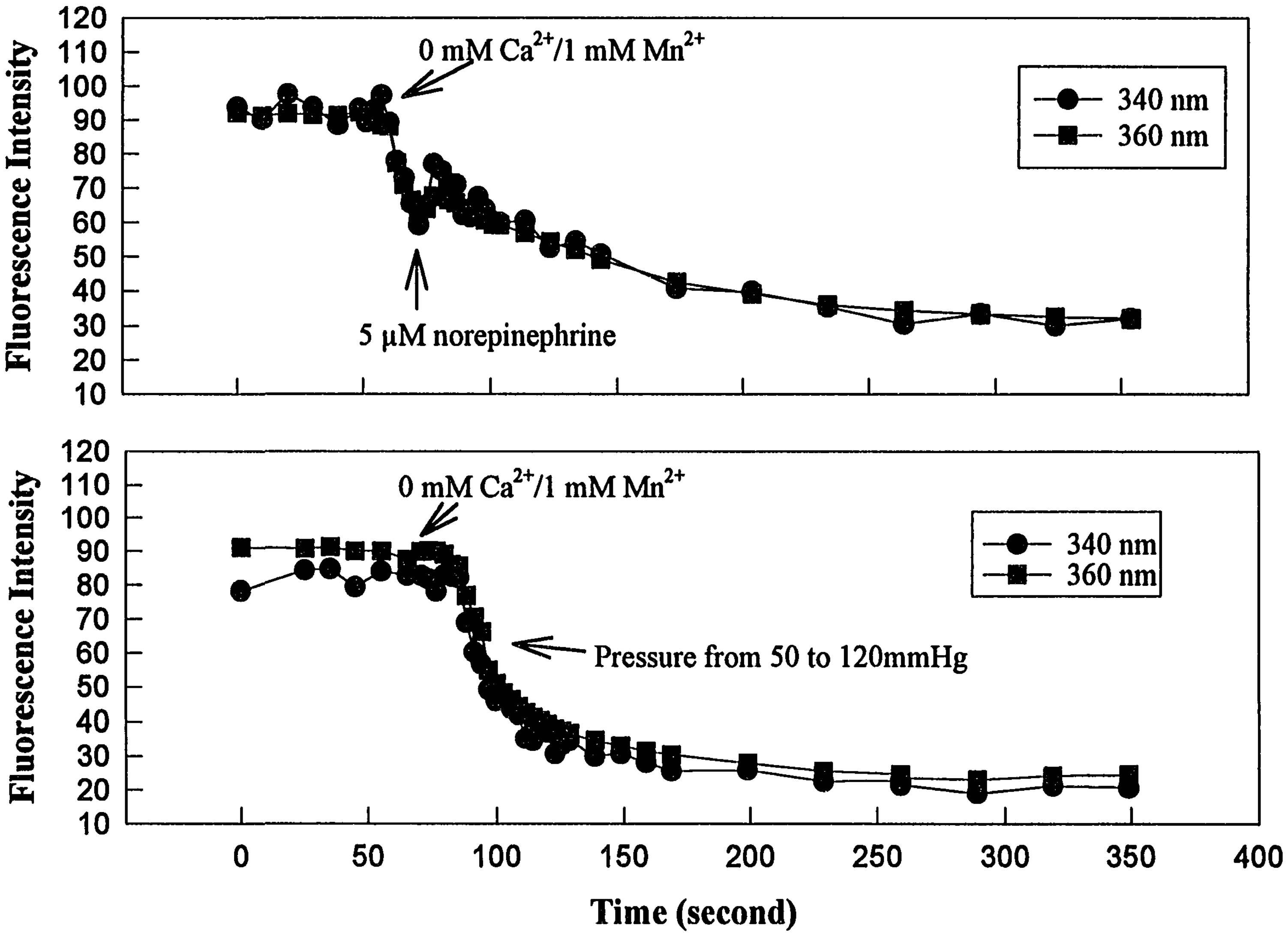
Fluorescence Intensity
120
110
100
90
80
70
60
50
40
30
20
10
0 mM Ca2+/1 mM Mn2+
5 μM norepinephrine
340 nm
360 nm
Fluorescence Intensity
0 mM Ca2+/1 mM Mn2+
Pressure from 50 to 120mmHg
0
50
100
150
200
250
300
350
400
Time (second)

1987; Jackson and Duling, 1989), however, $[Ca^{2+}]_i$ were not measured in those studies. With the use of fluorescent Ca^{2+} indicator, fura-2, we were able to more closely examine this issue. A decrease in $[Ca^{2+}]_i$ was found in a dose dependent manner to the addition of verapamil to superfusing solution, which confirmed the inhibitory effect of verapamil on Ca^{2+} entry. With that, the isolated arterioles also lost their basal tone verapamil dose dependently (Figure 6-1). The arteriolar myogenic contraction is totally inhibited by 1μM verapamil when the vessels still exhibited certain amount of spontaneous tone (Figure 6-2), indicating, at least for the tone developed in the presence of active VOC's, less Ca^{2+} is required to maintain it than to initiate a myogenic contraction.

Laher et al. (1988) showed that stretching of rabbit facial vein smooth muscle will induce a maintained active tone which is associated with an increase in Ca^{2+} influx. Further, by using a dihydropyridine VOC blocker (PN 200-110), they demonstrated that this Ca^{2+} influx is not through the VOCs and hence suggested a direct entry pathway. More recently, stretch activated Ca^{2+} channels were reported to be present in vascular smooth muscle cells (Davis, Donovitz and Hood, 1992) and have been implicated to be involved in the myogenic response (Meininger and Davis, 1992). In the present study, the observed transient Ca^{2+} increase in presence of VOC blockade, verapamil, may be due to the Ca^{2+} entry through these SACs (Figures 6-2, 6-3). However, SACs alone may not be able to totally explain the transient Ca^{2+} increase, because a $[Ca^{2+}]_i$ increase was observed even in the presence of Gd^{3+}, a trivalent cation that has been reported to block SACs (Yang and Sachs, 1989). It is possible that at the concentration we used (10μM), Gd^{3+} does not provide a total inhibition of the SACs although it has been shown that this concentration is sufficient to block the SACs in some other cell types, e.g. frog kidney proximal cells and *Xenopus* oocytes (Robson and Hunter, 1994; Yang and Sachs, 1989). The observations that Gd^{3+} did further decrease $[Ca^{2+}]_i$ and have an effect on the NE response suggest that Gd^{3+} reached the tissue and, at that concentration, could be effective. However, electrophysiological studies will be needed to determine the effective concentration for Gd^{3+} to block vascular smooth muscle SACs.

Kwan et al. (1990) has shown that another trivalent cation Ca^{2+} channel blocker, La^{3+}, has an effect on fura-2 fluorescence excitation/emission similar to Ca^{2+}. If this also applies to Gd^{3+}, the transient increase in fluorescence ratio (which is usually taken as an indication of $[Ca^{2+}]_i$) could, at least partly, be explained by the Gd^{3+} entering into the cell through SACs upon pressure increase. So far, there is no data show the permeability of vascular smooth muscle SACs to Gd^{3+}.

Ca^{2+} entry through T-type VOCs is also an alternative mechanism for this transient increase. However, the T-type VOCs are not found to be present in all smooth muscle cell types (Nelson, et al., 1990) and to date there has been no direct evidence for their functioning in cremaster first order arterioles. The observation that Gd^{3+} did not block this increase argues against the role of T-type VOCs in this situation because this nonspecific Ca^{2+} channel blocker has been demonstrated to block both T- and L-type VOCs at lower concentrations (Biagi and Enyeart, 1990; Song et al., 1992). Moreover, their low conductance (~1/3 of that of L-type VOC) and short lasting (20-50ms) characteristics plus their wide activation range (positive to -70mV) also makes T-type VOCs less likely to be a major contributor to this Ca^{2+} rise (Tsien, et al., 1988).

Another explanation to the transient $[Ca^{2+}]_i$ increase is that Ca^{2+} has been released from intracellular stores following an acute pressure step stimulation. Although the results from the Mn^{2+} studies do not favor this suggestion (Figures 6-13 and 6-14), it is possible that this technique is not sensitive enough to detect the relative smaller release induced by pressure stimulation. Another observation from the present studies also support the possibility of intracellular Ca^{2+} release: the $[Ca^{2+}]_i$ rise was slower when the intracellular stores were emptied by ryanodine (time required to reach half-maximum level were 8.5 ± 0.1 and 14.8 ± 2.0 seconds respectively, $p < 0.05$). This idea is also indirectly supported by the findings of other investigators, e.g. depolarization alone requires 30-60 seconds to produce a detectable change in $[Ca^{2+}]_i$ in bovine coronary arterial cells (Wagner-Mann, et al., 1991). Further, the diffusion of Ca^{2+} in the cytosol is much slower than that of any other second messengers, due to the presence of a large number of almost immobile Ca^{2+} binding sites (Allbritton, et al., 1992). More direct evidence came from the reports that stretch-induced intracellular Ca^{2+} release being observed both in single smooth muscle cells (Davis, Meininger and Zawieja, 1992) and in isolated arterial tissues (Tanaka, et al., 1993). For example, Davis, Meininger and Zawieja (1992) found that, when applying stretch to single pig coronary arterial smooth muscle cells in a Ca^{2+} free solution, a 24% stretch could cause Ca^{2+} release while a 10% stretch showed no change in $[Ca^{2+}]_i$. It therefore appears that there is a threshold for the intracellular Ca^{2+} release or the two phases of Ca^{2+} rise have different "stretch-sensitivities". Although the cellular mechanism for this Ca^{2+} release is not clear at this time, the idea of Ca^{2+} release is consistent with the suggestion that PLC activation is involved in myogenic reactivity (Narayanan, et al., 1994; Osol, 1995). Stretch has been recently reported to cause a significant increase in PLC activity in aortic smooth muscle within 275~375ms (Matsumoto, et al., 1995). However, further studies are still needed to determine whether similar activation is present in myogenic response because aortic rings, used in the above experiments, rarely show stretch induced contraction.

It is interesting to notice that the maintained opening state of Ca^{2+} channels on intracellular Ca^{2+} store, by ryanodine treatment resulted in a greater spontaneous tone in these arterioles while the increase in $[Ca^{2+}]_i$ was not significant. However, since a relatively higher R340/380 level was consistently observed in each of the experiments in the presence of ryanodine, statistical significance may be evident with additional experiments (statistics were performed with n=4 observations). On the other hand, this unaffected Ca^{2+} level can possibly be explained by the superficial buffer barrier model that an empty store will have the greatest buffering capacity for Ca^{2+} entering across the plasma membrane. Moreover, there might also be an enhanced Ca^{2+} efflux mechanism that helps to remove the cytosolic Ca^{2+} in this specific situation.

Although the intracellular Ca^{2+} release is not required for the arteriolar myogenic contraction and basal tone maintenance (Figure 6-11), it does not necessarily contradict the suggestion that PLC can be activated following an acute pressure increase, as in the situation of stretching of smooth muscle cells. PLC activation generally produce two major cellular messengers, IP_3 and DAG. While IP_3 might not be able to demonstrate its effect due to the emptiness of intracellular stores (supported by the observation that NE resulted little increase in $R_{340/380nm}$ in presence of ryanodine, data not shown), the role of PKC activated by DAG in the myogenic contraction can not be ruled out. There has been evidence showing that activation of PKC enhances the stretch-induced tone and PKC inhibitors attenuate myogenic responsiveness in isolated arterial preparations (Hill, et al., 1990; Laher and Bevan, 1987).

The observations that 1μM verapamil (and 1μM nifedipine, data not shown) significantly inhibited spontaneous tone and blocked myogenic constriction are at variance with the previous finding that VOCs are not the prime determinant of constrictor response to acute increase in intravascular pressure (Hill and Meininger, 1994). Although both studies used rat cremaster arterioles, the previous study was carried out *in vivo* while the present study employed an *in vitro* isolated preparation. Additional factors which make comparison of these studies difficult include, 1. data from the *in vivo* study was based on the response of third order arterioles instead of the first order vessels (which were used in this *in vitro* preparation); and 2. the first order arterioles do not exhibit spontaneous tone in such preparations probably as a result of the extensive surgery required for preparations of the cremaster muscle for *in vivo* microscopy (Hill, et al., 1990). Therefore, the inconsistency may come from either the differences in tissue preparation, *in vivo* vs. *in vitro*, or from the differences in the size or branch order of the vessels because functional variation appears to occur at different levels within a microvascular network.

Arterioles stimulated with norepinephrine showed a transient spike followed by a sustained elevation of $[Ca^{2+}]_i$ which is consistent with the other reported studies (Hill, et al., 1990; Meininger, et al., 1990). It is interesting to find from the present studies that while the transient increase in Ca^{2+} was less affected by the Ca^{2+} channel blockers, the sustained elevation was significantly attenuated (Figures 6-5, 6-6 and 6-7). Moreover, higher concentration of NE (5μM) showed a greater ability to increase $[Ca^{2+}]_i$ during the plateau phase even in the presence of 10μM verapamil, however, this was abolished by the further addition of 10μM Gd^{3+} and so was the arteriolar contraction. Although the specific mechanisms for Gd^{3+} blocking Ca^{2+} channels are not clear, it is likely that this cation acts as a non-specific, competitive blocker that also block other Ca^{2+} channels (Song, et al, 1992). The observation that Gd^{3+} blocked the NE induced Ca^{2+} increase that was not sensitive to VOC blockade implicates, as some investigators suggested in other tissues, that receptor operated Ca^{2+} channels may be present in cremaster first order arteriolar smooth muscle cells. Moreover, the contractions demonstrated following an agonist stimulation under an similar condition when no pressure-induced contraction occurred, e.g. a similar $[Ca^{2+}]_i$ increase in presence of 1μM verapamil, gave additional supports to the notion of smooth muscle sensitization in response to agonists.

It has been suggested that distention of vascular smooth muscle or elevation of transmural pressure will enhance the arterial response to agonist (Lombard, et al., 1990; Nilsson and Sjoblom, 1985). Further, the observed higher $[Ca^{2+}]_i$ at elevated pressures, as presented in the studies in chapter 4, may suggests a more active state of arterioles. However, the observation that arteriolar contractile responses to caffeine (20mM) at 120mmHg smaller that at 50mmHg (Figure 6-12) argues against the proposition of arteriolar sensitization at higher pressures. However, the variation may be due to the different stimuli applied, caffeine vs. NE, because caffeine also inhibits phosphodiesterase and results in an elevated cAMP/cGMP level(s) and consequent vasodilatation.

In summary, results from the present studies demonstrate that while Ca^{2+} entry from extracellular compartment, mostly via VOCs, is a mandatory process for maintaining arteriolar basal tone and the initiation of myogenic contraction, the release of Ca^{2+} from intracellular stores is not an absolute requirement. However, the Ca^{2+} release may actually be involved during a myogenic response especially when the stimulus (pressure increase/stretch) is relatively larger as, in the presence of Ca^{2+} channel blockers, a transient Ca^{2+} increase was observed in response to an acute pressure increase from 50 to 120mmHg. On the other hand, NE induced arteriolar contractions showed more dependency on intracellular store release while the Ca^{2+} entry may play a more important role in the sustained phase of contraction instead of force initiation. Further, the Ca^{2+} entry following an agonist stimulation may include a mechanism, e.g. receptor operated channels, that is not activated during myogenic contractions.

CHAPTER VII

CONCLUDING STATEMENTS AND FUTURE DIRECTIONS

Results from the studies presented in this thesis provided substantial evidence to demonstrate the obligatory roles of $[Ca^{2+}]_i$ and MLC phosphorylation in arteriolar myogenic reactivity and further demonstrate the major contribution of Ca^{2+} entry from the extracellular environment. The studies also provided evidence to suggest that agonist-induced arteriolar contractions are dependent on the Ca^{2+}/CaM activated MLCK pathway with possible modulation by other mechanisms. Additional results support the notion that contractile protein expression in resistance vessels may also underlie differences in reactivity of large and small vessels and therefore could conceivably contribute to myogenic reactivity. These conclusions, and some avenues for future research, are discussed below together with a summary of the cellular events involved in the genesis of arteriolar tone and myogenic reactivity.

Contractile Isoform Expression May Set the Structural Basis for Arteriolar Myogenic Reactivity

The results from the present study demonstrated differences in contractile isoform expression in more active vessels. For example, the expression of α-actin isoform is inversely correlated with vessel diameter perhaps consistent with functional variations between vessels of different sizes. Similarly, arterial vessels showed more α-actin than did the corresponding venous vessels. Therefore, myogenic reactivity, which is most prevalent in small arteries and arterioles may, in part, relate to differences in structural composition of proteins participating in the contractile process.

Structural differences are not limited to the level of contractile proteins but also other aspects such as intracellular Ca^{2+} stores, cell membrane composition, the distribution and characteristics of ion channels [e.g. K^+ channels which have been implicated to serves as feedback mechanism during myogenic reactivity (Nelson, 1993)] et al.. Future studies directed towards revealing these differences, if they do exist, will help to further understand the dependency of cell functions (e.g. myogenic reactivity) on structural variations and signal transduction pathways.

Wall Tension or a Related Parameter May Be the Sensing Factor and the Controlled Variable During Myogenic Reactivity.

The present studies suggest that the effect of intraluminal pressure changes may be detected, by the arterioles, as alterations in wall tension or a related variable, and also, wall tension appears to be a regulatory factor that the arterioles attempt to maintain at a controlled level.

Although a number of studies, including the present experiments, suggest the regulatory role of wall tension in myogenic reactivity a definite conclusion has not been reached. Basic questions still remain such as: how is the wall tension being sensed, where is the site of this hypothetical tension sensor, and how the mechanical signal is translated into a chemical process. In the present studies, when arteriolar responses to acute pressure increases were examined, increases in wall tension were always associated with abrupt stretch of the vessel which made it difficult to interpret the results (i.e. what is the effect of change in tension vs. change in length). Further experiments need to be designed in such a way that these two related factors can be separated to allow the role of wall tension to be specifically addressed. For example, the study of arteriolar responses to slow (ramp) increases in transmural pressure when no obvious change in vessel diameter occurs.

$[Ca^{2+}]_i$ and MLC Phosphorylation Play Obligatory Roles in Arteriolar Myogenic Reactivity

Data presented in this thesis demonstrated that increased wall tension (elevated intraluminal pressure) is associated with increases in $[Ca^{2+}]_i$ and MLC phosphorylation. Further, the MLCK inhibitor, ML-7, inhibits myogenic tone by dissociating the Ca^{2+} response from arteriolar contraction. These data suggest that increases in $[Ca^{2+}]_i$ and MLC phosphorylation are obligatory requirements for the setting of pressure-dependent steady-state arteriolar spontaneous tone. Moreover, the arteriolar myogenic contraction to an acute pressure increase also showed dependencies on $[Ca^{2+}]_i$ and MLC phosphorylation. Additional studies that examine this pathway in the arteriolar responses to pulsatile pressures or in the presence of intraluminal flow will provide further information more closely related to the *in vivo* physiological conditions.

Extracellular Space is the Major Source for the Increased Ca^{2+} During Myogenic Reactivity.

The extracellular source, rather than the intracellular stores, is most important in providing of the Ca^{2+} required for the maintenance of arteriolar basal tone and the initiation of myogenic contraction. This conclusion is drawn from two lines of experimental evidence: 1) blockade of VOCs with verapamil abolished the spontaneous tone and the constriction to acute pressure increase; 2) arterioles still exhibited basal tone and myogenic contraction with an observed $[Ca^{2+}]_i$ rise when intracellular Ca^{2+} stores were depleted with ryanodine treatment. While Ca^{2+} entry from the extracellular environment, largely via VOCs, is a mandatory process, Ca^{2+} release from intracellular stores may play a supportive role in myogenic reactivity, especially during the response to acute pressure increases. This is suggested by the observation of transient increase in $[Ca^{2+}]_i$ in response to pressure step while the Ca^{2+} entry was blocked in presence of verapamil and Gd^{3+}. While evidence for the exact mechanism for this Ca^{2+} release is not provided from the present studies, stretch activated PLC activity could be a possible candidate as suggested by studies form other investigators (Matsumoto, et al., 1995; Osol, 1995). Another possible mechanism is Ca^{2+} mobilization due to the Ca^{2+} entry through SACs, via a calcium induced calcium release mechanism, upon stretch (pressure increase). Although the present studies show that Ca^{2+} entry blockade abolished the arteriolar response to acute pressure increase, the data were acquired when vessels were significantly dilated with lower levels of $[Ca^{2+}]_i$ because of the prolonged exposure to Ca^{2+} channel blockers. In order to examine this issue more closely, future experiments need to be designed so that the arteriolar responses to acute pressure increases can be monitored immediately after the Ca^{2+} entry blockade while the $[Ca^{2+}]_i$ and vessel diameter are not significantly affect. Moreover, the mechanism for VOC activation during myogenic contraction is another subject that needs to be further examined. Current evidence suggests both direct activation by stretch and, indirectly, by the cell depolarization due to the cation entry through SACs upon stretch (Davis, Donovitz and Hood, 1992; McCarron, et al., 1995).

Dependency of the Ca^{2+}/CaM Activated MLCK Pathway is Modulated by Other Mechanisms During Agonist-Induced Arteriolar Contraction

α-adrenergic agonist, norepinephrine, induced arteriolar contraction also depends on the increase in $[Ca^{2+}]_i$ and MLC phosphorylation as demonstrated in the present studies. However, the distinct patterns in temporal responses between myogenic and agonist-induced contraction indicate that different signal transduction pathways are present. For example, other regulatory mechanisms, such as the sensitization of the contractile elements perhaps by pathways involving PKC, may contribute to the agonist-induced arteriolar response. While the role of PLC is less obvious during myogenic contractions, activation of PLC in arteriolar responses to agonist stimulation appears more important. Arteriolar contraction showed much stronger dependency on Ca^{2+} release from intracellular stores, especially for the initiation of the contraction. The observation that Gd^{3+}, a non-specific Ca^{2+} channel blocker, inhibited arteriolar contraction to agonist indicates that a Ca^{2+} entry mechanism which is not exhibited in the myogenic contractions, possibly receptor-operated Ca^{2+} channels as suggested by others, is involved in the agonist-induced contractions.

Relationship with Other Vasoregulatory Mechanisms

Since these vessels are also under neuronal control and the influence of local metabolism, it is important to examine the interactions that occur between arteriolar responses to pressure changes and to metabolic/agonist stimulation. The interaction between endothelium, which underlies the smooth muscle cells on vessel wall, and vascular smooth muscle is another important issue need to be considered. These studies will help us in better understanding the arteriolar functions and characteristics under *in situ* conditions.

Signal Transduction Pathways Underlying Myogenic Reactivity

Based on the results from this thesis and published studies from other investigators, a schematic diagram is presented in Figure 7-1 to illustrate the signaling pathways involved in the arteriolar myogenic responses. Stretch of smooth muscle cells or an increase in tension, as would be expected to occur when vascular pressure increases, leads to the opening of stretch activated channels and allows cations (including Ca^{2+}) to enter from extracellular space. This event may serve several purposes: 1) it may cause membrane depolarization, due to the influx of cations, and subsequently activation of voltage operated Ca^{2+} channels (recent evidence suggested that VOC can also be directly modified by stretch); 2) the Ca^{2+} came in through this channel may induce a Ca^{2+} release from intracellular stores; 3) This Ca^{2+}, itself, also contribute to the increase in $[Ca^{2+}]_i$. The opening of VOCs allows more Ca^{2+} to enter and further increase $[Ca^{2+}]_i$. IP_3, together with DAG, is generated by PLC which is somehow activated following the stretch. Binding of IP_3 to its receptors on SR will cause a Ca^{2+} release which may represent another mechanism for the $[Ca^{2+}]_i$ rise. While all these events contribute to the elevation in $[Ca^{2+}]_i$ and lead to MLC phosphorylation, DAG activated PKC may exert its inhibitory effect on MLC phosphatase, hence, potentiates the levels of MLC phosphorylation and cause the sensitization of contractile apparatus to Ca^{2+}. The smooth muscle cell contraction then becomes an inevitable consequence.

Figure 7-1. Possible signaling pathways involved in the arteriolar myogenic responses.

Cell Signaling Pathways Involved in Arteriolar Myogenic Reactivity

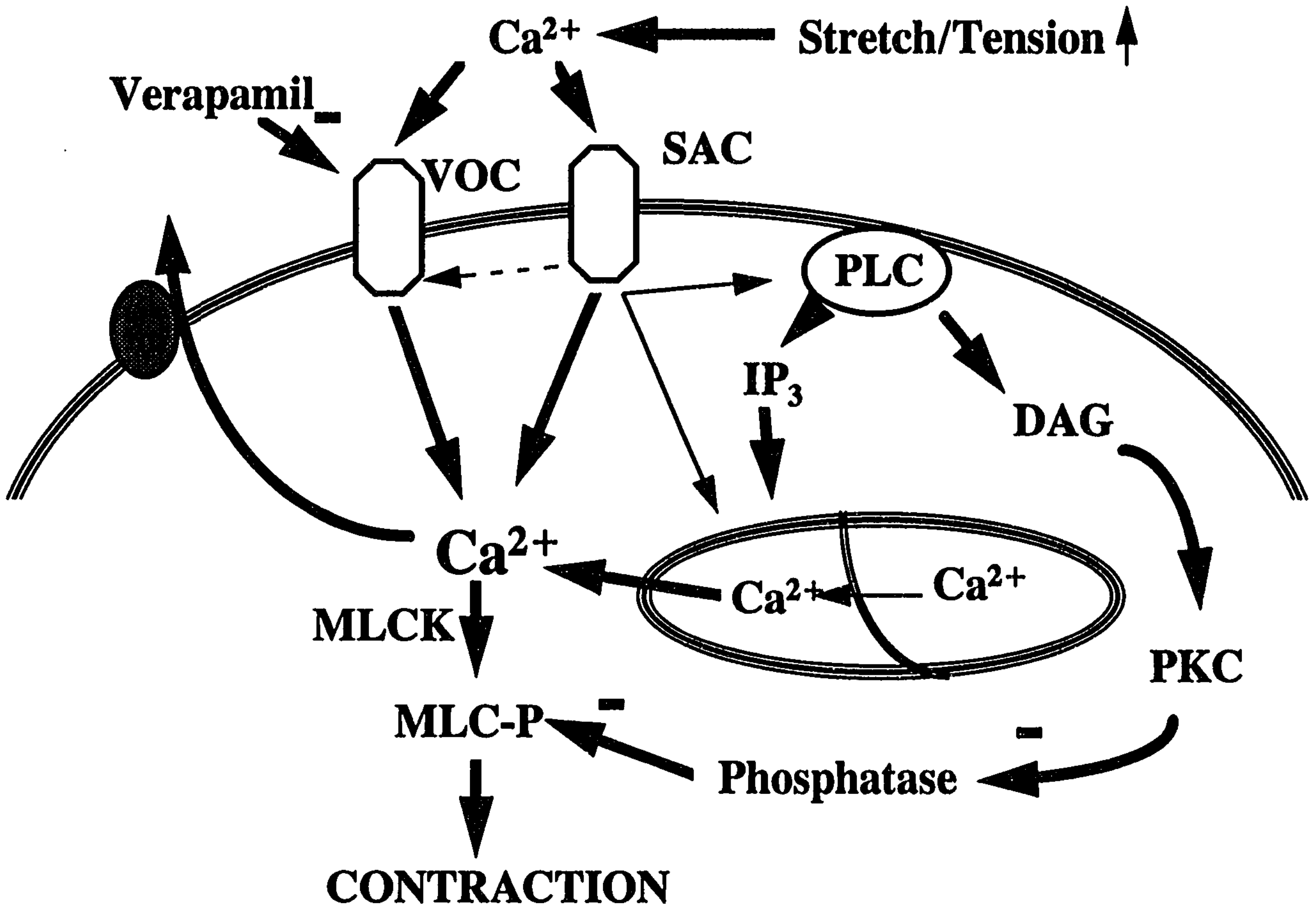
Ca2+
Stretch/Tension ↑
Verapamil
–
VOC
SAC
PLC
IP3
DAG
Ca2+
Ca2+
Ca2+
MLCK
MLC-P
–
–
PKC
Phosphatase
CONTRACTION

REFERENCES

1. **Adam, L. P., and D. R. Hathaway.** Identification of mitogen-activated protein kinase phosphorylation sequences in mammalian h-Caldesmon. *FEBS Lett.* 322:56-60, 1993.
2. **Aikawa, M., P. N. Sivam, M. Kuro-o, K. Kimura, K. Nakahara, S. Takewaki, M. Ueda, H, Yamaguchi, Y. Yazaki, M. Periasamy, R. Nagai.** Human smooth muscle myosin heavy chain isoforms as molecular markers for vascular development and atherosclerosis. *Circ. Res.* 73: 1000-1012, 1993.
3. **Aksoy, M. O., S. Mras, K. E. Kamm, and R. A. Murphy.** Ca^{2+}, cAMP, and changes in myosin phosphorylation during contraction of smooth muscle. *Am. J. Physiol.* 245 (*Cell Physiol.* 14): C255-C270, 1983.
4. **Allbritton, N. L., T. Meyer, and L. S. Stryer.** Range of messenger action of calcium ion and inositol 1,4,5-trisphosphate. *Science Wash. DC* 258: 1812-1815, 1992.
5. **Andrea, J. E., and M. P. Walsh.** Protein kinase C of smooth muscle. *Hypertension* 20: 585-595, 1992.
6. **Babij, P., and M. Periasamy.** Myosin heavy chain isoform diversity in smooth muscle is produced by differential RNA processing. *J. Mol. Biol.* 210: 673-679, 1989.

7. **Barany, K., A. Rokolya,. and M. Barany.** Stretch activates myosin light chain kinase in arterial smooth muscle. *Biochem. Biophys. Res. Comm.* 173:164-171, 1990.

8. **Bayliss, W. M.** On the local reaction of the arterial wall to changes of internal pressure. *J. Physiol. London* 28: 220-231, 1902.

9. **Bengur, A. R., E. A. Robinson, E. Appella, and J. R. Sellers.** Sequence of the sites phosphorylated by protein kinase C in the smooth muscle myosin light chain. *J. Biol. Chem.* 262: 7613-7617, 1987.

10. **Benham, C. D., P. Hess, and R. W. Tsien.** Two types of calcium channels in single smooth muscle cells from rabbit ear artery studied with whole-cell and single-channel recordings. *Circ. Res.* 61 (Suppl. I): I10-I16, 1987.

11. **Berridge, M. J.** Inositol trisphosphate and calcium signaling. *Nature Lond.* 361: 315-325, 1993.

12. **Biagi, B. A., and J. J. Enyeart.** Gadolinium blocks low- and high-threshold calcium currents in pituitary cells. *Am. J. Physiol.* 259 (*Cell Physiol.* 28): C515-C520, 1990.

13. **Birnbaumer, L., and A. M. Brown.** G proteins and the mechanism of action of hormones, neurotransmitters, and autocrine and paracrine regulatory factors. *Am. Rev. Respir. Dis.* 141: S106-S114, 1990.

14. **Blatte, L. A., and W. G. Wier.** Agonist-induced $[Ca^{2+}]_i$ wave and Ca^{2+}-induced Ca^{2+} release in mammalian vascular smooth muscle cells. *Am. J. Phsiol.* 263 (*Heart Circ. Physiol.* 32): H576-H586, 1992.

15. **Boels, P. J., M. Troschka, J. C. Ruegg, and G. Pfitzer.** Higher Ca^{2+} sensitivity of triton-skinned guinea pig mesenteric microarteries as compared with large arteries. *Circ. Res.* 69: 989-996, 1991.

16. **Borrione, A. C., A. M. C. Zanellato, G. Scannapieco, P. Pauletto, and S. Sartore.** Myosin heavy-chain in adult and developing rabbit vascular smooth muscle. *Eur. J. Biochem.* 183: 413-417, 1989.

17. **Brayden, J. E., and M. T. Nelson.** Regulation of arterial tone by activation of calcium-dependent potassium channels. *Science Wash. DC* 256: 532-535, 1992.

18. **Bulow, A., and H. Nilsson.** Myogenic activity in isolated resistance arteries from skeletal muscle of the rat. *Blood Vessels* 28: 278-279, 1991.

19. **Butler, T. M., M. J. Siegman, and S. U. Moers.** Chemical energy usage during shortening and work production in mammalian smooth muscle. *Am. J. Physiol. 244 (Cell Physiol. 13)*: C234-C242, 1983.

20. **Caiozzo, V. J., E. Ma, S. A. McCue, E. Smith, R. E. Herrick, and K. M. Baldwin.** A new animal model for modulating myosin isoform expression by altered mechanical activity. *J. Appl. Physiol.* 73: 1432-1440, 1992.

21. **Cassidy, P., P. E. Hoar, and W. G. Kerrick.** Irreversible thiophosphorylation and activation of tension in functionally skinned rabbit ileum strips by $[^{35}S]ATP\gamma S$. *J. Biol. Chem.* 254: 11148-11153, 1979.

22. **Chadwick, C. C., A. Saito, and S. Fleischer.** Isolation and characterization of the inositol 1,4,5-trisphosphate receptor from smooth muscle. *Proc. Natl. Acad. Sci. USA.* 87: 2132-2136, 1990.

23. **Chang, K. S., W. E. Zimmer, Jr., D. J. Bergsma, J, B. Dodgson, and R. J. Schwartz.** Isolation and characterization of six different chicken actin genes. *Mol. Cell. Biol.* 4: 2498-2508, 1984.

24. **Chatterjee, M., and R. A. Murphy.** Calcium-dependent stress maintenance without myosin phosphorylation in skinned smooth muscle. *Science Wash. DC* 221: 464-466, 1983.

25. **Clapham, D. E., and E. J. Neer.** New roles for G-protein βγ-dimers in transmembrane signaling. *Nature Lond.* 365: 403-406, 1993.

26. **Clayton, L., F. C. Reinach, G. M. Chumbley and A. R. Macleod.** Organization of the hTM_{nm} gene implications for the evolution of muscle and non-muscle tropomyosin. *J. Mol. Biol.* 201: 507-515, 1988.

27. **Cohen, D. M., and R. A. Murphy.** Differences in cellular contractile protein contents among porcine smooth muscles. *J. Gen. Physiol.* 72: 369-380, 1978.

28. **Collins, E. M., M. P. Walsh, and K. G. Morgan.** Contraction of single vascular smooth muscle cells by phenylephrine at constant $[Ca^{2+}]_i$. *Am. J. Physiol.* 262 (*Heart Circ. Physiol.* 31): H754-H762, 1992.

29. **Csabina, S., M. Barany, and K. Barany**. Stretch-induced myosin light chain phosphorylation in rat uterus. *Arch. Biochem. Biophys.* 249: 374-381, 1986.

30. **Cummins, P., and S. V. Perry.** Chemical and immunochemical characteristics of tropomyosins from striated and smooth muscle. *Biochem. J.* 141: 43-49, 1974.

31. **Davis, M. J.** Myogenic response gradient in an arteriolar network. *Am. J. Physiol.* 264 *(Heart Circ. Physiol. 33)*: H2168-H2179, 1993.

32. **Davis, M. J., J. A. Donovitz, and J. D. Hood.** Stretch-activated single-channel and whole currents in vascular smooth muscle cells. *Am. J. Physiol.* 262 (*Cell Physiol.* 31): C1083-C1088, 1992.

33. **Davis, M. J., G. A. Meininger, and D. C. Zawieja.** Stretch-induced increase in intracellular calcium of isolated vascular smooth muscle cells. *Am. J. Phsiol.* 263 (*Heart Circ. Physiol.* 32): H1292-H1299, 1992.

34. **Defeo, T. T., G. M. Briggs, and K. G. Morgan.** Ca^{2+} signals obtained with multiple indicators in vascular smooth muscle cells. *Am. J. Physiol.* 253 (*Heart Circ. Physiol.* 22): H1456-H1461, 1987

35. **Demirel, E., J. Rusko, D. J. Adams, and C. Van Breemen.** TEA inhibits ACh-induced EDRF release: endothelial Ca^{2+}-dependent K^+ channels contribute to vascular tone. *Am. J. Physiol.* 267 (*Heart Circ. Physiol.* 36): H1135-H1141, 1994.

36. **Dillon, P. F., M. O. Aksoy, S. P. Driska, and R. A. Murphy.** Myosin phosphorylation and the cross-bridge cycle in arterial smooth muscle. *Science Wash. DC* 211: 495-497, 1981.

37. **Driska, S. P., M. O. Aksoy, and R. A. Murphy.** Myosin light chain phosphorylation associated with contraction in arterial smooth muscle. *Am. J. Physiol.* 240 (*Cell Physiol.* 9): C222-233, 1981.

38. **Duling, B. R., R. M. Berne, and G. V. R. Born.** Microiontophoretic application of vasoactive agents to the microcirculation of the hamster cheek pouch. *Microvasc. Res.* 1: 158-173, 1968.

39. **Dunn, W. R., G. C. Wellman, and J. A. Bevan.** Enhanced resistance artery sensitivity to agonists under isobaric compared with isometric conditions. *Am. J. Phsiol.* 266 (*Heart Circ. Physiol.* 35): H147-H155, 1994.

40. **Eddinger, T. J., and R. A. Murphy.** Two smooth muscle myosin heavy chains differ in their light meromyosin fragment. *Biochemistry* 27: 3807-3811, 1988.

41. **Eddinger, T. J., and R. A. Murphy.** Developmental changes in actin and myosin heavy chain isoform expression in smooth muscle. *Arch. Biochem. Biophys.* 284: 232-237, 1991.

42. **Eddinger, T. J., and J. A. Wolf.** Four myosin heavy chain isoforms in mouse uterus. *Cell Motil. Cytoskeleton* 25: 358-368, 1993.

43. **Eiichi, S. M. Resnick, and K. G. Morgan.** Change of Ca^{2+} requirement for myosin phosphorylation by prostagladin $F_{2\alpha}$. *Am. J. Physiol.* 261 (*Cell Physiol.* 30): C253-C258, 1991.

44. **Emerson, C. P., and S. I. Bernstein.** Molecular genetics of myosin. *Annu. Rev. Biochem.* 56: 695-726, 1987.

45. **Falcone, J. C., M. J. Davis, and G. A. Meininger.** Endothelial independence of the myogenic response in skeletal muscle arterioles. *Am. J. Physiol. 260 (Heart Circ. Physiol. 29):* H130-H135, 1991.

46. **Fatigati, V., and R. A. Murphy.** Actin and tropomyosin variants in smooth muscles: Dependence on tissue type. *J. Biol. Chem.* 259: 14383-14388, 1984.

47. **Fay, F. S., S. Yagi, T. Itoh, J. McCarron, G. McGeown, J. Walsh, M. Ikebe, E. D. W. Moore.** Cellular and molecular physiology of calcium signaling in smooth muscle cells. *Jpn. J. Pharmacol.* 58 (Suppl. 2): 55P-40P, 1992.

48. **Felder, C. C., M. O. Poulter, and J. Wess.** Muscarinic receptor-operated Ca^{2+} influx in transfected fibroblast cells is independent of inositol phosphates and release of intracellular Ca^{2+}. *Proc. Natl. Acad. Sci. USA* 89: 509-513, 1992.

49. **Finch, E. A., T. J. Turner, and S. M. Goldin.** Calcium as a coagonist of inositol 1,4,5-trisphosphate-induced calcium release. *Science Wash. DC* 252: 443-446, 1991.

50. **Folkow, B.** Intravascular pressure as a factor regulating the tone of the small vessels. *Acta Physiol. Scand.* 17: 289-310, 1949.

51. **Folkow, B.** A study of the factors influencing the tone of denervated blood vessels perfused at various pressures. *Acta Physiol. Scand.* 27: 118-129, 1952.

52. **Folkow, B., K. Haeger, and G. Hahlson.** Observations on reactive hyperemia as related to histamine on drugs antagonizing vasodilatation induced by histamine and one vasodilator properties of adenosine triphosphate. *Acta Physiol. Scand.* 15: 264-278, 1948.

53. **Gaylinn, B. D., T. J. Eddinger. P. A. Martino, P. L. Monical, D. F. Hunt, and R. A. Murphy.** Expression of nonmuscle myosin heavy and light chain in smooth muscle. *Am. J. Phsiol.* 257 (*Cell Physiol.* 26): C997-C1004, 1989.

54. **Gilon, P., G. J. Bird, X. Bian, J. L. Yakel, and J. W. Putney, Jr..** The Ca^{2+}-mobilizing actions of a Jurkat cell extract on mammalian cells and Xenopus laevis oocytes. *J. Biol. Chem.* 270: 8050-8055, 1995.

55. **Giulian, G. G., R. L. Moss, and M. L Greaser.** Improved methodology for analysis and quantitation of proteins on one-dimensional silver-stained slab gels. *Anal. Bioch.* 129: 277-287, 1983.

56. **Gong, M. C., A. Fuglsang, D. Alessi, S. Kobayashi, P. Cohen, A. V. Somlyo, and A. P. Somlyo.** Arachidonic acid inhibits myosin light chain phosphatase and sensitizes smooth muscle to calcium. *J. Biol. Chem.* 267: 21492-21498, 1992.

57. **Goodman, A. H.** Un calibreur video simple pour l'utilisation en microscopie video. *Innov Tech. Biol. Med.* 9: 350-356, 1988.

58. **Gore, R. W.** Wall Stress: a determinant of regional differences in response of frog microvessels to norepinephrine. *Am. J. Physiol.* 222: 82-91, 1972.

59. **Graceffa, P.** In-register homodimers of smooth muscle myosin. *Biochemstry* 28: 1282-1287, 1989.

60. **Granger, H. J., M. E. Schelling, R. E. Lewis, D. C. Zawieja, and C. J. Meininger.** Physiology and pathobiology of the microcirculation. *Am. J. Otolarygol.* 9: 264-277, 1988.

61. **Grynkyewicz, G., M. Poenie, and R.Y. Tsien.** A new generation of Ca^{2+} indicators with greatly improved fluorescence properties. *J. Biol. Chem.* 260: 3440-3450, 1985.

62. **Haeberle, J. R., D. R. Hathaway, and C. L. Smith.** Caldesmon content of mammalian smooth muscles. *J. Muscle Res. Cell Motil.* 13: 81-89, 1992.

63. **Hai, C., and R. A. Murphy.** Cross-bridge phosphorylation and regulation of latch state in smooth muscle. *Am. J. Phsiol.* 254 (*Cell Physiol.* 23): C99-C106, 1988.

64. **Harder, D. R.** Pressure-dependent membrane depolarization in cat middle cerebral artery. *Circ. Res.* 55: 197-202, 1984.

65. **Harder, D. R.** Pressure-induced myogenic activation of cat cerebral arteries is dependent on intact endothelium. *Circ. Res.* 60: 102-107, 1987.

66. **Harder, D. R.** Increased sensitivity of cat cerebral arteries to serotonin upon elevation of transmural pressure. *Pflugers Arch.* 411: 698-700, 1988.

67. **Harder, D. R., R. Gilbert, and J. H. Lombard.** Vascular muscle cell depolarization and activation in renal arteries on elevation of transmural pressure. *Am. J. Physiol.* 253 (*Renal Fluid Electrolyte Physiol.* 22): F778-F781, 1987.

68. **Helper, D. J., J. A. Lash, and D. R. Hathaway.** Distribution of the isoelectric variants of the 17,000-dalton myosin light chain in mammalian smooth muscle. *J. Biol. Chem.* 263: 15748-15753, 1988.

69. **Herlihy, J. T., and R. A. Murphy.** Length-tension relationship of smooth muscle of the hog carotid artery. Circ. Res. 33: 275-283, 1973.

70. **Heukeshoven, J., and R. Dernick.** Simplified method for silver staining of proteins in polyacrylamide gels and the mechanism of silver staining. *Electrophoresis* 6: 103-112, 1985.

71. **Hill, M. A., M. J. Davis, J. Song, and H. Zou.** Calcium dependence of indolactam mediated contractions in resistance vessels. *J. Pharmacol. Exp. Ther.* in press, 1996.

72. **Hill, M. A., J. C. Falcone, and G. A. Meininger.** Evidence for protein kinase C involvement in arteriolar myogenic reactivity. *Am. J. Physiol.* 259 (*Heart Circ. Physiol.* 28): H1586-H1594, 1990.

73. **Hill, M. A., and G. A. Meininger.** Calcium entry and myogenic phenomena in skeletal muscle arterioles. *Am. J. Physiol.* 267 (*Heart Circ. Physiol.* 36): H1085-H1092, 1994.

74. **Hill, M. A., M. J. Davis, V. Miriel and J. Song.** Ca^{2+} and PKC-mediated contractions in resistance vessels. *Microcirculation* 2: (abstract), 1995.

75. **Himpens, B., L. Missiaen, and R. Casteels.** Ca^{2+} homeostasis in vascular smooth muscle. *J. Vasc. Res.* 32: 207-219, 1995.

76. **Iino, M.** Calcium-induced calcium release mechanisms in guinea-pig taenia caeci. *J. Gen. Physiol.* 94: 363-383, 1989.

77. **Iino, M.** Calcium release mechanisms in smooth muscle. *Jpn. J. Pharmacol.* 54: 345-354, 1990.

78. **Ikebe, M. and D. J. Hartshorne.** Phosphorylation of smooth muscle myosin at two distinct sites by myosin light chain kinase. *J. Biol. Chem.* 260: 10027-10031, 1985.

79. **Ikebe, M., D. J. Hartshorne, and M. Elzinga.** Phosphorylation of the 20,000-dalton light chain of smooth muscle myosin by the calcium-activated, phospholipid-dependent protein kinase. *J. Biol. Chem.* 262: 9569-9573, 1987.

80. **Itoh, H., A. Shimomura, S. Okubo, K. Ichikawa, M. Ito, T. Konishi, and T. Nakano.** Inhibition of myosin light chain phosphatase during Ca^{2+}-independent vasocontraction. *Am. J. Physiol.* 265 (*Cell Physiol.* 34): C1319-C1324. 1993.

81. **Itoh, T., M. Ikebe, G. J. Kargacin, D. J. Hartshorne, B. E. Kemp, and F. S. Fay.** Effect of modulators of myosin light-chain kinase activity in single smooth muscle cells. *Nature Lond.* 338: 164-167, 1989.

82. **Jackson, P. A., and B. R. Duling.** Myogenic response and wall mechanics of arterioles. *Am. J. Phsiol.* 257 (*Heart Circ. Physiol.* 26): H1147-H1155, 1989.

83. **Jancsó, A., and P. Graceffa.** Smooth muscle tropomyosin coiled-coil dimer. *J. Biol. Chem.* 266: 5891-5897, 1991.

84. **Jiulian, G. G., R. L. Moss, and M. Greaser.** Improved methodology for analysis and quantitation of proteins on one-dimensional silver-stained slab gels. *Anal. Biochem.* 129: 277-287, 1983.

85. **Johnson, P. C.** The myogenic response. In, *Handbook of Physiology*, section 2, The Cardiovascular System, vol. II, Vascular Smooth Muscle, Ed. Bohr, D. R., Somlyo, A. P. and Sparks, H. V. Jr., American Physiological Society, Bethesda, MD. pp.409-442, 1980.

86. **Johnson, P. C.** Autoregulation of blood flow. *Circ. Res.* 59: 483-495, 1986.

87. **Kamm, K. E., and J. T. Stull.** The function of myosin and myosin light chain kinase phosphorylation in smooth muscle. *Ann. Rev. Pharmacol. Toxicol.* 25: 593-620, 1985.

88. **Kamm, K. E., and J. T. Stull.** Myosin phosphorylation, force, and maximal shortening velocity in neurally stimulated tracheal smooth muscle. *Am. J. Physiol.* 249 (*Cell Physiol.* 18): C238-C247, 1985b.

89. **Katoch, S. S., and R. S. Moreland.** Agonist and membrane depolarization induced activation of MAP kinase in the swine carotid artery. *Am. J. Physiol.* 269 (*Heart Circ. Physiol.* 38): H222-H229, 1995.

90. **Katsuragawa, Y., M. Yanagisawa, A. Inoue, and T. Masaki.** Two distinct nonmuscle myosin-heavy-chain mRNAs are differentially expressed in various chicken

tissues. Identification of a novel gene family of vertebrate non-sarcomeric myosin heavy chains. *Eur. J. Biochem.* 184: 611-616, 1989.

91. **Katsuyama, H., C.-L. A. Wang, and K G. Morgan.** Regulation of vascular smooth muscle tone by caldesmon. *J. Biol. Chem.* 267: 14555-14558, 1992.

92. **Katsuyama, H., and K. G. Morgan.** Mechanisms of Ca^{2+}-independent contraction in single permeabilized ferret aorta cells. *Circ. Res.* 72: 651-657, 1993.

93. **Katusic, Z. S., J. T. Shepherd, and P. M. Vanhoutte.** Endothelial-dependent contraction to stretch in canine basilar arteries. *Am. J. Physiol.* 252 (*Heart Circ. Physiol.* 21): H671-H673, 1987.

94. **Kawamoto, S., and R. S. Adelstein.** Characterization of myosin heavy chains in cultured aorta smooth muscle cells. *J. Biol. Chem.* 262: 7282-7288, 1987.

95. **Kelly, C. A., J. R. Sellers, P. K. Goldsmith, and R. S. Adelstein.** Smooth muscle myosin is composed of homodimeric heavy chains. *J. Biol. Chem.* 267: 2127-2130, 1992.

96. **Kirber, M. T., R. W. Ordway, L. H. Clapp, J. V. Walsh, Jr., and J. J. Singer.** Both membrane stretch and fatty acids directly activate large conductance Ca^{2+}-activated K^+ channels in vascular smooth muscle cells. *FEBS Lett.* 297: 24-28, 1992.

97. **Kirber, M. T., J. V. Walsh, Jr., and J. J. Singer.** Stretch-activated ion channels in smooth muscle: a mechanism for the initiation of stretch-induced contraction. *Pflügers Arch.* 412:-339-345, 1988.

98. **Kitazawa, T., M. Masuo, and A. P. Somlyo.** G protein-mediated inhibition of myosin light-chain phosphatase in vascular smooth muscle. *Proc. Natl. Acad. Sci.* USA. 88: 9307-9310, 1991.

99. **Kuo, L., Chilian, W. M., and M. J. Davis.** The coronary arteriolar myogenic response is independent of the endothelium. *Circ. Res.* 66: 860-866, 1990.

100. **Kuo, L., W. M. Chilian, and M. J. Davis.** Interaction of pressure- and flow-induced responses in porcine coronary resistance vessels. *Am. J. Physiol.* 261 (*Heart Circ. Physiol.* 30): H1707-H1705, 1991.

101. **Kuo, L., M. J. Davis, and W. M. Chilian.** Endothelial modulation of arteriolar tone. *NIPS* 7: 5-9, 1992.

102. **Kwan, C. Y.** Signal transduction in smooth muscle as studied by the subcellular membrane approach. *Can. J. Physiol. Pharmacol.* 70: 501-508, 1991.

103. **Kwan, C. Y., H. Takemura, J. F. Obie, O. Thastrup, and J. W. Putney, Jr.** Effect of Mech, thapsigargin, and La^{3+} on plasmalmmal and intracellular Ca^{2+} transport in lacrimal acinar cells. *Am. J. Physiol.* 258 (*Cell Physiol.* 27): C1006-C1015, 1990.

104. **Kwan, C. Y., and J. W. Putney, Jr.** Uptake and intracellular sequestration of divalent cations in resting and methacholine-stimulated mouse lacrimal acinar cells. *J. Biol. Chem.* 265(2): 678-684, 1990.

105. **Laemmli, U. K.**, Cleavage of structural proteins during the assembly of the head of bacteriophage T4. *Nature Lond.* 227: 680-685, 1970

106. **Laher, I., and J. A. Bevan.** Protein kinase C activation selectively augments a stretch-induced, calcium-dependent tone in vascular smooth muscle. *J. Pharmacol. Exp. Ther.* 242: 566-572, 1987.

107. **Laher, I. and J. A. Bevan.** Stretch of vascular smooth muscle activates tone and $^{45}Ca^{2+}$ influx. *J. Hypertens. Suppl.* 7: S17-S20, 1989.

108. **Laher, I., C. van Breemen, and J. A. Bevan.** Stretch-dependent calcium uptake associated with myogenic tone in rabbit facial vein. *Circ. Res.* 63: 669-772. 1988.

109. **Laporte, R., J. R. Haeberle, and I. Laher.** Phorbol ester-induced potentiation of myogenic tone is not associated with increases in Ca^{2+} influx, myoplasmic free Ca^{2+} concentration, or 20-kDa myosin light chain phosphorylation. *J. Mol. Cell. Cardiol.* 26: 297-302, 1994.

110. **Ledvora, R. F., K. Barany, D. L. VanderMuelen, J. T. Barron,. and M. Barany.** Stretch-induced phosphorylation of the 20,000-dalton light chain of myosin in arterial smooth muscle. J. Biol. Chem. 258: 14080-14083, 1983.

111. **Lee, M. W., and D. L. Severson.** Signal transduction in vascular smooth muscle: diacylglycerol second messengers and PKC action. *Am. J. Physiol.* 267 (*Cell Physiol.* 36): C659-C678, 1994.

112. **Lehman, W.** Calponin and the composition of smooth muscle thin filaments. *J. Muscle Res, Cell Mot.* 12: 221-224, 1991.

113. **Lehman, W., C. Moody, and R. Craig.** Caldesmon and the structure of vertebrate smooth muscle thin filaments. *Ann. N. Y. Acad. Sci.* 599: 75-84, 1990.

114. **Lincoln, T. M., and T. L. Cornwell.** Towards an understanding of the mechanism of action of cyclic AMP and cyclic GMP in smooth muscle relaxation. *Blood Vessels* 28: 129-137, 1991.

115. **Lincoln, T. M., and T. L. Cornwell.** Intracellular cyclic GMP receptor proteins. *FASEB. J.* 7:328-338, 1993.

116. **Liu, Y., D. R. Harder, and J. H. Lombard.** Myogenic activation of canine small renal arteries after nonchemical removal of the endothelium. *Am. J. Physiol.* 267 (*Heart Circ. Physiol.* 36): H302-H307, 1994.

117. **Llopis, J., G. E. N. Kass, A. Gahm, and S. Orrenius.** Evidence for two pathways of receptor-mediated Ca^{2+} entry in hepatocytes. *Biochem. J.* 284: 243-247, 1992.

118. **Lombard, J. H., H. Eskinder, K. Kauser, J. L. Osborn, and D. R. Harder.** Enhanced norepinephrine sensitivity in renal arteries at elevated transmural pressure. *Am. J. Phsiol.* 259 (*Heart Circ. Physiol.* 28): H29-H33, 1990.

119. **Low, A. M., C. Y. Kwan, and E. E. Daniel.** Evidence for two types of internal Ca^{2+} stores in canine mesenteric artery with different refilling mechanisms. *Am. J. Physiol.* 262 (*Heart Circ. Physiol.* 31): H31-H37, 1992.

120. **Mabuchi, K., J. J.-C. Lin, and C.-L. A. Wang.** Electron microscopic images suggest both ends of caldesmon interact with actin filaments. *J. Muscle Res. Cell Motil.* 14: 54-64, 1993.

121. **MacPherson, R. S., L. J. McLeod, and R. L. Rasiah.** Myogenic response of isolated pressurized rabbit ear artery is independent of endothelium. *Am. J. Physiol.* 260 (*Heart Circ. Physiol.* 29): H779-H784, 1991.

122. **Marston, S. B., and C. S. Redwood.** Inhibition of actin-tropomyosin activation of myosin Mg^{2+}-ATPase activity by the smooth muscle regulatory protein caldesmon. *J. Biol. Chem.* 267: 6796-16800, 1992.

123. **Marston, S. B., and W. Lehman.** Caldesmon is a Ca^{2+}-regulatory component of native smooth-muscle thin filament. *Biochem. J.* 231: 517-522, 1985.

124. **Matlib, M. A.** Role of sarcolemmal membrane sodium-calcium exanger in vascular smooth muscle tension. *Ann. N. Y. Acad. Sci.* 639: 531-541, 1991.

125. **Matsuda, J. J., K. A. Volk, and E. F. Shibato.** Calcium currents in isolated rabbit coronary arterial smooth muscle myocytes. *J. Physiol. Lond.* 427: 657-680, 1990.

126. **Matsumoto, H., C. B. Baron, and R. F. Coburn.** Smooth muscle stretch-activated phospholipase C activity. *Am. J. Phsiol.* 268 (*Cell Physiol.* 37): C458-C465, 1995.

127. **Matsuoka, R.** Molecular cloning and characterization of a gene coding for human cardiac myosin heavy-chain. *Nippon Rinsho* 51: 1441-1447, 1993.

128. **McCarron, J. G., G. Osol, and W. Halpern.** Myogenic responses are independent of the endothelium in rat pressurized posterior cerebral arteries. *Blood Vessels* 26: 315-319, 1989.

129. **McPherson, P. S., and K. P. Campbell.** The ryanodine receptor/Ca^{2+} release channel. *J. Biol. Chem.* 268: 13765-23768, 1993.

130. **Meininger, G. A. and M. J. Davis.** Cellular mechanisms involved in the vascular myogenic response. *Am. J. Physiol.* 263 (*Heart Circ. Physiol.* 32): H647-H659, 1992.

131. **Meininger, G. A., and J. E. Faber.** Adrenergic facilitation of myogenic response in skeletal muscle arterioles. *Am. J. Phsiol.* 260 (*Heart Circ. Physiol.* 29): H1424-H1432, 1991.

132. **Meininger, G. A., D. C. Zaweija, J. C. Falcone, M. A. Hill, and J. P. Davey.** Calcium measurement in isolated arterioles during myogenic and agonist stimulation. *Am. J. Physiol.* 261 (*Heart Circ. Physiol.* 30): H950-H959, 1991.

133. **Meyer, T., T. Wensel, and L. Stryer.** Kinetics of calcium channel opening by inositol 1,4,5-trisphosphate. *Biochemistry* 29: 32-37, 1990.

134. **Mohammad, M. A., and M. P. Sparrow.** The heavy-chain stoichiometry of smooth muscle myosin is a characteristic of smooth muscle tissues. *Aust. J. Biol. Sci.* 41: 409-419, 1988.

135. **Morano, I., G. Erb, and B. Sogl.** Different expression and post-translational modification of myosin heavy and light chains increased shortening velocity in the pregnant rat uterus. *Pflugers Arch.* 420: R102, 1992.

136. **Moreland, S., L. M. Antes, D. M. McMullen, P. G. Sleph, and G. J. Grover.** Myosin light-chain phosphorylation and vascular resistance in canine anterior tibial arteries in situ. *Pflugers Arch.* 417: 180-184, 1990.

137. **Moreland. S., J. Nishimura, C. van Breemen, H. Y. Ahn, and R. S. Moreland.** Transient myosin phosphorylation at constant Ca^{2+} during agonist activation of permeabilized arteries. *Am. J. Physiol.* 263 (*Cell Physiol.* 32): C540-C544, 1992.

138. **Morgan, J. P. and K. G. Morgan.** Stimulus-specific patterns of intracellular calcium levels in smooth muscle of the ferret portal vein. *J. Physiol. Lond.* 355: 155-167, 1984.

139. **Murphy, R. A.** Myosin phosphorylation and crossbridge regulation in arterial smooth muscle. *Hypertension* 4: (Suppl II): II-3-II-7, 1982.

140. **Murphy, R. A.** Do the cytoplasmic and muscle-specific isoforms of actin and myosin heavy and light chains serve different functions in smooth muscle? *Jpn J. Pharmacol.* 58: 67P-74P, 1992.

141. **Murphy, R. A.** What is special about smooth muscle? The significance of covalent crossbridge regulation. *FASEB J.* 8: 311-318, 1994.

142. **Narayanan, J., M. Imig, R. J. Roman, and D. R. Harder.** Pressurization of isolated renal arteries increases inositol triphosphate and diacylglycerol. *Am. J. Physiol.* 266 (*Heart Circ. Physiol.* 35): H1840-H1845, 1994.

143. **Nelson, M. T., J. B. Patlak, J. F. Worley, and N. B. Standen.** Calcium channels, potassium channels, and voltage dependent of arterial smooth muscle tone. *Am. J. Physiol.* 259 (*Cell Physiol.* 28): C3-C18, 1990.

144. **Nelson, M. T., and J. F. Worley.** Dihydropyridine inhibition of single calcium channels and contraction in rabbit mesenteric artery depends on voltage. *J. Physiol. Lond.* 412: 65-91, 1989.

145. **Ngai, P. K., and M. P. Walsh.** Inhibition of smooth muscle actin-activated myosin Mg^{2+}-ATPase activity by caldesmon. *J. Biol. Chem.* 259: 13656-13659, 1984.

146. **Nilsson, H., and N. Sjoelblom.** Distention-dependent changes in noradrenaline sensitivity in small arteries from the rat. *Acta Physiol. Scand.* 125: 429-435, 1985.

147. **Nishikawa, M., P. deLanerolle, T. M. Lincoln, and R. S. Adelstein.** Phosphorylation of smooth muscle myosin light chain kinase by protein kinase C. Comparative study of the phosphorylated sites. *J. Biol. Chem.* 260: 8978-8983, 1985.

148. **Nishimura, J., R. A. Khalil, J. P. Drenth, and C. van Breemen.** Evidence for increased myofilament Ca^{2+} sensitivity in norepinephrine-activated vascular smooth muscle. *Am. J. Physiol.* 259 (*Heart Circ. Physiol.* 28): H2-H8, 1990.

149. **Nixon, G. F., K. Lizuka, C. M. M. Haystead, T. A. J. Haystead, A. P. Somlyo, and A. V. Somlyo.** Phosphorylation of caldesmon by mitogen-activated protein kinase with no effect on Ca^{2+} sensitivity in rabbit smooth muscle. *J. Physiol. Lond.* 487: 283-289, 1995.

150. **O'Donnell, M. E., and N. E. Owen.** Regulation of ion pumps and carriers in vascular smooth muscle. *Physiol. Rev.* 74(3): 683-720, 1994.

151. **Omote, M., and H. Mizusawa.** Effects of cyclopiazonic acid on phenylephrine-induced contractions in the rabbit ear artery. *Br. J. Pharmacol.* 111: 233-237, 1994.

152. **Osage, O. S., J. E. Merritt, T. J. Hallam, and T. J. Rink.** Receptor-mediated calcium entry in fura-2-loaded human platelets stimulated with ADP and thrombin. *Biochem. J.* 258: 923-926, 1989.

153. **Osol, G., I. Laher, and M. Cipolla.** Protein kinase C modulates basal myogenic tone in resistance arteries from the cerebral circulation. *Circ. Res.* 68: 359-367, 1991.

154. **Osol, G., I. Laher, and M. Kelly.** Myogenic tone is coupled to phospholipase C and G protein activation in small cerebral arteries. *Am. J. Physiol* 265 (*Heart Circ. Physiol.* 34): H415-H420, 1993.

155. **Owens, G. K., A. Loeb, D. Gordon, and M. M. Thompson.** Expression of smooth muscle specific α-isoactin in cultured vascular smooth muscle cells: Relationship between growth and cytodifferentiation. *J. Cell Biol.* 102: 343-352, 1986.

156. **Parente, J. E., M. P. Walsh, W. G. L. Kerrick, and P. E. Hoar.** Effects of constituitively active proteolytic fragment of protein kinase C on the contractile properties of demembranated smooth muscle fibers. *J. Muscle Res. Cell Motil.* 13: 90-99, 1992.

157. **Pfitzer, G, C. Zeugner, M. Troschka, and J. M. Chalovich.** Caldesmon and a actin-binding fragment of caldesmon inhibit tension development in skinned gizzard muscle fiber bundles. *Proc. Natl. Acad. Sci. USA.* 90: 5904-5908, 1993.

158. **Pinter, K., and S. B. Martson.** Phosphorylation of vascular smooth muscle caldesmon by endogenous kinase. *FEBS Lett.* 305: 192-196, 1992.

159. **Putney, J. W., Jr.** Capacititative calcium entry revisited. *Cell Calcium* 11: 611-624, 1990.

160. **Raeymaekers, L., and L. R. Jones.** Evidence for the presence of phospholamban in the endoplasmic reticulum of smooth muscle. *Biochem. Biophys. Acta.* 882: 258-265, 1986.

161. **Raeymaekers, L., and F. Wuytack.** Ca^{2+} pump in smooth muscle cells. *J. Muscle Res. Cell Motil.* 14: 141-157, 1993.

162. **Randriamampita, C., and R. Y. Tsien.** Emptying of intracellular Ca2+ stores releases a novel small messenger that stimulates Ca2+ influx. *Nature Lond.* 364: 809-814, 1993.

163. **Rasmussen, H., Y. Tanuwa, and S. Park.** Protein kinase C in the regulation of smooth muscle contraction. *FASEB J.* 1: 177-185, 1987.

164. **Ratz, P. H.** High α_1-adrenoceptor occupancy decreases relaxing potency of nifedipine by increasing myosin light chain phosphorylation. *Circ. Res.* 72: 1308-1316, 1993.

165. **Ratz, P. H., and R. A. Murphy.** Contribution of intracellular and extracellular Ca2+ pools to activation of myosin phosphorylation and stress in swine carotid media. *Cir. Res.* 60: 410-421, 1987.

166. **Rembold, C. M. and R. A. Murphy.** $[Ca^{2+}]_i$-dependent myosin phosphorylation in phorbol diester stimulated smooth muscle contraction. *Am. J. Physiol.* 255 (*Cell Physiol.* 24): C719-C723, 1988.

167. **Rhodin, J. D. D.** The ultrastructure of mammalian arterioles and precapilary sphincters. *J. Ultrasruc. Res.* 18: 181-223, 1967.

168. **Robson, L., and M. Hunter.** Volume-activated, gadolinium-sensitive whole-cell currents in single proximal cells of frog kidney. *Pflugers Arch.* 429: 98-106, 1994.

169. **Rovner, A. S., R. A. Murphy, and G. K. Owens.** Expression of smooth muscle and non-muscle myosin heavy chains in cultured vascular smooth muscle cells. *J. Biol. Chem.* 261: 14740-14745, 1986.

170. **Rovner, A. S., M. M. Thompson. and R. A. Murphy.** Two different heavy chains are found in smooth muscle myosin. *Amer. J. Physiol.* 250 (*Cell Physiol.* 19): C861-C870, 1986.

171. **Rubanyi, G. M.** Endothelium-dependent pressure-induced contraction of isolated canine carotid arteries. *Am. J. Physiol.* 255 (*Heart Circ. Physiol.* 24): H783-H788, 1988.

172. **Sage, S. O., J. E Merrit, T. J. Hallam and T. J. Rink.** Receptor-mediated calcium entry in fura-2-loaded human platelets stimulated with ADP and thrombin: Dual wavelengths study with Mn^{2+}. *Biochem. J.* 258: 923-926, 1989.

173. **Saitoh, M., T. Ishikawa, S. Matsushima, M. Naka, and H. Hidaka.** Selective inhibition of catalytic activity of smooth muscle myosin light chain kinase. *J. Biol. Chem.* 262: 7796-7801, 1987.

174. **Sanders, C., L. D. Burtnick, and L. B. Smillie.** Native chicken gizzard tropomyosin is predominantly a βγ-heteodimer. *J. Biol. Chem.* 261: 12774-12778, 1986.

175. **Satoh, S., H. Rensland, and G. Pfitzer.** *Ras* proteins increase Ca^{2+}-responsiveness of smooth muscle contraction. *FEBS Lett.* 324(2): 211-215, 1993.

176. **Schwartz, A., E. McKenna, and P. L. Vaghy.** Receptors for calcium antagonists. *Am. J. Cardiol.* 62 (Suppl): 3G-6G, 1988.

177. **Seidel, C. L., D. Rickman, H. Steuckrath, J. C. Allen, and A. M. Kahn.** Control and function of alterations in contractile protein isoform expression in vascular smooth muscle. In, *Regulation of Smooth Muscle Contraction*, (R. S. Moreland, Ed) Plenum Press, pp. 315-325, 1991.

178. **Silver, P. J., and J. T. Stull.** Quantitation of myosin light phosphorylation in small tissue samples. *J. Biol. Chem.* 257: 6137-6144, 1982.

179. **Singer, H. A., J. W. Oren, and H. A. Benscoter.** Myosin light chain phosphorylation in ^{32}P-labeled rabbit aorta stimulated by phorbol 12,13-dibutyrate and phenylephrine. *J. Biol. Chem.* 264: 21215-21222, 1989.

180. **Sobieszek, A.** Ca^{2+}-linked phosphorylation of a light chain of vertebrate smooth-muscle myosin. *Eur. J. Biochem.* 73: 477-483, 1977.

181. **Sobue, K., K. Morimoto, M. Inui, K. Kanda, and S. Kakiuchi.** *Biomed. Res.* 3: 188-192, 1982.

182. **Sobue, K., and J. R. Sellers.** Caldesmon, a novel regulatory protein in smooth muscle and nonmuscle actomyosin system. *J. Biol. Chem.* 266: 12115-12118, 1991.

183. **Somlyo, A. P.** Myosin isoforms in smooth muscle: how they may affect function and structure? *J. Musc. Res. Cell Motil.* 14: 557-564, 1993.

184. **Somlyo, A. P., and A. V. Somlyo.** Signal transduction and regulation in smooth muscle. *Nature Lond.* 372: 231-236, 1994.

185. **Song, J. B., J. D. Hood, and M. J. Davis.** Gadolinium blocks calcium channels in coronary artery smooth muscle cells. *Biophys. J.* 61: A515, 1992.

186. **Stull, J. T., L-C. Hsu, M. G. Tansey, and K. E. Kamm.** Myosin light chain kinase phosphorylation in tracheal smooth muscle. *J. Biol. Chem.* 265: 16683-16690, 1990.

187. **Stull, J. T., P. J. Gallagher, B. P. Herring, and K. E. Kamm.** Vascular smooth muscle contractile elements: cellular regulation. *Hypertension* 17: 723-732, 1991.

188. **Sun, D., E. J. Messina, G. Kaley, and A. Koller.** Characteristic and origin of myogenic response in isolated mesenteric arterioles. *Am. J. Physiol.* 263 (*Heart Circ. Physiol.* 32): H1486-1491, 1992.

189. **Takahashi, K., Hiwada, K. and Kokubu, T.** Isolation and characterization of a 34000-dalton calmodulin- and F-actin -binding protein from chicken gizzard smooth muscle. *Biochem. Biophys. Res. Commun.* 141: 20-26, 1986.

190. **Takemura, H., A. R. Hughes, O. Thastrup, and J. W. Putney, Jr.** Activation of calcium entry by the tumor promoter, thapsigargin, in parotid acinar cells. Evidence that an intracellular calcium pool, and not an inositol phosphate, regulates calcium influxes at the plasma membrane. *J. Biol. Chem.* 264: 12266-12272, 1989.

191. **Takemura, H., and J. W. Putney, Jr.** Capacitative calcium entry in parotid acinar cells. *Biochem. J.* 258: 409-412, 1989.

192. **Tanaka, Y., S. Hata, H. Ishiro, K. Ishii, and K. Nakayama.** Quick stretch increase the production of inositol 1,4,5-trisphosphate (IP_3) in porcine coronary artery. *Life Sci.* 55: 227-235. 1994.

193. **Tanaka, Y., S. Hata, H. Ishiro, K. Ishii, and K. Nakayama.** Stretching releases Ca^{2+} from intracellular storage sites in canine cerebral arteries. *Can. J. Physiol. Pharmacol.* 72: 19-24, 1993.

194. **Thastrup, O., P. J. Cullen, B. K. Drobak, M. R. Hanley, and A. P. Dawson.** Thapsigargin, a tumor promoter, discharges intracellular Ca^{2+} stores by specific inhibition of the endoplasmic reticulum Ca^{2+}-ATPase. *Proc. Natl. Acad. Sci.* 87: 2466-2470, 1990.

195. **Tsien, R. Y.** Fluorescent probes of cell signaling. *Ann. Rev. Neurosci.* 12: 227-253, 1989.

196. **Towbin, H., T. Staehelin, and G. Gordon.,** Electrophoretic transfer of proteins from polyacrylamide gels to nitrocellulose sheets: Procedure and some applications. *Proc. Natl. Acad. Sci.* 76: 4350-4354, 1979.

197. **Tsao, A. E., and T. J. Eddinger.** Smooth muscle myosin heavy chains combine to form three native myosin isoforms. *Am. J. Physiol.* 264 (Heart Circ. Physiol. 33): H1653-H1662, 1993.

198. **VanBavel, E., and M. J. Mulvany.** Role of wall tension in the vasoconstrictor response of cannulated rat mesenteric small arteries. *J. Physiol. London.* 477: 103-115, 1994.

199. **van Breemen, C., Q. Chen, and I. Laher.** Superficial buffer barrier function of smooth muscle sarcoplasmic reticulum. *Tips* 16: 98-105, 1995.

200. **van Breemen, C., and K. Saida.** Cellular mechanisms regulating $[Ca^{2+}]_i$ smooth muscle. *Annu. Rev. Physiol.* 51: 315-329, 1989.

201. **Vandekerckhove, J., and K. Weber.** At least six actins are expressed in a higher mammal: an analysis based on the amino acid sequence of the amino-terminal tryptic peptide. *J. Mol. Biol.* 126: 783-802, 1978.

202. **Watanabe, J., A. Karibe, S. Horiguchi, M. Keitoku, S. Satoh, T. Takishima, and K. Shirato.** Modification of myogenic intrinsic tone and $[Ca^{2+}]_i$ of rat isolated arterioles by ryanodine and cyclopiazonic acid. *Circ. Res.* 73: 465-472, 1993.

203. **Walsh, M. P.** Calcium-dependent mechanisms of regulation of smooth muscle contraction. *Biochem. Cell Biol.* 69: 771-780, 1991.

204. **Walsh, M. P.** Regulation of vascular smooth muscle tone. *Can. J. Physiol. Pharmacol.* 72: 919-936, 1994.

205. **Walsh, M. P., J. D. Carmichael, and G. J. Kargacin.** Characterization and confocal imaging of calponin in gastrointestinal smooth muscle. *Am. J. Phsiol.* 265 (*Cell Physiol.* 34): C1371-C1378, 1993.

206. **Williams, D. A., and F. S. Fay.** Calcium transients and resting levels in isolated smooth muscle cells as monitored with quin 2. *Am. J. Phsiol.* 250 (*Cell Physiol.* 19): C779-C791, 1986.

207. **Winder, S. J., B. G. Allen, E. D. Fraser, H. M. Kang, G. J. Kargacin, and M. P. Walsh.** Calponin phosphorylation in vitro and in intact muscle. *Biochem. J.* 296: 827-836, 1993.

208. **Winder, S. J., G. J. Kargacin, A. A. Bonet-Kerrache, M. D. Pato, and M. P. Walsh.** Calponin: localization and regulation of smooth muscle actomyosin Mg^{2+}-ATPase. *Jpn. J. Pharmacol.* 58(Suppl. 2): 29P-34P, 1992.

209. **Winder, S. J., and M. P. Walsh.** Smooth muscle calponin. Inhibition of actomyosin Mg^{2+}-ATPase and regulation by phosphorylation. *J. Biol. Chem.* 265: 10148-10155, 1990.

210. **Yang, X. C., and F. Sachs.** Block of stretch-activated ion channels in *Xenopus* oocytes by gadolinium and calcium ions. *Science Wash. DC* 243: 1068-1071, 1989.

211. **Zanellato, A. M. C., A. C. Borrione, L. Giuriato, M. Tonello, G. Scannapieco, P. Pauletto, and S. Sartore.** Myosin isoforms and cell heterogeneity in vascular smooth muscle. I. Developing and adult bovine aorta. *Develop. Biol.* 141: 431-446, 1990.

VITA

Name: Hui Zou
SSN: 223-61-9521

Address:

University of Massachusetts
Department of Physiology
Worcester, MA 01605

63 Frank street
Apartment 86
Worcester, MA 01604

Date of Birth: March 14, 1964
Tianjin, China

Education:

1995 Doctor of Philosophy
Eastern Virginia Medical School and Old Dominion University (Biomedical Sciences)
Field of Study: Microvascular Physiology
Thesis: Cellular Mechanisms underlying Basal Tone and Myogenic Reactivity in Isolated Arterioles
Advisor: Michael A.Hill, Ph. D

1989 Master of Engineering
Tianjin University, China
Field of Study: Biomedical Engineering and Instrumentation
Thesis: Design of an ECG monitor with Functions of Pacing and Defibrillation.
Advisor: Ming Shi Wang

1986 Bachelor of Engineering
Tianjin University, China
Field of Study: Biomedical Engineering and Instrumentation
Thesis: Design of a Digital Thermometer
Advisor: Ming Shi Wang

Honors:

1992-1995 3 years Graduate Fellowship
Eastern Virginia Medical School

Professional Society Memberships:

American Physiology Society